NUREG/CR-1557
BMI-2038

Steam-Water Mixing and System Hydrodynamics Program Task 4

Quarterly Progress Report April-June 1979

Prepared by R. P. Collier, T. A. Bishop, J. A. Dworak, L. J. Flanigan, R. E. Kurth, J. S. Liu, A. Segev

Battelle Columbus Laboratories

Prepared for U.S. Nuclear Regulatory Commission

Available from

GPO Sales Program
Division of Technical Information and Document Control
U. S. Nuclear Regulatory Commission
Washington, D. C. 20555

Printed copy price: $4.25

and

National Technical Information Service
Springfield, Virginia 22161

NUREG/CR-1557
BMI-2038
R2

STEAM-WATER MIXING AND SYSTEM HYDRODYNAMICS PROGRAM

QUARTERLY PROGRESS REPORT
April 1979 - June 1979

by

Robert P. Collier
Thomas A. Bishop
Joseph A. Dworak
Lawrence J. Flanigan
Robert E. Kurth
Jim S. Liu
Aryeh Segev

Manuscript Completed: June 1980
Manuscript Published: July 1980

BATTELLE
Columbus Laboratories
505 King Avenue
Columbus, Ohio 43201

Prepared for
Division of Reactor Safety Research
Office of Nuclear Regulatory Research
U.S. Nuclear Regulatory Commission
Washington, D.C. 20555
NRC FIN No. A4048

ABSTRACT

During this quarter analysis included additional development of the I^* scaling parameter for tubes, review of results from air-water tests in distorted geometries, and correlation of results from countercurrent flow condensation tests in a rectangular test section.

Experimental work this quarter included completion of condensation tests and heat partitioning studies in the rectangular test section, and air-water and steam-water tests in the 2/15-scale model with shortened and extended annulus lengths. The instrumented break leg spool piece was received from INEL and installed in the 2/15-scale facility.

SUMMARY

This report describes progress during the third quarter of FY '79 on the BCL Steam-Water Mixing and System Hydrodynamics Program. Progress during the quarter is reported under four technical tasks: analysis, testing and data reduction, RIL support and technical assistance, and acquisition and application of advanced instrumentation.

Analysis

A theoretical model for countercurrent flow flooding in tubes has been presented previously. This model expresses the relationship between the dimensionless gas and liquid fluxes in terms of a ratio of modified Bessel functions. During the quarter an approximation of the Bessel function ratio as a function of the characteristic dimension and the critical wave number was developed.

Results from air-water tests conducted in the 2/15-scale model with shortened and extended annulus lengths were reviewed. Short annulus tests show a dependence on injection rate but not on water temperature. Long annulus tests showed the reverse. For a given liquid injection flow rate, temperature and air flow rate, penetration decreases with increasing annulus length. The data can be correlated in the Wallis form, but the slope and intercept parameters, m and C, are not constant.

Countercurrent flow steam-water condensation tests in a rectangular test section were evaluated. Local condensation heat transfer coefficients were determined from liquid temperature measurements along the channel. Their dependence on local steam and water flow rates, liquid subcooling, and test section inclination angle was studied. The results were correlated in terms of the local hydrodynamic and thermal conditions for different experimentally observed wave structure regions. The correlations define the local Nusselt number in terms of the local steam and liquid Reynolds numbers and the liquid Prandtl number. A correlation for the dimensionless surface temperature was also developed from which the condensation efficiency can be determined.

Testing and Data Reduction

Testing in the heated wall rectangular channel during the quarter included studies of heat partitioning between the steam and liquid phases when rapidly cooling a heated wall and completion of the countercurrent flow condensation tests began during the last quarter. Testing in the 2/15-scale model included air-water and steam-water experiments with both standard and distorted annulus lengths. Emphasis was placed on obtaining high bypass data.

RIL Support and Technical Assistance

BCL staff participated in an ECC Bypass Review Group meeting and reviewed draft material for the RIL.

Acquisition and Application of Advanced Instrumentation

The instrumented break leg spool piece was received from INEL, installed and checked out. VDM assembly and check out continued.

TABLE OF CONTENTS

LIST OF TABLES

PART I

Progress for the Quarter
April 1, 1979 - June 30, 1979

LIST OF FIGURES

PART I

Progress for the Quarter
April 1, 1979 - June 30, 1979

LIST OF FIGURES
(continued)

LIST OF FIGURES
(continued)

PART II

Steam Condensation on a Subcooled Film in Countercurrent Flow

Page

LIST OF FIGURES
(continued)

PREVIOUS REPORTS IN THIS SERIES

Report No.	Period Covered	Date Issued
BMI-X-657	January-March 1975	April, 1975
BMI- 1936	April-June 1975	August, 1975
BMI- 1940	July-September 1975	November, 1975
BMI-NUREG-1945	October-December 1975	March, 1976
BMI-NUREG-1949	January-March 1976	May, 1976
BMI-NUREG-1962	April-June 1976	November, 1976
BMI-NUREG-1964	July-September 1976	December, 1976
BMI-NUREG-1968	October-December 1976	February, 1977
BMI-NUREG-1972	January-March 1977	May, 1977
BMI-NUREG-1979	April-June 1977	September, 1977
BMI-NUREG-1987	July-September 1977	December, 1977
NUREG/CR-0034 (BMI-1993)	October-December 1977	March, 1978
NUREG/CR-0147 (BMI-2003)	January-March 1978	June, 1978
NUREG/CR-0526 (BMI-2011)	April-June 1978	November, 1978
NUREG/CR-0565 (BMI-2013)	July-September 1978	December, 1978
NUREG/CR-0845 (BMI-2028)	October-December 1978	May, 1979
NUREG/CR-0897 (BMI-2029)	January-March 1979	June, 1979

INTRODUCTION

The U.S. Nuclear Regulatory Commission is responsible for assessing and assuring the safety of nuclear reactors under abnormal conditions such as a postulated loss-of-coolant accident (LOCA), as well as under normal operating conditions. Prediction of the thermal-hydraulic behavior of the reactor system following such a LOCA is of particular interest, and NRC supports a very large research effort aimed at increasing that predictive capability. In the Steam-Water Mixing and System Hydrodynamics Program currently in progress at Battelle-Columbus Laboratories (BCL) both analytical and experimental work are directed toward a more thorough understanding and description of steam-water interaction and its influence on the effectiveness of emergency core cooling systems under LOCA conditions. The phenomena of ECC penetration and bypass are of primary interest.

Fiscal Year 1979 activities include identification and establishment of the physical basis for scaling ECC bypass phenomena, development of and understanding of condensation and vaporization processes in the downcomer, determination of the validity of using steady-state results to predict transient behavior, and preparation of a summary technical report for the planned Research Information Letter (RIL).

The scope of technical work on the program has been subdivided into four tasks: (1) Analysis, (2) Testing and Data Reduction, (3) RIL Support and Technical Assistance and (4) Acquisition and Application of Advanced Instrumentation.

The quarterly Progress Reports consist of two parts, the first is a description of activities and progress during the quarter in the technical tasks. This part is more informational in nature as results are presented as early as possible to expedite the dissemination of data and analyses. The second part is a discussion of a specific topic or topics important to meeting the overall program objectives. In this sense, the second part is a "mini-topical" which may include results of work completed during several quarters. This part is more interpretational in nature.

This report summarizes progress made on the program during the quarter ending June 30, 1979, for the individual technical tasks. Although progress is reported by task, it should be recognized that there is significant interaction between the tasks in both the scope and conduct of the research. A section discussing steam condensation on a subcooled film in countercurrent flow is also included.

PART 1

Progress for the Quarter

April 1, 1979 - June 30, 1979

TASK 1.0 ANALYSIS

Objectives

The objectives of this task are to:

(1) Develop an improved theoretical understanding of steam-water interaction phenomena,

(2) Analyze and correlate the experimental data obtained from the studies conducted under Task 2.0,

(3) Evaluate and interpret experimental data from offsite steam-water mixing experimental efforts, and

(4) Use this knowledge to verify and improve current LOCA/ECC analysis methods.

Work During Quarter

During this quarter we carried out additional analytical development for the I^* scaling parameter, analyzed results from air-water tests in distorted geometries, and analyzed results from countercurrent condensation tests in the rectangular test section. An informal review of results from heat partitioning tests in the rectangular test section was also carried out.

Further I^* Development for Tubes

A theoretical model for countercurrent flow flooding in tubes based on the Helmholtz instability concept has been developed previously.[1] The model is given by

$$J_g^{*1/2} + (\rho_g/\rho_L)^{1/4} J_L^{*1/2} = \left[\frac{Tk}{g(\rho_L - \rho_g)D} \cdot \frac{I_1(kR)}{I_o(kR)}\right]^{1/4} \qquad (1)$$

where T is the surface tension, k is the wave number, D is a characteristic dimension, and R is the tube radius. I_1 and I_o are modified Bessel functions of the first and zero order respectively.

The objective of this work is to approximate the Bessel function ratio as a function of the characteristic dimension so that

$$D^{\alpha} = I_1(kR)/I_o(kR) \tag{2}$$

If Equation (2) is substituted into Equation (1), it is obvious that for $\alpha = 0$ we have K^* scaling and for $\alpha = 1$, J^* scaling is obtained.

Defining a new variable, z, as

$$z \equiv \frac{kD}{2} \quad , \tag{3}$$

thus

$$D^{\alpha} = I_1(z)/I_o(z) \quad . \tag{4}$$

Differentiation of Equation (4) yields

$$\alpha D^{\alpha-1} = \{[(I_o - I_1/z)I_o - I_1^{\,2}]/I_o^{\,2}\}k/2 \quad . \tag{5}$$

Substitution of Equation (2) into Equation (5) gives

$$\alpha D^{\alpha-1} = (1 - D^{\alpha}/z - D^{2\alpha})k/2 \quad , \tag{6}$$

or finally

$$\alpha = z(D^{-\alpha} - D^{\alpha}) - 1 \quad . \tag{7}$$

We define the function, f, as

$$f = z(D^{-\alpha} - D^{\alpha}) - 1 - \alpha \quad , \tag{8}$$

and find the roots of f to determine values of α which satisfy Equation (7). In Figure 1, f is plotted as a function of α. Since the function is nearly linear around zero, a simple iterative technique using linear interpolation was used to find the roots which are summarized in Table 1. This approach provides a simple method for determining α for given values of k and D for tubes.

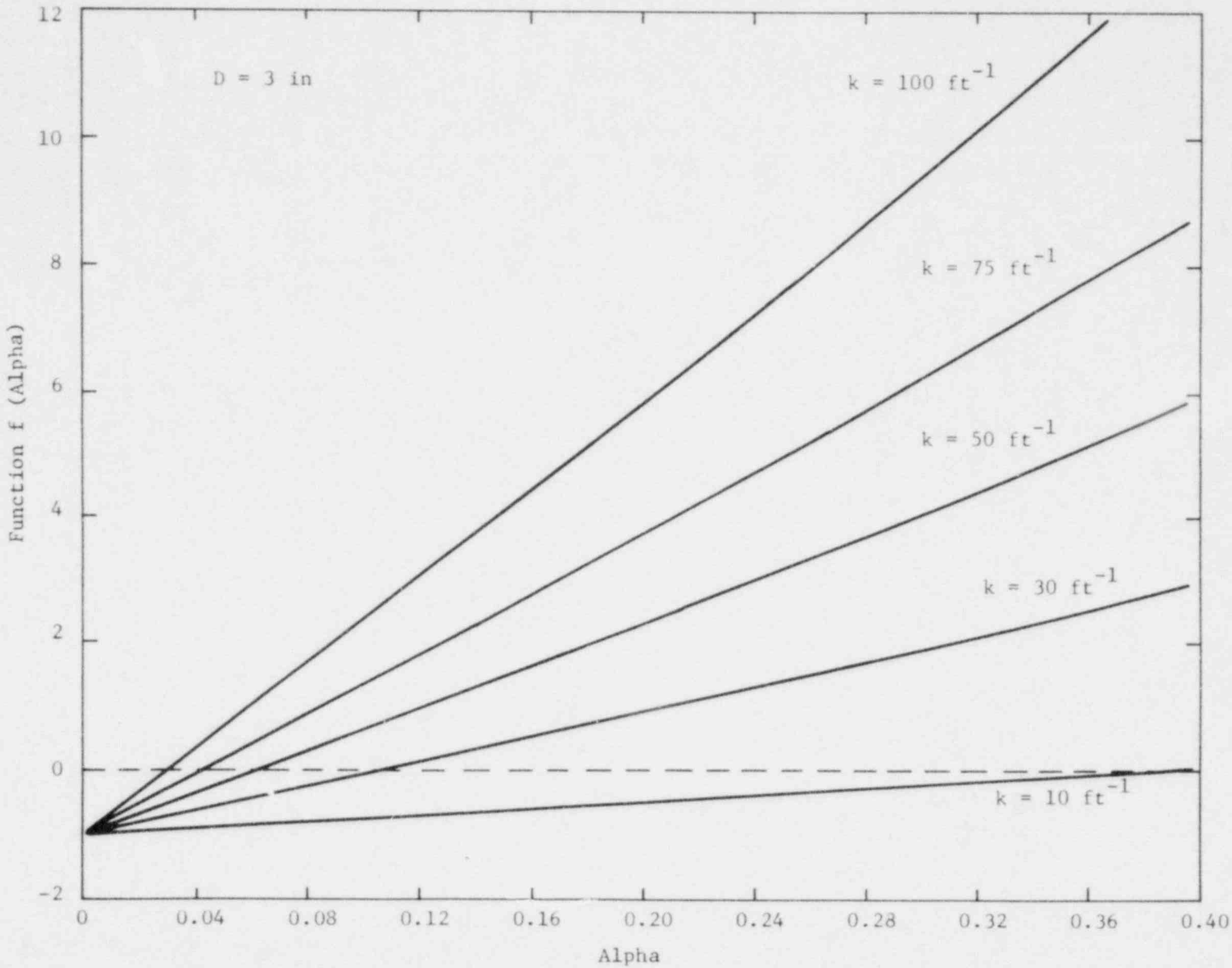

Figure 1. Roots of the Function f as a Function of α

TABLE 1. ROOTS OF THE FUNCTION f FOR A RANGE OF CHARACTERISTIC DIMENSIONS AND WAVE NUMBERS

D	k	α	D	k	α
1 in	25 ft^{-1}	0.2247	4 in	25 ft^{-1}	0.1222
	50	0.1056		50	0.0577
	75	0.0685		75	0.0378
	100	0.0506		100	0.0281
	150	0.0332		150	0.0185
	200	0.0247		200	0.0138
2 in	25	0.1525	5 in	25	0.1229
	50	0.0716		50	0.0580
	75	0.0467		75	0.0379
	100	0.0346		100	0.0282
	150	0.0228		150	0.0186
	200	0.0170		200	0.0139
3 in	25	0.1297	6 in	25	0.1303
	50	0.0612		50	0.0612
	75	0.0400		75	0.0400
	100	0.0297		100	0.0297
	150	0.0196		150	0.0196
	200	0.0146		200	0.0146

Analysis of Air-Water Tests in Distorted Geometries

Air-water plenum fill tests were conducted in the 2/15-scale model with short and long core barrels. Details of the geometries are given in Reference (2). Nominal operating conditions are given in Tables 2 and 3. Results of the tests are tabulated in Tables A-1 and A-2 in Appendix A.

Short Core Barrel Results. Figures 2 and 3 show the short core barrel penetration data listed in Table A-1. Figure 2 shows the effect of different ECC injection rates on penetration for a fixed water temperature. For the short core barrel higher injection rates increase penetration for a fixed reverse core air flow. This effect was not seen in our previous air-water tests in the standard geometry. Figure 2 also indicates the reproducibility of the short core barrel air-water data. The circles and squares represent data taken on two different days at approximately the same operating conditions. The data from the different runs agree very closely. Figure 3 shows the effect of varying water temperature on penetration for a fixed injection rate. Water temperature does not seem to affect the penetration rate for the short core barrel geometry.

Long Core Barrel Results. The results of tests conducted with the long core barrel are shown in Figures 4 through 10. These figures show the effect of varying the ECC injection rate for a fixed water temperature and varying the water temperature for a fixed ECC injection rate. In Figures 4 through 6 we can see that, excluding the lowest injection rate, there is no clear dependence on the penetration curve on injection flow rate for the long core barrel. For the lowest flow rate the water flow pattern at zero gas flow is different than at higher flow rates. Thus the shifted penetration curve for the low injection rate may be due to different injected water flow patterns.

While there is no effect of injection flow rate on penetration for the long core barrel, there is a well defined effect of injected water

TABLE 2. AIR-WATER PLENUM FILL TEST MATRIX FOR SHORT CORE BARREL TESTS

Test No.	Model Pressure, psia	ECC Water Temp., F	ECC Water Injection Flow Rate, gpm	J^*_{Lin}	J^*_g
1	as low as operating conditions permit	70	250	0.063	air flow to span range from full penetration to full bypass
2		70	380	0.098	
3		170	380	0.098	
4		70	475	0.121	

TABLE 3. AIR-WATER PLENUM FILL TEST MATRIX FOR EXTENDED CORE BARREL TESTS

Test No.	Model Pressure, psia	ECC Water Temp., F	ECC Water Injection Flow Rate, gpm	J^*_{Lin}	J^*_g
1	as low as operating conditions permit	70	125	0.032	air flows to span range from full penetration to full bypass
2		170	"	"	
3		210	"	"	
4		70	250	0.063	
5		170	"	"	
6		210	"	"	
7		70	380	0.098	
8		170	"	"	
9		210	"	"	
10		70	475	0.121	
11		170	"	"	
12		210	"	"	

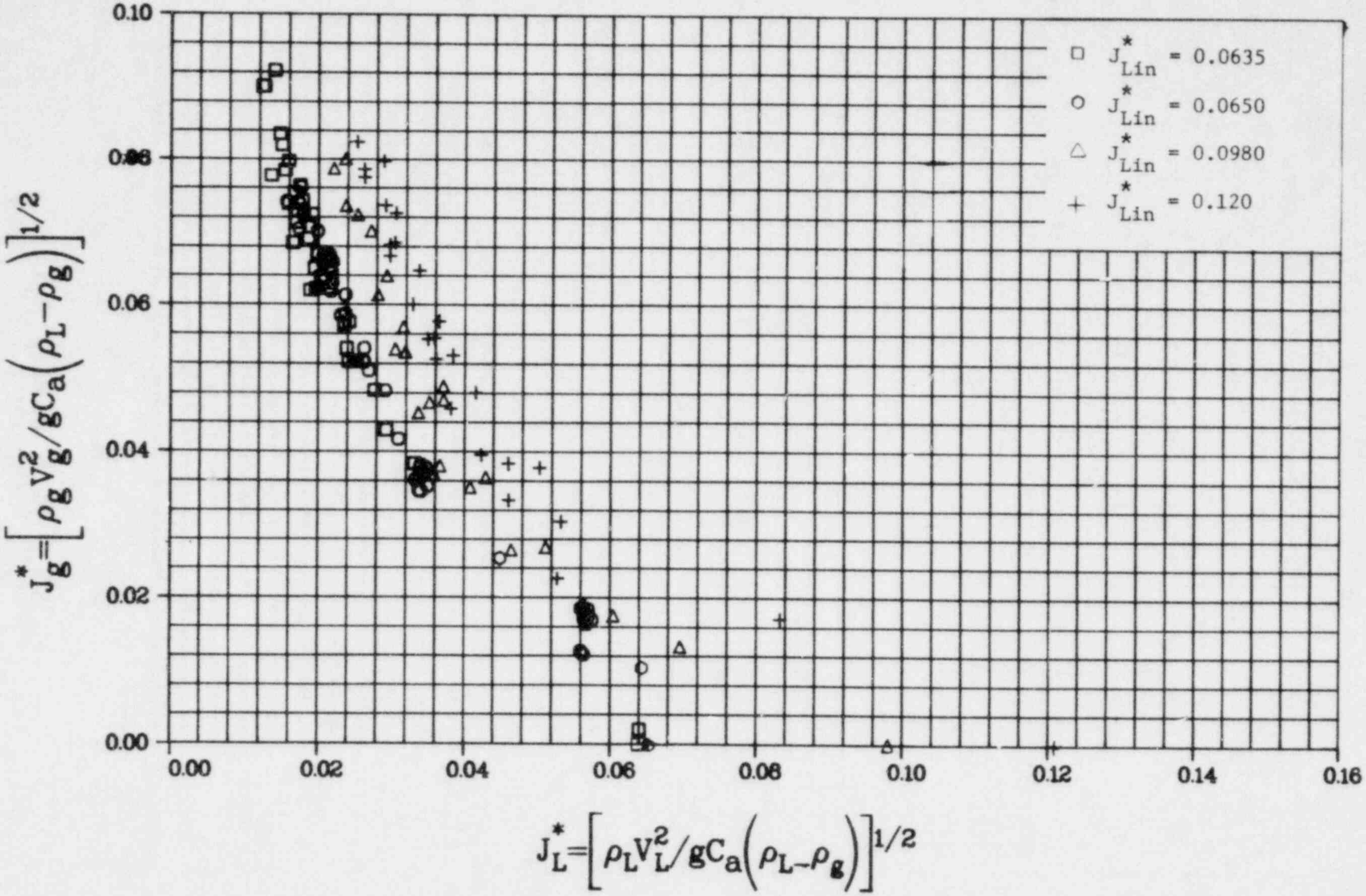

Figure 2. Air-Water Plenum Fill Penetration Data Obtained With T_{Lin} = 21 C (70 F) and PV = 136 kPa (20 psia) for Short Core Barrel Tests

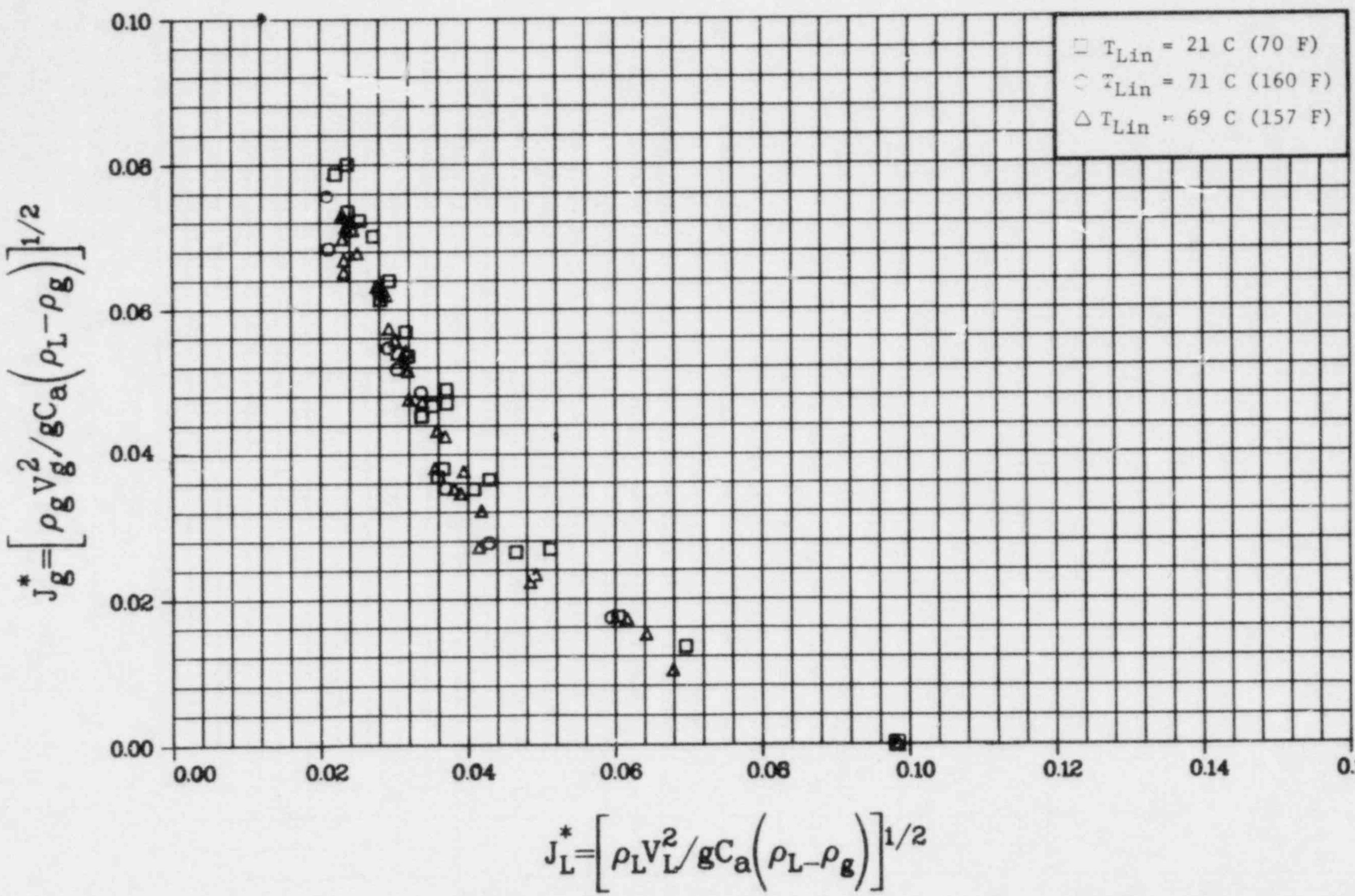

Figure 3. Air-Water Plenum Fill Penetration Data Obtained With J^*_{Lin} = 0.098 and PV = 136 kPa (20 psia) for Short Core Barrel Tests

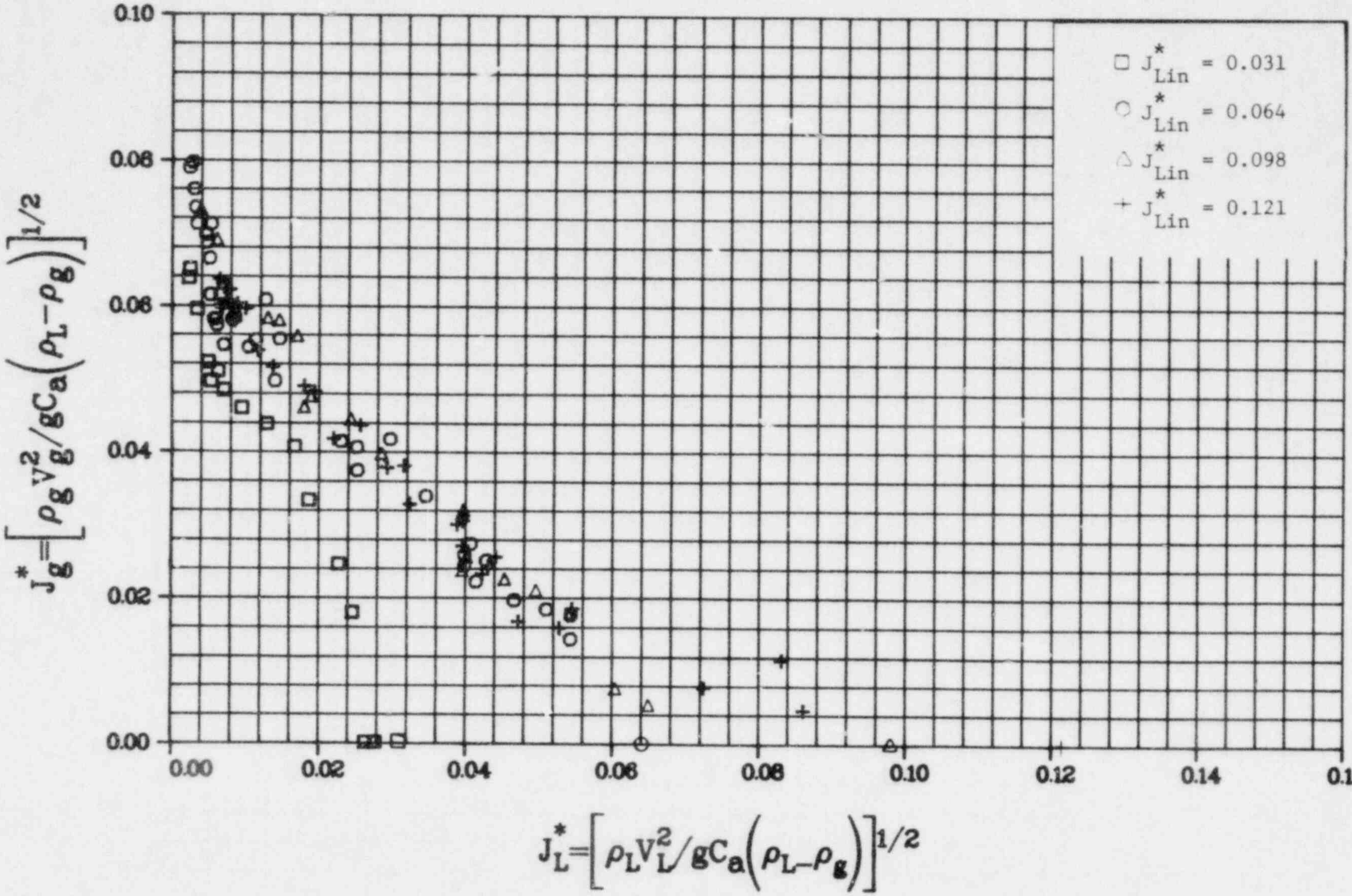

Figure 4. Air-Water Plenum Fill Penetration Data Obtained With T_{Lin} = 21 C (70 F) and PV = 149 kPa (22 psia) for Exended Core Barrel Tests

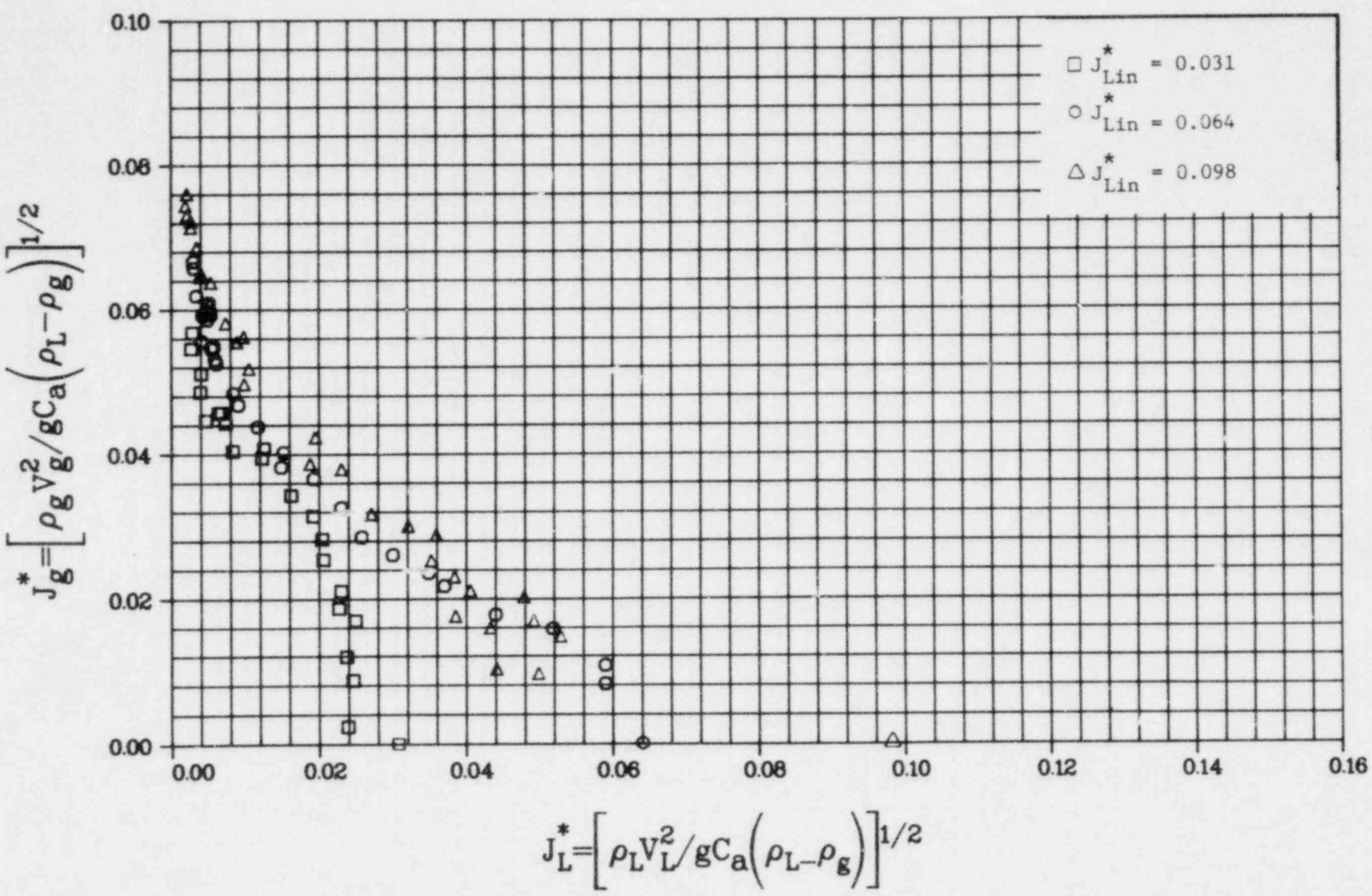

Figure 5. Air-Water Plenum Fill Penetration Data Obtained With T_{Lin} = 74 C (165 F) and PV = 149 kPa (22 psia) for Extended Core Barrel Tests

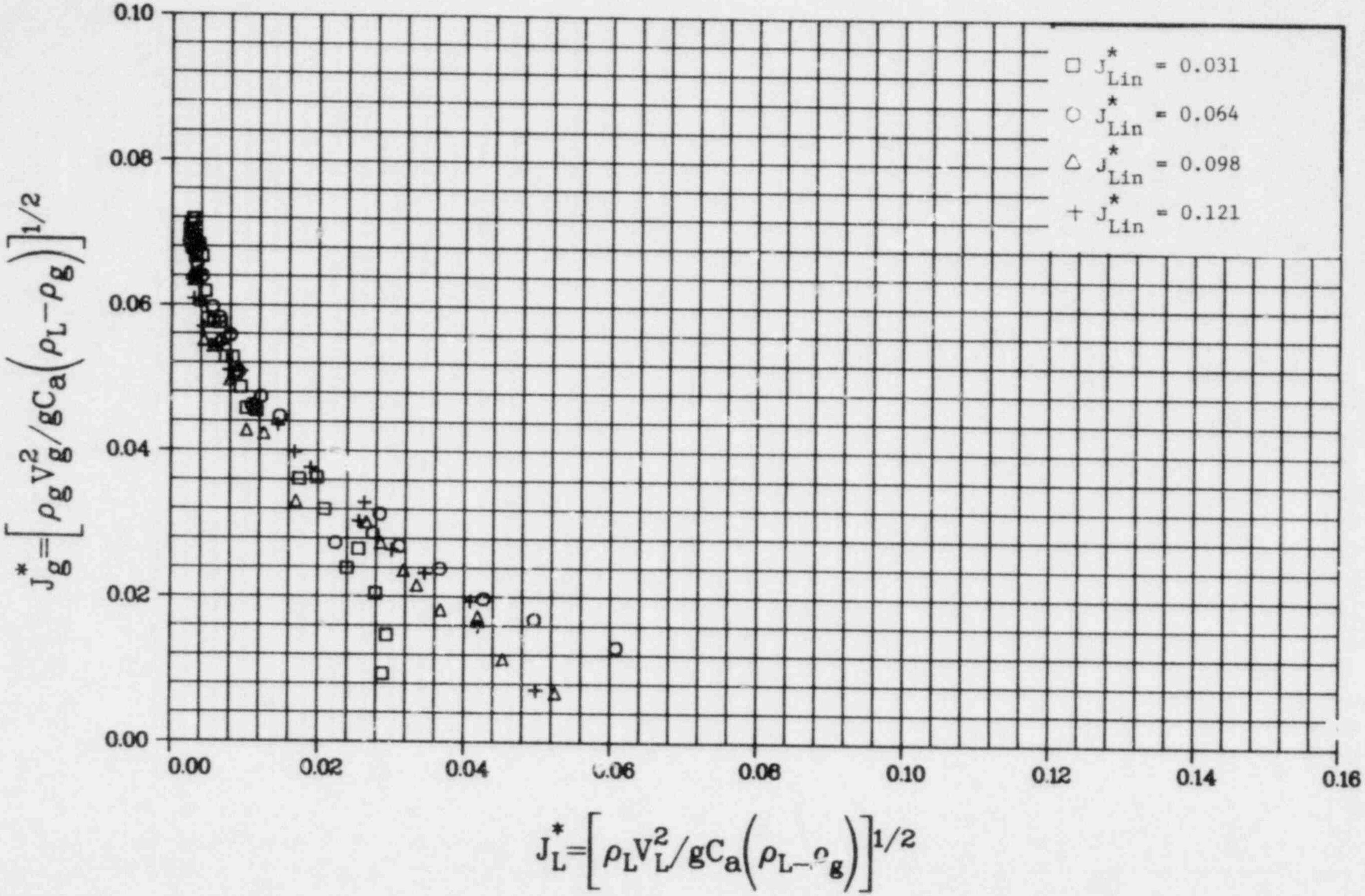

Figure 6. Air-Water Plenum Fill Penetration Data Obtained With T_{Lin} = 96 C (205 F) and PV = 149 kPa (22 psia) for Extended Core Barrel Tests

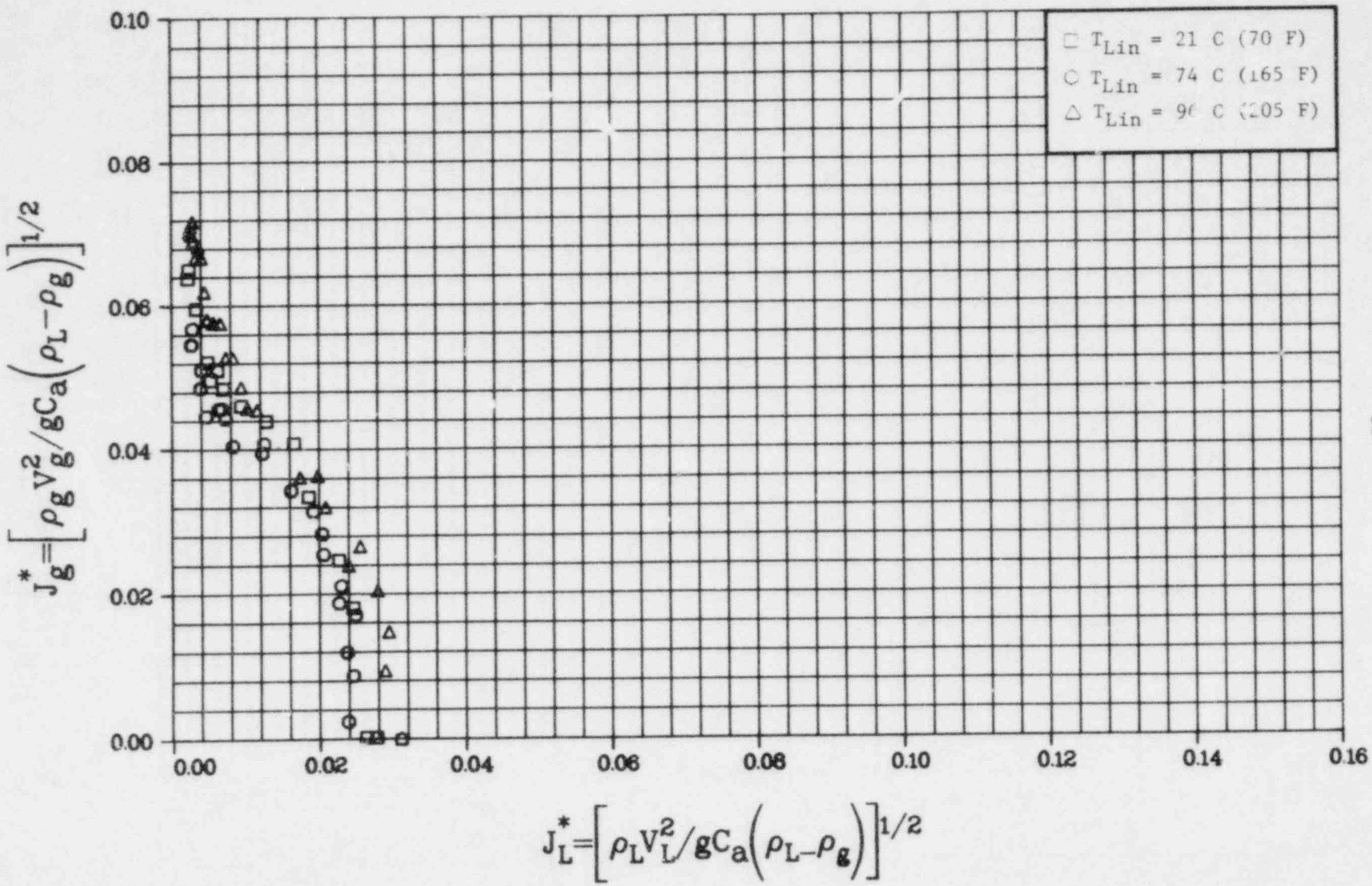

Figure 7. Air-Water Plenum Fill Penetration Data Obtained With J^*_{Lin} = 0.031 and PV = 149 kPa (22 psia) for Extended Core Barrel Tests

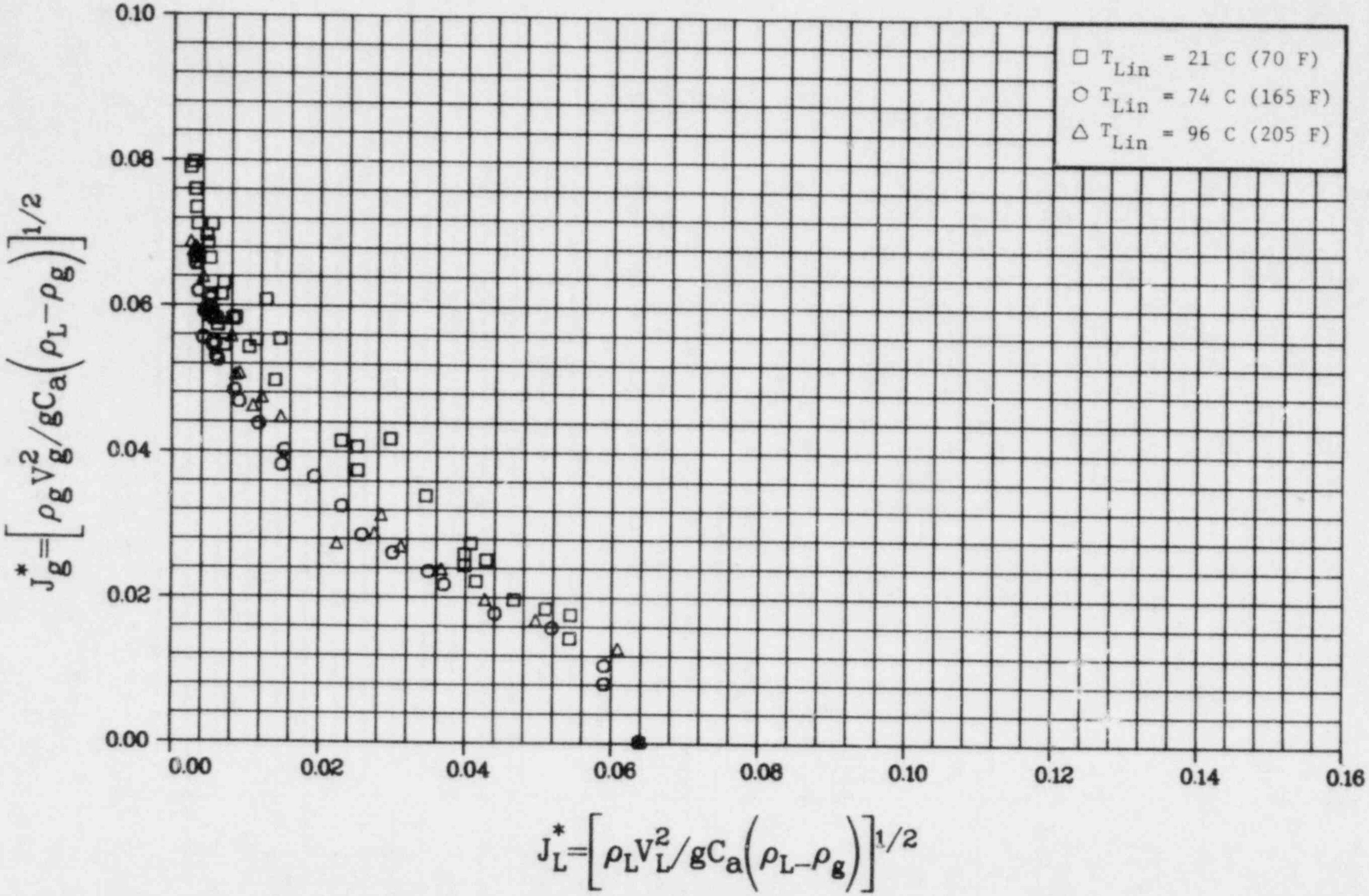

Figure 8. Air-Water Plenum Fill Penetration Data Obtained With J^*_{Lin} = 0.064 and PV = 149 kPa (22 psia) for Extended Core Barrel Tests

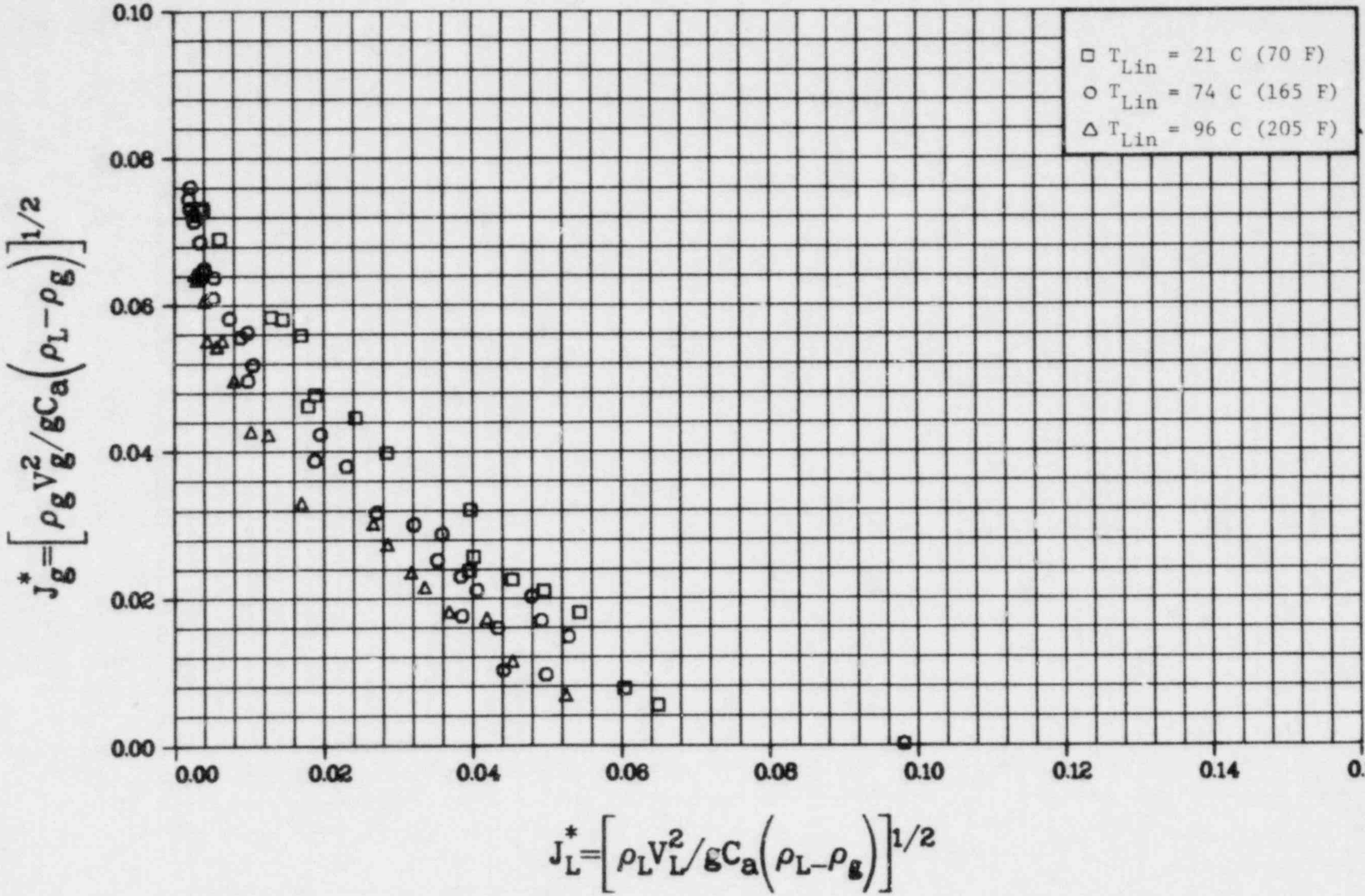

Figure 9. Air-Water Plenum Fill Penetration Data Obtained With J^*_{Lin} = 0.098 and PV = 149 kPa (22 psia) for Extended Core Barrel Tests

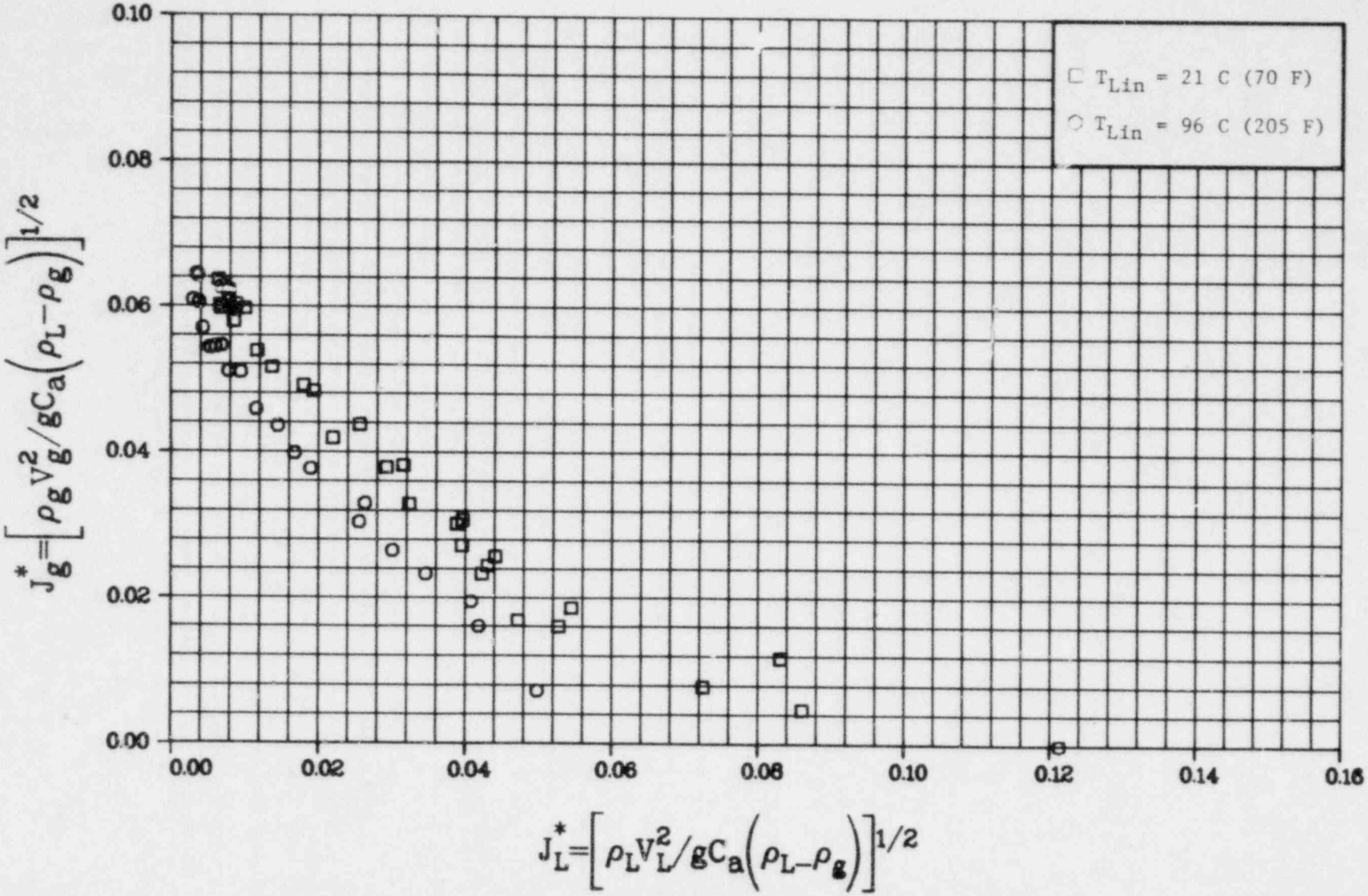

Figure 10. Air-Water Plenum Fill Penetration Data Obtained With J^*_{Lin} = 0.121 and PV = 149 kPa (22 psia) for Extended Core Barrel Tests

temperature. Figures 7 through 10 present penetration curves for fixed ECC injection rates and varying ECC temperatures. In each figure the penetration curve is shifted down and to the left as temperature increases. For a fixed reverse core air flow rate the penetration decreases as the temperature increases. This is in the direction that we would expect changes in surface tension to affect the penetration. The magnitude of the shift cannot be explianed by surface tension effects, however, as shown in Figure 11, where the data of Figure 9 are replotted on K^* coordinates. The individual penetration curves do not collapse to a single line, indicating that surface tension, as accounted for by K^*, is not the primary cause of the difference in penetration curves.

One explanation may be that the effective gas phase is a mixture of air and water vapor, with the maximum amount of vapor defined by saturation of the air. As temperature increases, the amount of water vapor which the air can carry also increases. This would be rather like a hot wall effect, in that fluid evaporated from the liquid would add to the reverse core gas flow and decrease penetration. In this case the fluid would merely evaporate rather than boil. Calculations in which the air is assumed to be saturated with water at the injected liquid temperature indicate that the additional gas momentum could easily be large enough to explain the deviation of the penetration curves with temperature.

This explanation is consistent with results from both short and long core barrels. That is, the effect is pronounced when the contact time between the air and water is long, but within the experimental scatter when the contact time is brief.

Comparison of Results from Different Geometries. Direct comparison of data from tests with short, standard, and long core barrels are shown in Figures 12 and 13. In these figures it is quite clear that the short core barrel data lie well above data from the standard and extended core barrel tests. Standard and extended core barrel data lie close together, however there is a consistent trend for the extended core barrel data to lie below the standard core barrel data.

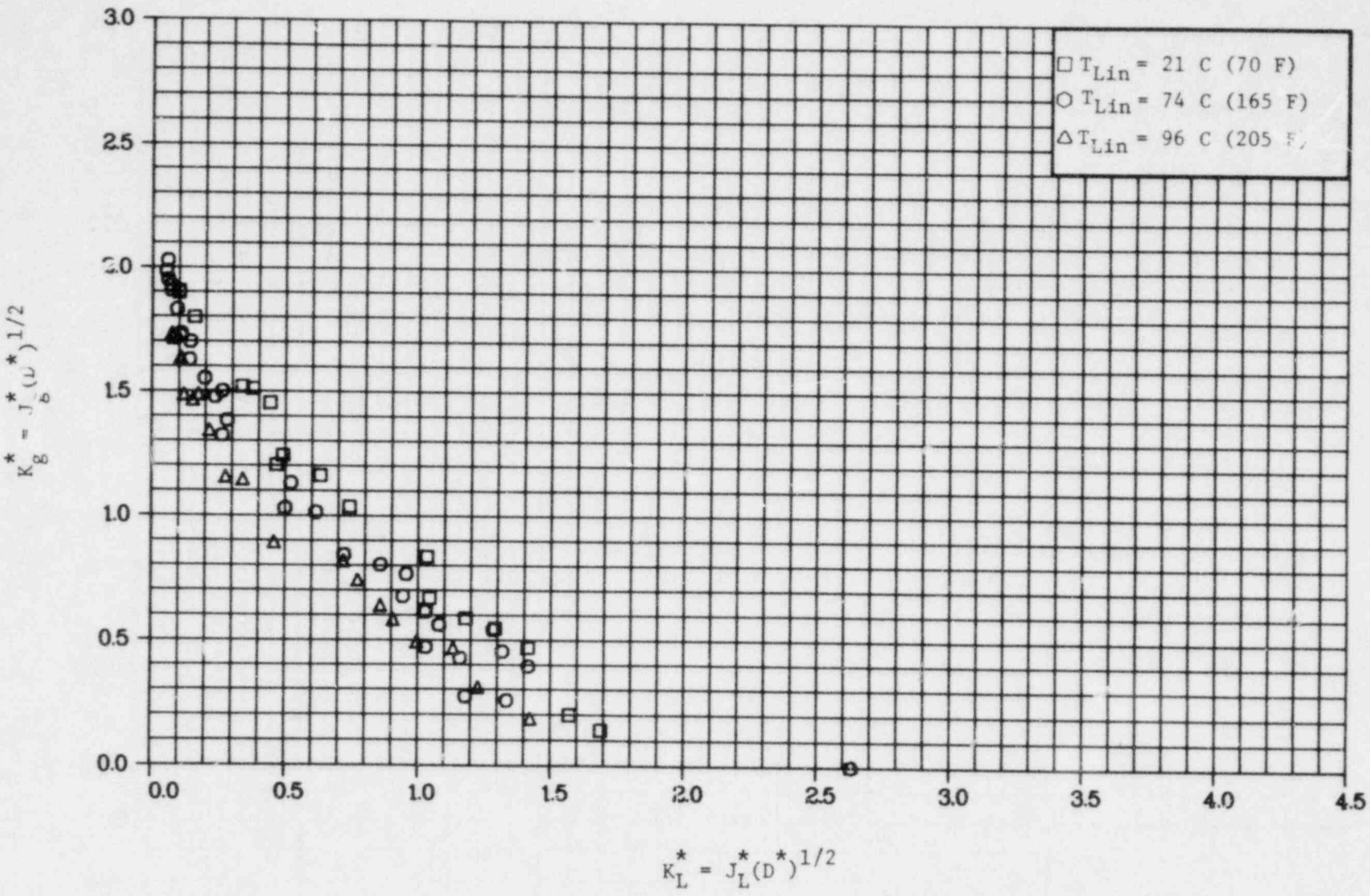

Figure 11. Air-Water Plenum Fill Penetration Data Obtained With $K_{Lin}^* = 2.62$ and PV = 149 kPa (22 psia) for Extended Core Barrel Tests

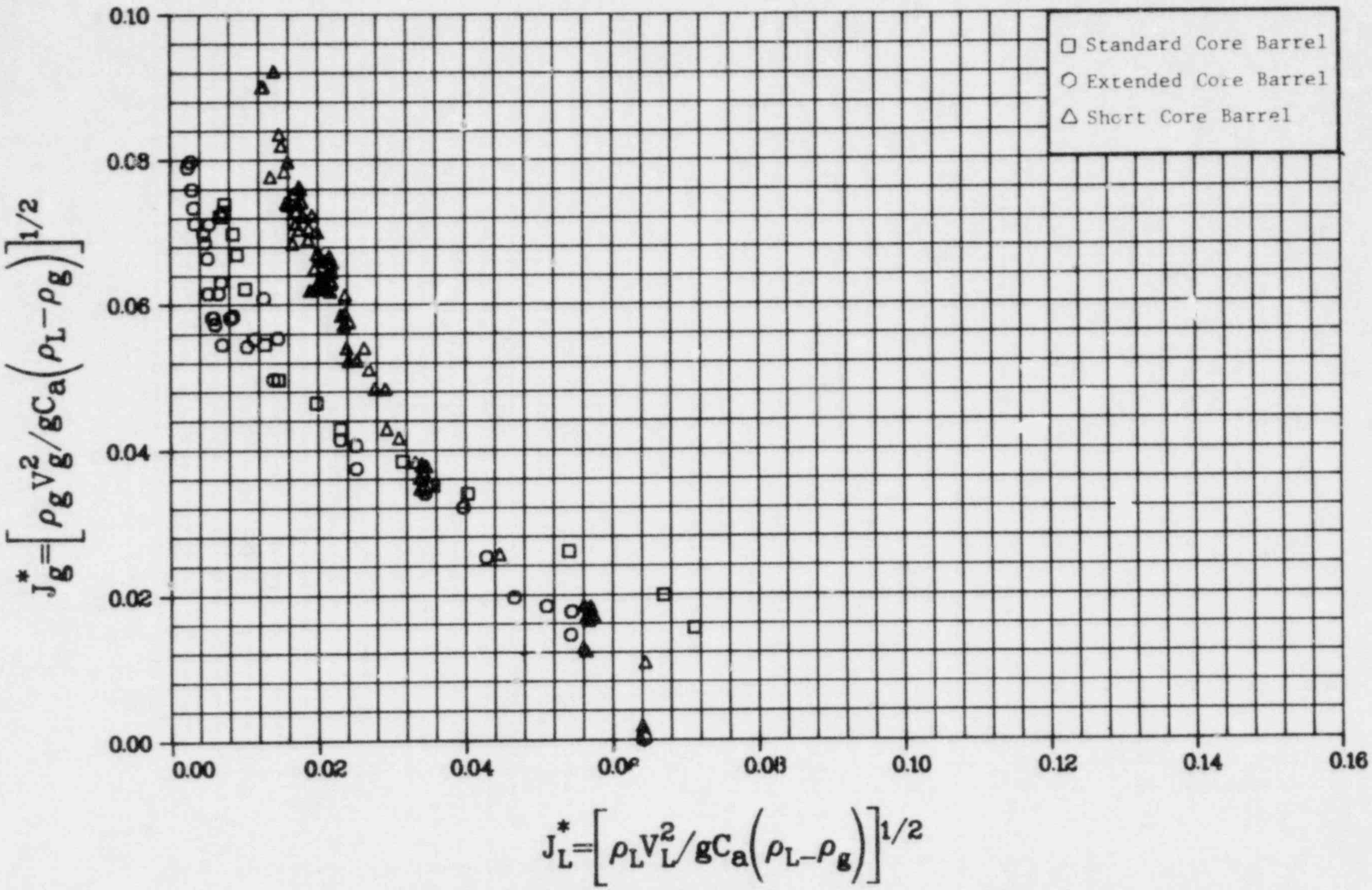

Figure 12. Comparison of Penetration Data from Standard, Extended and Short Core Barrel Tests for $J_{Lin}^* = 0.064$ and $T_{Lin} = 21$ C (70 F)

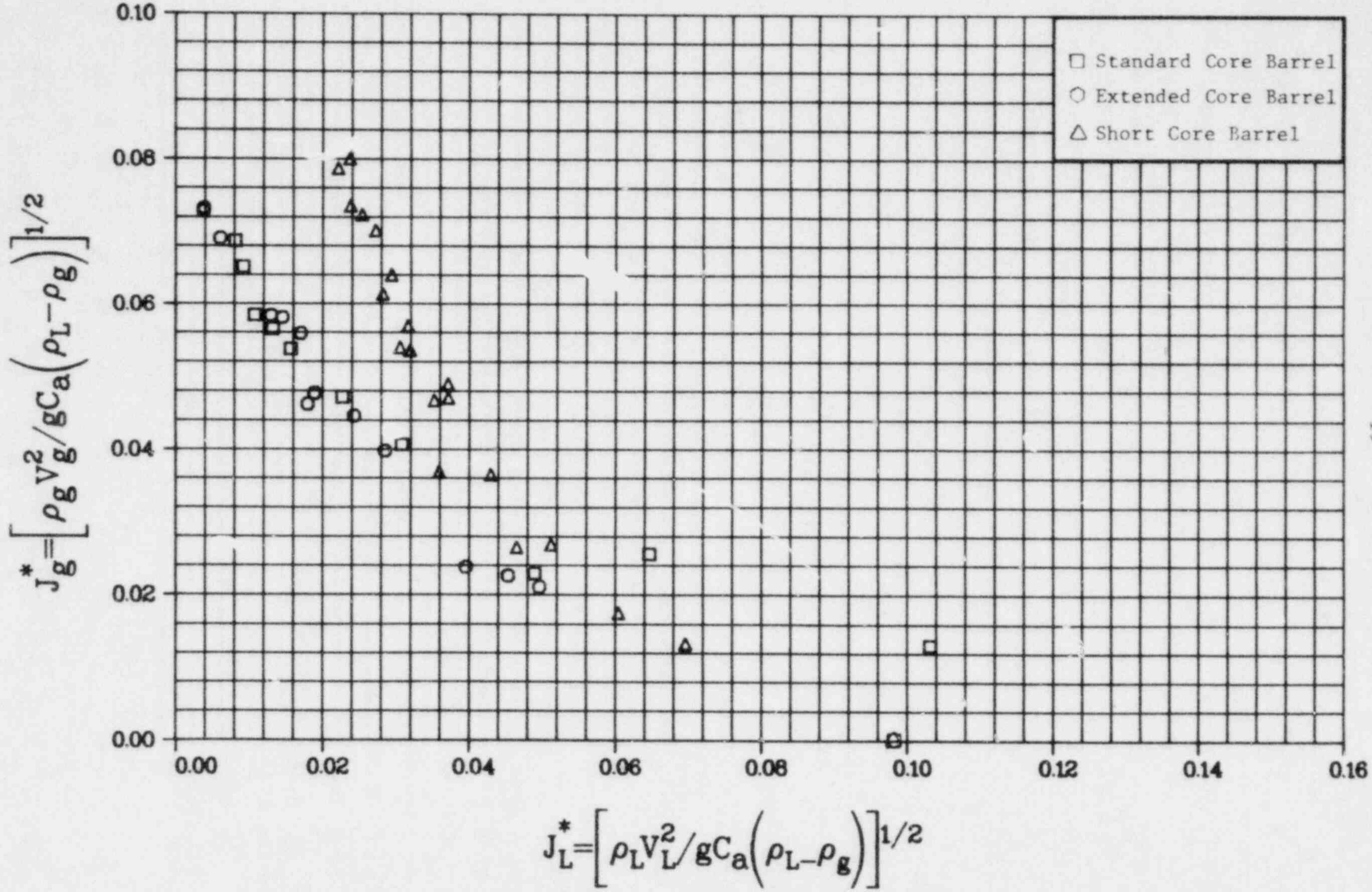

Figure 13. Comparison of Penetration Data from Standard, Extended and Short Core Barrel Tests for J^*_{Lin} = 0.098 and T_{Lin} = 21 C (70 F)

It seems clear that there is a definite effect of annulus length on flooding in the absence of condensation in the 2/15-scale model It is also clear that the effect becomes smaller as length increases. This is consistent with previous work in tubes[3,4] and small annuli[5]. Results of previous tests with steam-water in distorted 2/15-scale geometries indicate that the length effect is, if anything, more pronounced when condensation is present.

Correlation of Results. Test results were analyzed with the NLINMLE statistical program assuming a Wallis correlation form,

$$J_g^{*1/2} + mJ_L^{*1/2} = C \quad .$$

Results of some of the analyses are shown in Figures 14-20, in which data are plotted on $J_x^{*1/2}$ coordinates. These figures show that, at least over the range tested, the data are well represented by straight lines on square root coordinates. In Figure 19 for example, for liquid penetration rates ranging from less than 2% to more than 95% of the injected water flow rate the data are scattered uniformly about the best fit straight line. Similar results are seen in Figure 18 where penetration ranges from about 2% to about 90% of the injected liquid flow rate. No upward trend of the data is observed at the low penetration end of the curves.

Figures 14 through 17 present short core barrel data for three different injection flow rates. Slightly different values of the parameters m and C are obtained for these three figures since the short core barrel data show a dependence on injected liquid flow rate as illustrated in Figure 2. Extended core barrel data are shown in Figures 17 through 19 for three injected liquid temperatures. Again, slight variation in slope and intercept (m and C) are seen due to the dependence of long core barrel results on injected liquid temperature at higher penetration rates. Figure 20 presents standard core barrel data for comparison. Complete results of the statistical analysis are given in Table 4.

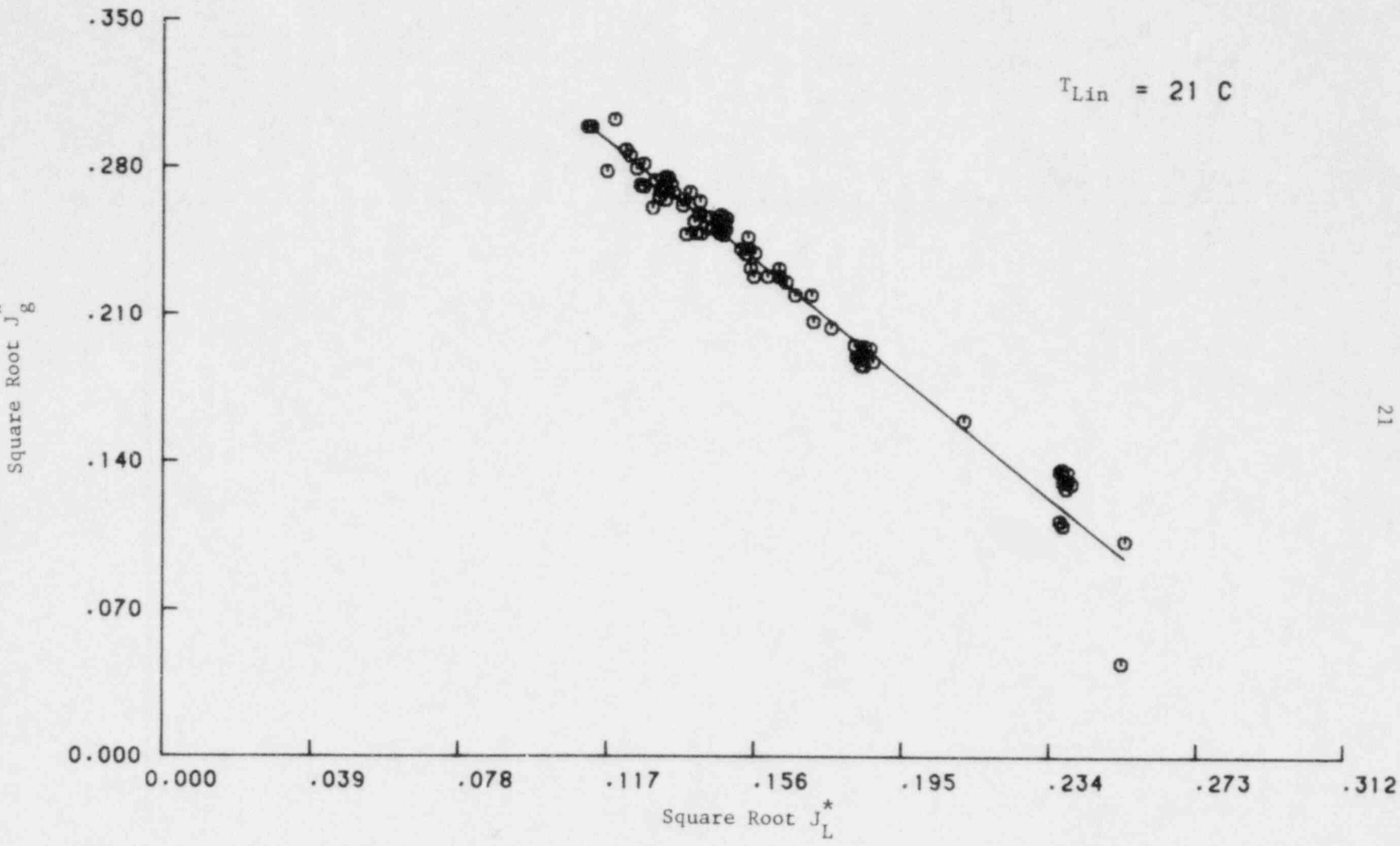

Figure 14. Penetration Data on Square Root Coordinates from Short Core Barrel Tests with J^*_{Lin} = 0.060 and T_{Lin} = 21°C

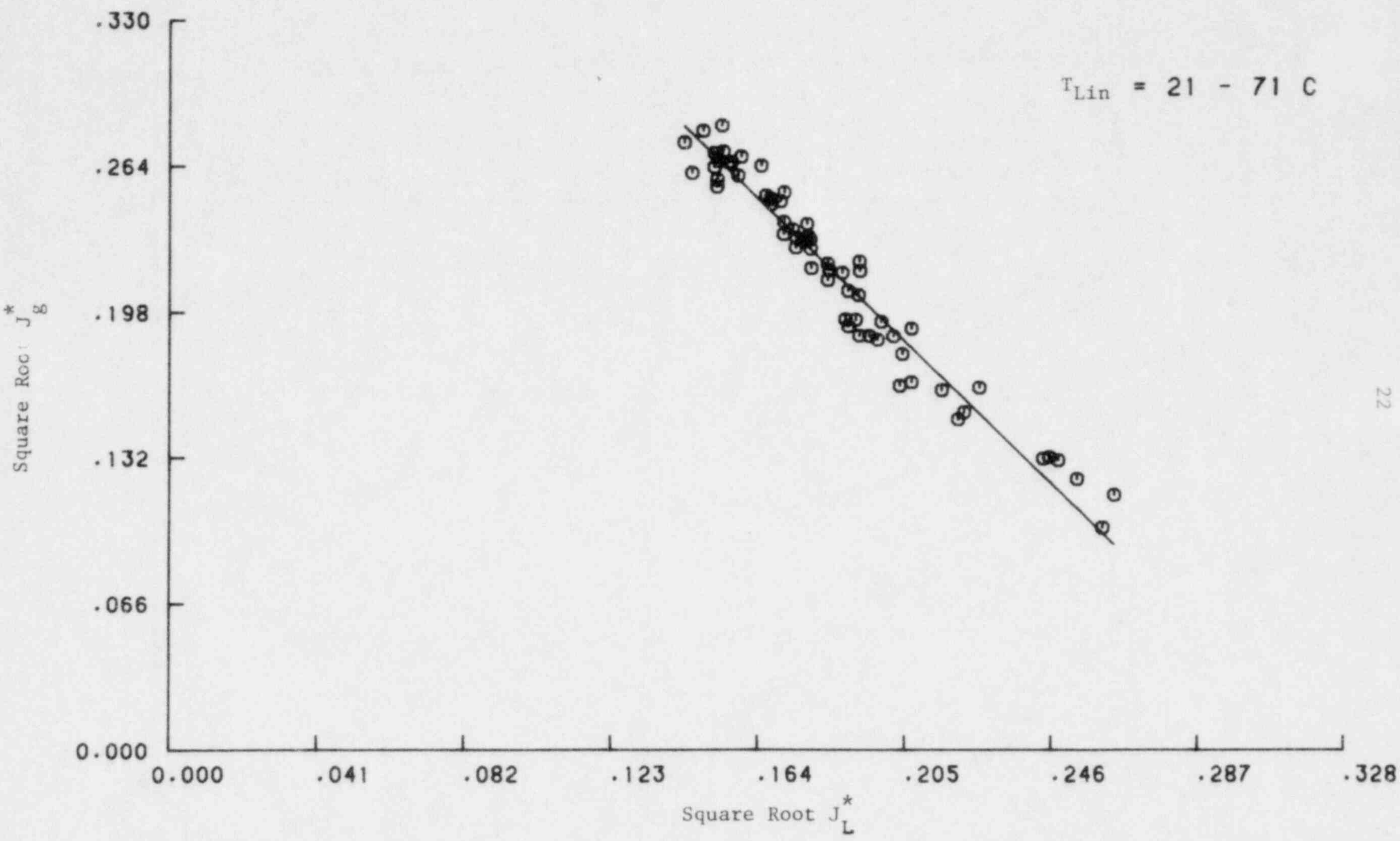

Figure 15. Penetration Data on Square Root Coordinates from Short Core Barrel Tests with $J_{Lin}^* = 0.098$ and $T_{Lin} = 21\text{-}71°C$

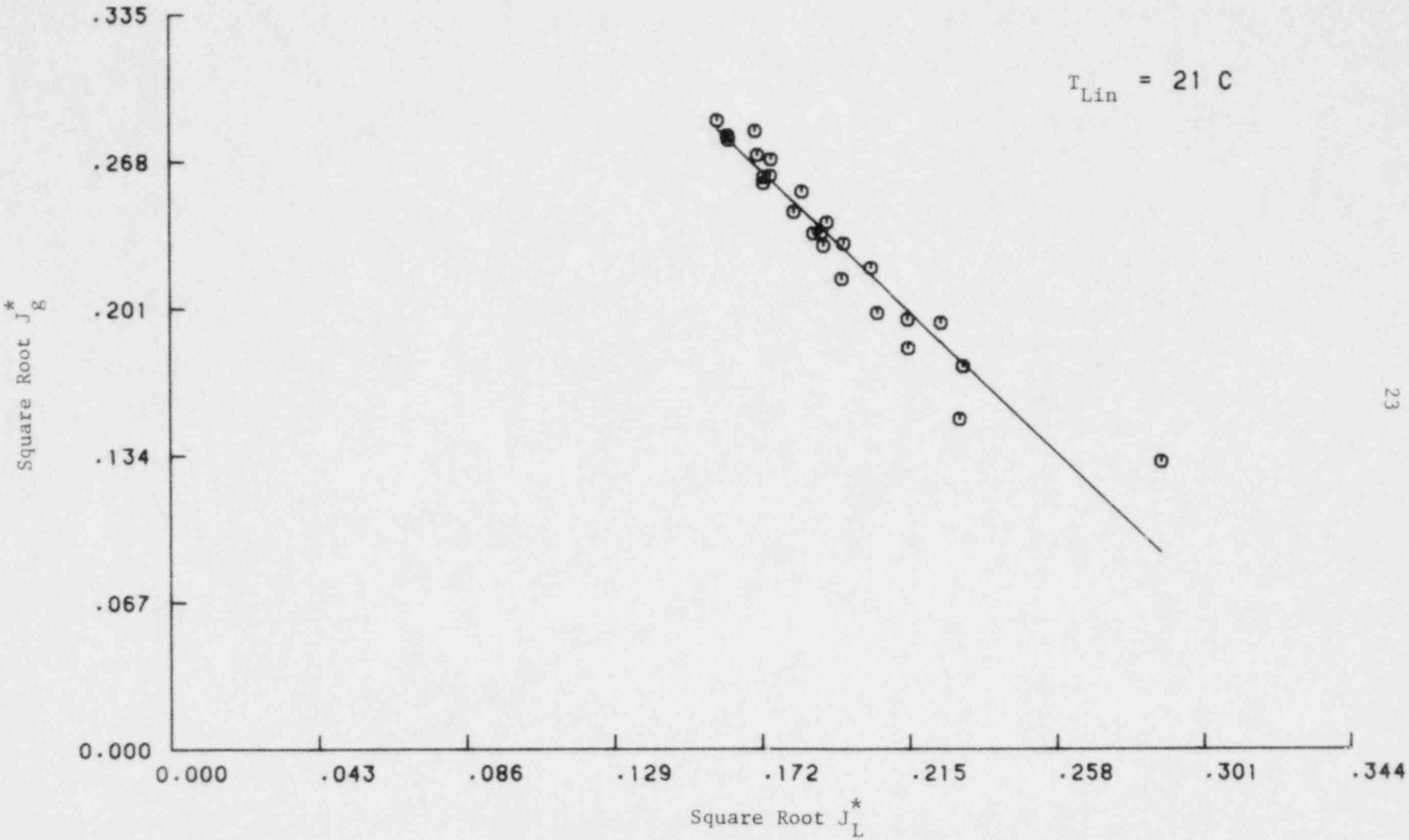

Figure 16. Penetration Data on Square Root Coordinates from Short Core Barrel Tests with J^*_{Lin} = 0.12 and T_{Lin} = 21°C

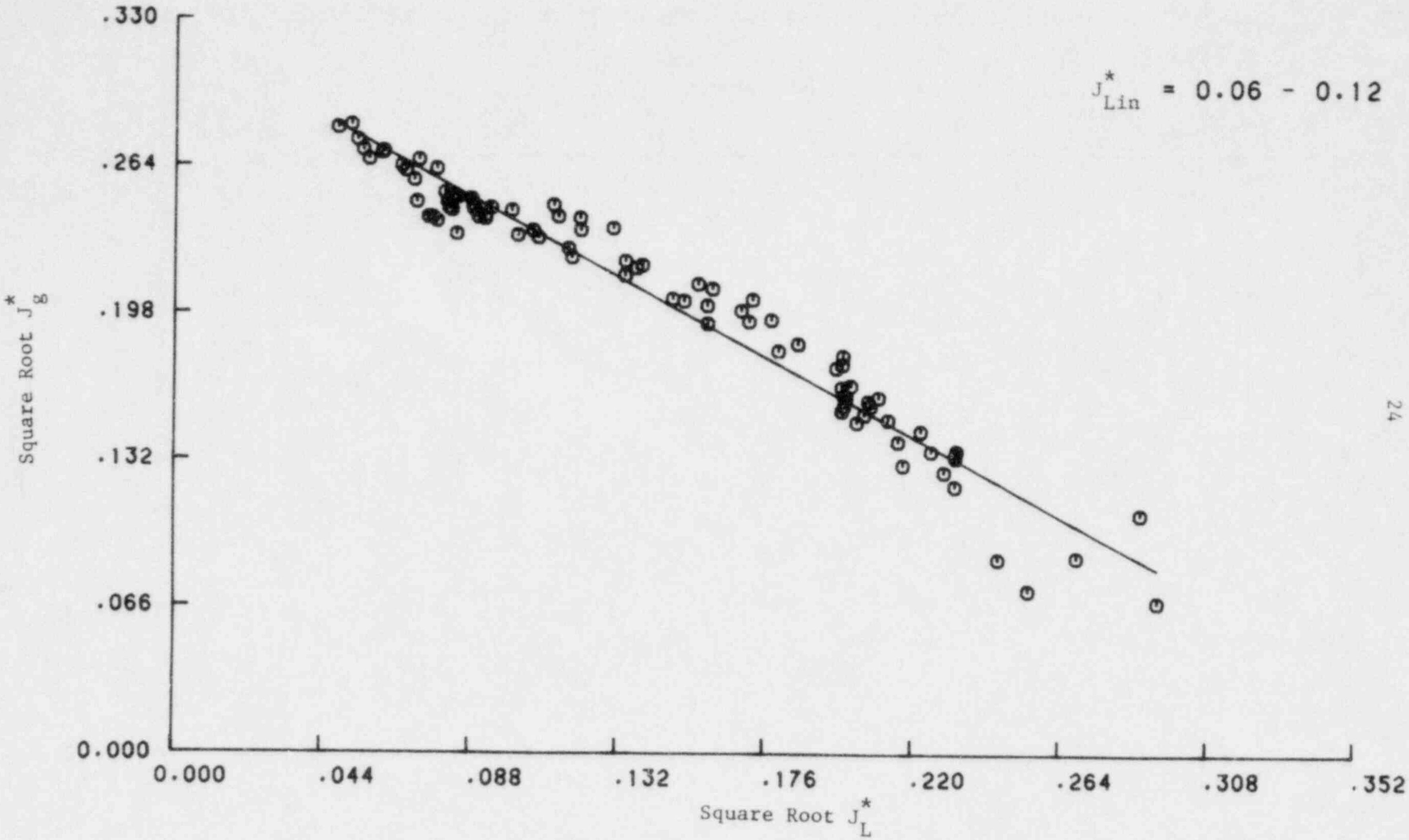

Figure 17. Penetration Data on Square Root Coordinates from Extended Core Barrel Tests with J_{Lin}^* = 0.06-0.12 and T_{Lin} = 21°C

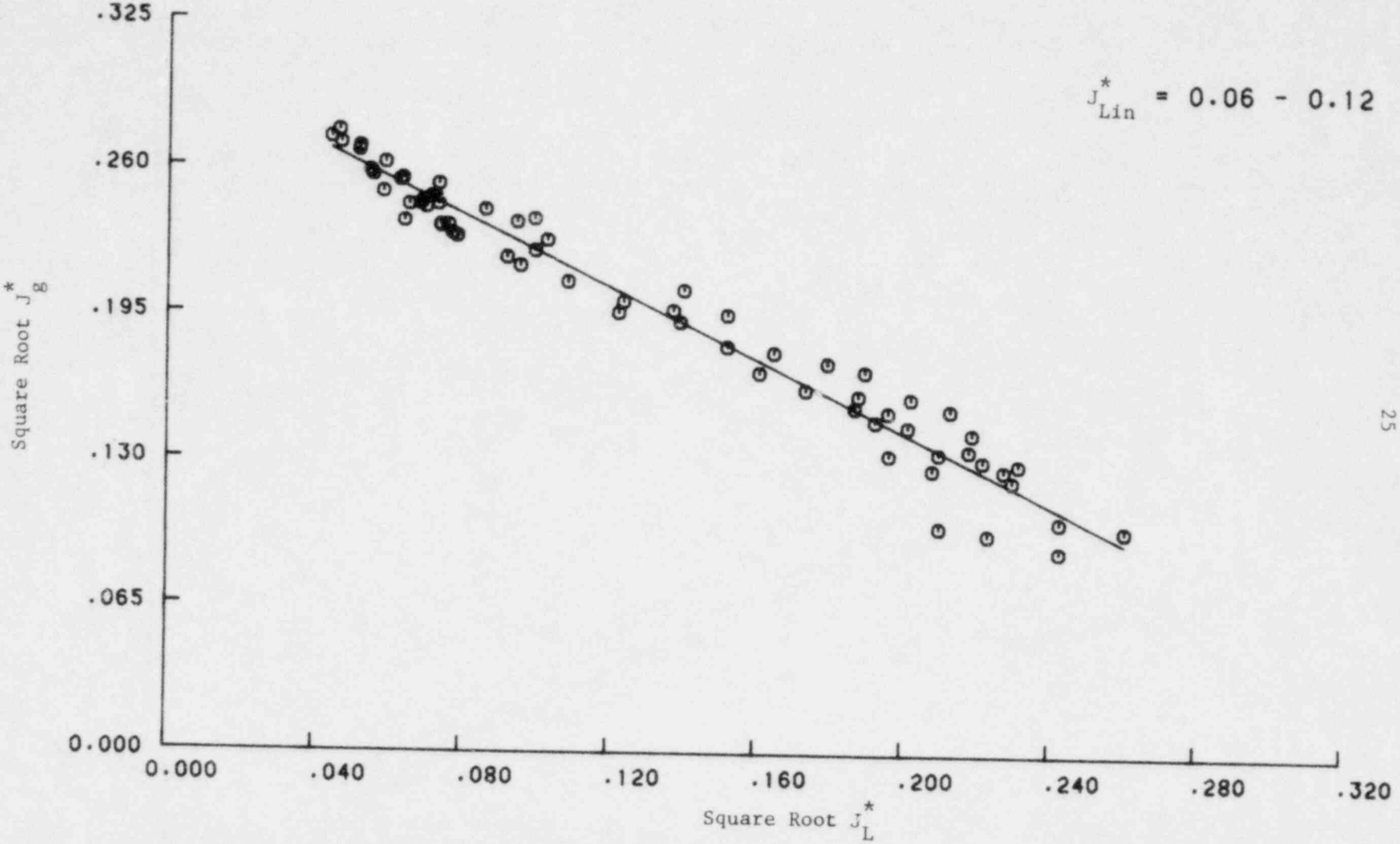

Figure 18. Penetration Data on Square Root Coordinates from Extended Core Barrel Tests with J^*_{Lin} = 0.06-0.12 and T_{Lin} = 74°C

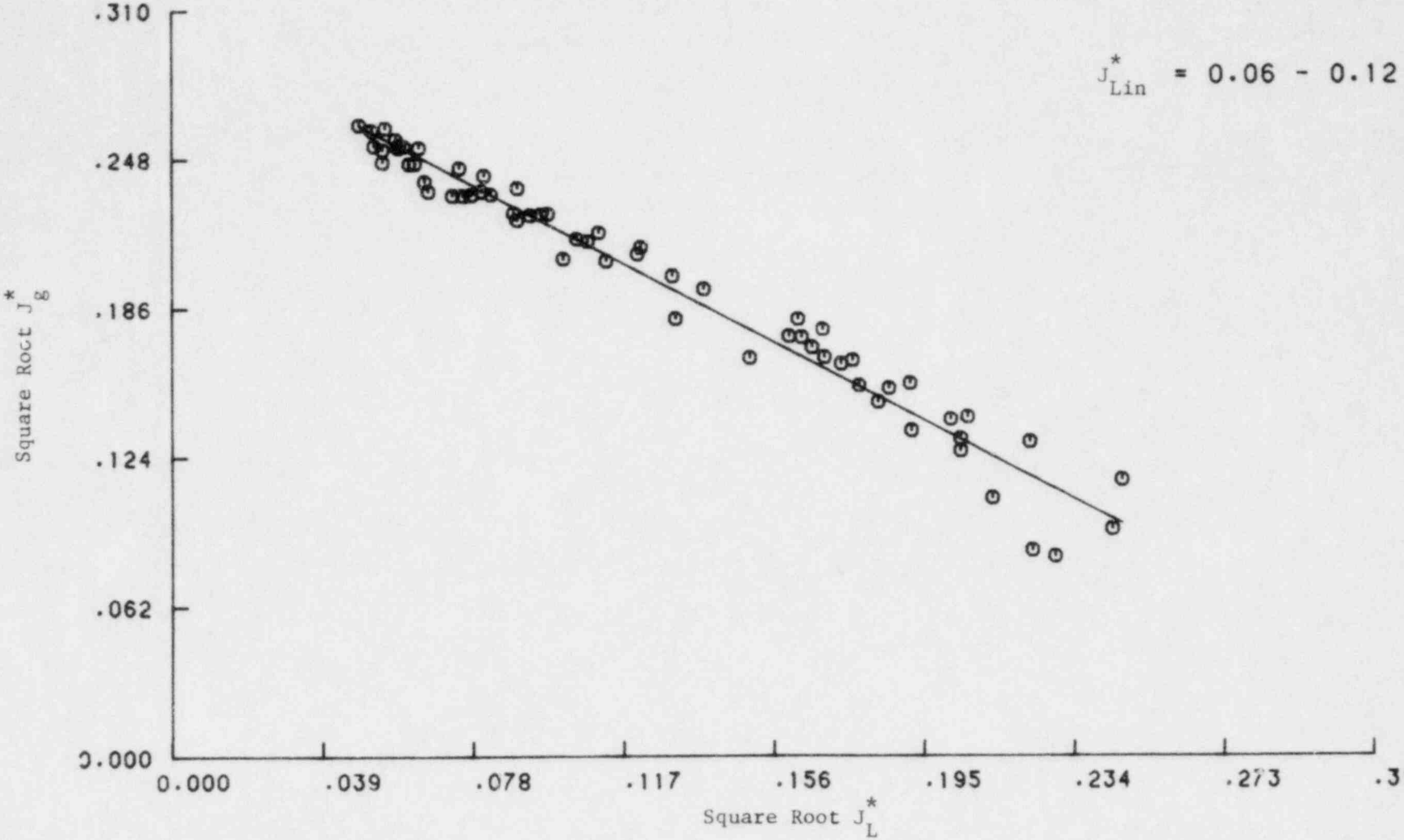

Figure 19. Penetration Data on Square Root Coordinates from Extended Core Barrel Tests with J_{Lin}^* = 0.06-0.12 and T_{Lin} = 96°C

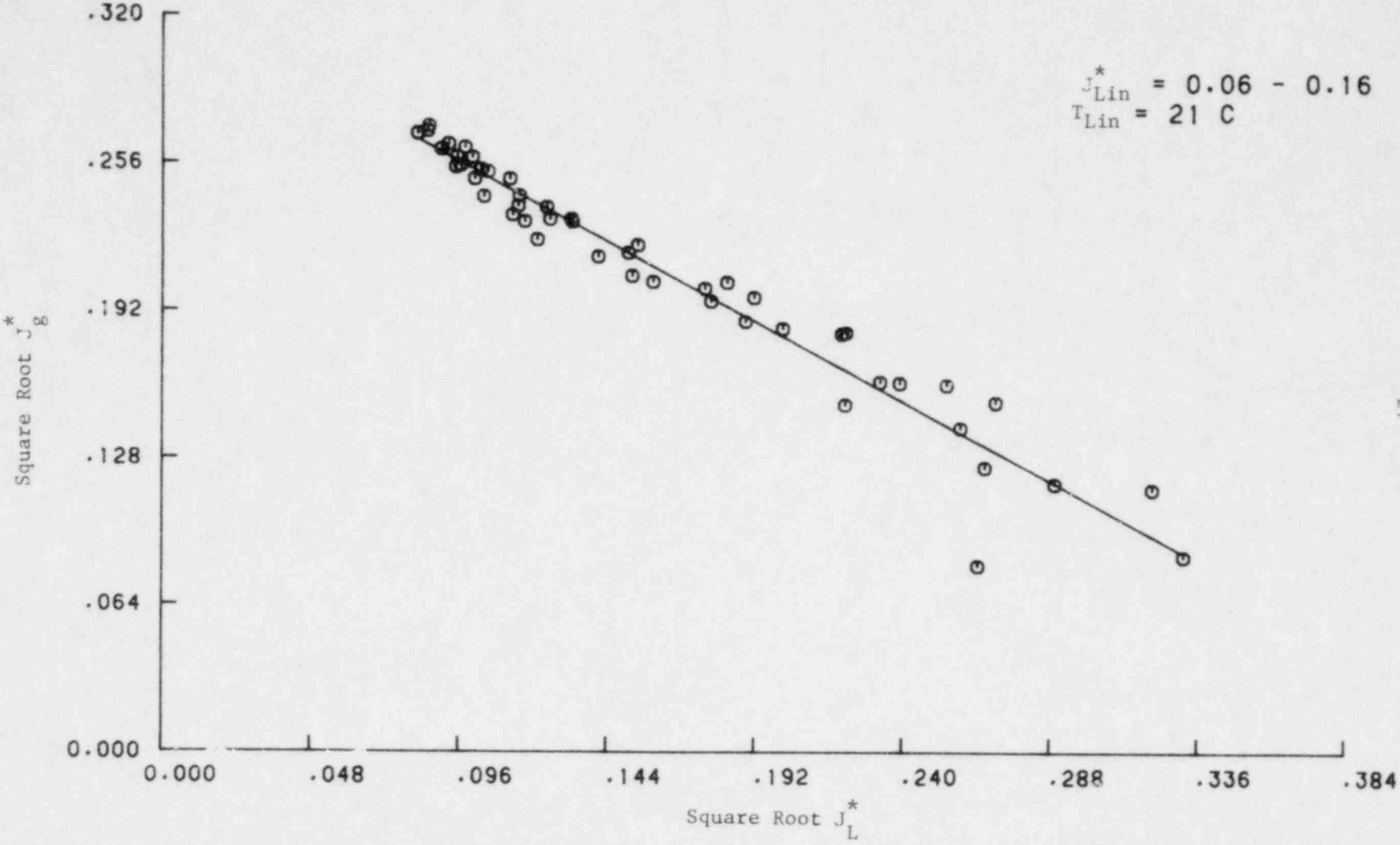

Figure 20. Penetration Data on Square Root Coordinates from Standard Core Barrel Tests with $J_{Lin}^* = 0.06\text{-}0.16$ and $T_{Lin} = 21°C$

TABLE 4. WALLIS CORRELATION OF AIR-WATER PENETRATION DATA FROM 2/15- SCALE DISTORTED GEOMETRY TESTS

Geometry	T_{Lin}, °C	J^*_{Lin}	m	C
SCB	21	0.06	1.448 ± 0.056	0.462 ± 0.009
"	21 - 71	0.098	1.574 ± 0.090	0.509 ± 0.017
"	21	0.12	1.494 ± 0.189	0.521 ± 0.037
ECB	21	0.06 - 0.12	0.813 ± 0.039	0.322 ± 0.006
"	74	0.06 - 0.12	0.800 ± 0.038	0.303 ± 0.006
"	96	0.06 - 0.12	0.837 ± 0.040	0.303 ± 0.006
STD	21	0.06 - 0.16	0.721 ± 0.049	0.326 ± 0.009

SCB - Shortened Core Barrel
ECB - Extended Core Barrel
STD - Standard Core Barrel

Summary. Air-water flooding tests have been conducted in the 2/15-scale model with shortened and extended core barrels for a range of injected water flow rates and temperatures. Short core barrel results show a dependence on injection rate but not on water temperature. Long core barrel results show the reverse, i.e., dependence on temperature but not on injection rate. Addition of water vapor to the air is suggested as a potentially important factor in the temperature dependence. For a given liquid injection flow rate and temperature there is a well defined effect of annulus length on penetration. Penetration decreases with increasing annulus length, for a fixed air flow rate. In general the data can be reasonably well correlated in the Wallis form, but the slope and intercept parameters, m and C, are not constant. Correlations for m and C are presented in Table 4.

Analysis of Countercurrent Flow Condensation Tests

Countercurrent flow condensation tests have been carried out in a rectangular test section. Data from those tests has been analyzed and is discussed more fully in Part II of this report.

Plans for Future Work

During the next quarter analysis effort will be concentrated on extension of the condensation/vaporization model to provide a mechanistic model for ECC penetration, and review of the data from the simple tube model.

TASK 2.0 EXPERIMENTAL TESTING AND DATA REDUCTION

Objectives

The objectives of this task are to:

(1) Provide experimental data on ECC penetration and lower plenum entrainment using scale models geometrically similar to a four-loop pressurized water reactor. These data should provide a base for establishing a better understanding of the bypass phenomenon in large-scale systems.

(2) Provide experimental data from small test facilities in support of analytical development programs.

(3) Provide lead-in information on steam-water interaction phenomena and operational information obtained in smaller scale models for future larger scale experiments.

Work During Quarter

The experimental testing carried out during this quarter consisted of studies in the heated flat plate model and in the 2/15-scale model with other than standard annulus lengths. Work was continued on the instrumented spool piece for the broken leg and on the instrumentation for determining liquid and vapor flow patterns in the annulus of the 2/15-scale model.

Heated Flat Plate Model

The experimental studies started last quarter were continued this quarter with tests run to determine the partitioning of heat initially stored in the model wall and to determine the effect of model inclination angle on steam condensation and liquid bypass.

In the heat partitioning studies the hot wall section of the model was heated to a uniform temperature significantly above the saturation temperature and the water flow was started. From the time of initiation of water flow until the surface of the plate cooled to below saturation, temperature, pressure and flow rate data were recorded using the high speed data acquisition system.

In the steam condensation studies the data obtained at a model inclination angle of 0.5 degrees was supplemented with data taken at inclination angles of 17 and 45 degrees from horizontal. A complete description of the experimental studies and the results are contained in Part II of this report.

2/15-Scale Model

In direct support of ongoing analytical development efforts at BCL, a series of air-water and steam-water studies were carried out in the 2/15-scale model with annulus lengths that were both shorter and longer than standard. The short annulus was 40% shorter than standard while the extended annulus was 60% longer. [illegible] tests were run with equilibrium walls and with data taken during plenum filling. The model was fitted with an oversized (8-inch diameter) simulated break leg. Table 5 shows the nominal operating conditions with the two annulus lengths. All tests were run using a range of air or steam flow rates to define the penetration curves as fully as possible.

Analyses of air-water data obtained with a standard length core barrel in the period July - September, 1978, showed a need for penetration data at air flow rates and consequently bypass rates above those obtainable with the BCL in-house air supply system. Additional air was obtained by supplementing the in-house system with a large portable air compressor leased from a local equipment rental company. With this system, essentially total bypass could be obtained at all ECC injection rates.

TABLE 5. NOMINAL OPERATING CONDITIONS FOR 2/15-SCALE MODEL DISTORTED ANNULUS LENGTH STUDIES

Test No.	Pressure, psia	Water Temperature, °F	Water Flow, gpm	J^*_{Lin}	Test Type	Annulus Length
1	15	70	250	0.064	Air-Water	Short
2			380	0.098		
3			475	0.122		
4		175	380	0.098		
5	30	130	380	0.098	Steam-Water	
6	15	70	250	0.064	Air-Water	Long
7			380	0.098		
8			475	0.122		
9		170	380	0.098		
10		70	125	0.032		
11			250	0.064		
12			380	0.098		
13			475	0.122		
14		170	125	0.032		
15			250	0.064		
16			380	0.098		
17			475	0.122		
18		210	125	0.032		
19			250	0.064		

TABLE 5. CONTINUED

Test No.	Pressure, psia	Water Temperature, °F	Water Flow, gpm	J^*_{Lin}	Test Type	Annulus Length
20	15	210	125	0.032	Air-Water	Long
21	↓	↓	475	0.122	↓	
22	30	80	250	0.064	Steam-Water	
23			380	0.098		
24		↓	475	0.122		
25		180	250	0.064		
26			380	0.098		
27	↓	↓	475	0.122	↓	↓

Table 6 shows the nominal operating conditions for the various air-water tests run with a standard annulus length and an oversized break leg

Other Work

Work on the void distribution measurement (VDM) system continued with fabrication of the high temperature probes that mount in the model annulus and initial checkout of the data acquisition system. For the instrumented spool piece, mounting adapters were fabricated and the additional channels in the data acquisition system that were installed earlier were activated and checked out.

Plans For Future Work

In the next quarter the instrumented spool piece and the annulus void distribution measurement system will become fully operational and model tests will be run. The purpose of these tests will be to obtain the additional fluid behavior data that these two instrument systems will provide.

TABLE 6. NOMINAL OPERATING CONDITIONS FOR 2/15-SCALE MODEL HIGH BYPASS AIR-WATER STUDIES

Test No.	Pressure, psia	Water Temperature °F	Water Flow Rate, gpm	J^*_{Lin}
1	15	75	250	0.064
2			380	0.098
3			475	0.122
4		135	250	0.064
5			380	0.098
6			475	0.122
7		210	250	0.064
8			380	0.098
9			475	0.122

TASK 3.0 RIL SUPPORT AND TECHNICAL ASSISTANCE

Objectives

The objectives of this task are to:

(1) Prepare a summary technical report, concentrating on scaling, in support of the Research Information Letter on ECC Bypass Research to be issued in FY '79,

(2) Participate in ECC Bypass Review Group activities as necessary during the program year, and

(3) Carry out additional technical support as necessary during the program year.

Work During Quarter

During this quarter BCL staff participated in an ECC Bypass Review Group meeting and reviewed draft material prepared for the Research Information Letter.

Plans for Future Work

We will participate in ECC Bypass Review Group meetings and carry out additional technical support as required.

TASK 4.0 ACQUISITION AND APPLICATION OF ADVANCED INSTRUMENTATION

Objectives

The objectives of this task are to:

(1) Modify the 2/15-scale test facility and install an instrumented spool piece to measure instantaneous two-phase flow conditions in the broken leg, and

(2) Modify the 2/15-scale test facility and install a system to measure void distribution in the annulus as a function of time.

Work During Quarter

The break leg spool piece was received from INEL and has been installed in the 2/15-scale facility. The spool piece instruments have been checked out and are in order. Assembly and shakedown of the VDM system continued.

Plans for Future Work

We now expect the VDM system to be completed the fourth quarter of this fiscal year. The break leg gamma densitometer is scheduled for completion and installation early in the fourth quarter. On completion of installation suitable tests will be carried out to measure break leg flows and annulus void distribution.

PART II

Steam Condensation on a Subcooled Film in Countercurrent Flow

STEAM CONDENSATION ON A SUBCOOLED FILM IN COUNTERCURRENT FLOW

by

Aryeh Segev

Abstract

To further the understanding of condensation effects on ECC penetration, an experimental study was conducted in a small test apparatus having a rectangular cross section. The main objective was to evaluate condensation heat transfer of saturated steam in direct contact with subcooled water films in countercurrent flow.

Tests were carried out for a range of steam and liquid injection flow rates and liquid temperatures for three different tube inclinations: 0.5° (nearly horizontal), 17°, and 45°.

Local condensation heat transfer coefficients were determined from liquid temperature measurements along the channel. Their dependence on local steam and water flow rates, liquid subcooling, and test section inclination angle was evaluated. The results were correlated in terms of local hydrodynamic and thermal conditions for the different wave structure regions observed experimentally.

In the inclined tube positions (17° and 45°), the local Nusselt Number (Nu) depends significantly on the local steam and liquid Reynolds Numbers (Re_g, Re_ℓ) and on the local liquid Prandtl Number (Pr) when no bypass occurs. In the bypass region, the Nusselt Number is almost independent of the steam flow rate and it drops sharply due to the strong effects of the reduced liquid flow rate as bypass increases. In the horizontal tube position it was found that up to a specific steam mass flow rate, the dependence of Nu on Re_g is very small, whereas for higher steam flow rates Nu is very sensitive to Re_g.

Tests with different inlet liquid temperatures have indicated a pronounced difference in the bypass mechanism. For highly subcooled inlet water, the bypass is controlled by waves which are initiated near the liquid outlet. For low inlet water subcooling, bypass is controlled by liquid sweepout which takes place near the liquid injector.

A correlation for the dimensionless surface temperature was also developed from which the condensation efficiency can be determined. This correlation will be incorporated into a one-dimensional analysis describing the downcomer behavior in scaled PWR models.

Introduction

Studies of the thermal-hydraulic behavior in the annulus of scale models of a pressurized water reactor (PWR) during a postulated loss-of-coolant accident (LOCA) have shown that steam condensation on the subcooled emergency core cooling (ECC) water has a significant effect on the rate at which the ECC water penetrates into the lower plenum of the pressure vessel[6,7]

Not a great deal is known about condensation of steam on subcooled water in countercurrent flows. The majority of work in this area has involved flows in small scale PWR models where the overall condensation efficiency, f, can only be estimated because of the complex hydrodynamic effects, such as surface wave development, instabilities leading to "bridging" and plug flow, entrainment and mixing. The condensation efficiency in these tests is defined so that $f = 1$ when the two countercurrent flows mix perfectly and achieve thermal equilibrium. The value for f is determined by a "best fit" approach to data from small scale models. In an effort to reduce the number of free parameters in the "best fit" correlations, Segev and Collier [8] have developed a one-dimensional model from which they showed that f is essentially a dimensionless temperature at the end of the core barrel which may be evaluated for adiabatic walls if the condensation heat transfer coefficient in countercurrent flow is known. Due to the lack of experimental data for condensation in countercurrent flow, they used the heat transfer correlation developed by Lee et al[9] for cocurrent flow in a rectangular horizontal channel. The theoretical predictions of the one-dimensional model agreed fairly well with experimental ECC penetration data taken in small scale reactor models.

To further the understanding of condensation effects on ECC penetration, an experimental study has been conducted in a small test apparatus having a rectangular cross section. The main objective of the study was to evaluate the condensation heat transfer of saturated steam in direct contact with the subcooled water in countercurrent flow. The dependence on steam and water flow rates, the degree of subcooling, and test section inclination angle were all studied.

Experiment

A schematic diagram of the experimental test section is shown in Figure 21. Saturated steam and subcooled liquid flow countercurrently through a rectangular cross section, 106.6 cm (42 inches) long and 15.2 cm (6 inches) wide. The channel height may be adjusted by moving the top plate, allowing operation at any desired gap height up to 15.2 cm (6 inches). Preliminary experiments with 2.5 cm (1.0 inch) gap height resulted in severe liquid oscillations due to liquid bridging over the gap. The present experiments have been conducted with a 5.1 cm (2.0 inc' g-r, which eliminated any bridging and consequent oscillations.

The test section is constructed of aluminum except for the sides which are formed from polished Pyrex glass. This makes possible visual observation and photography of flow behavior. The bottom plate is 1.3 cm (0.5 inch) thick with a 45.7 cm (18 inches) long, 7.6 cm (3 inches) thick section, which may be used for heat storage in non-adiabatic studies. To d te, all condensation experiments have been conducted with adiabatic walls. Heat losses were minimized by 3.8 cm (1.5 inches) thick fiber glass insulation.

To provide a uniform flow into the test section, steam is supplied through an inlet plenum chamber and a perforated plate as shown in Figure 21. A second plenum chamber is fitted to the test section at the steam outlet region to minimize additional steam condensation on the bypass water. Inlet and outlet volumetric steam flow rates were measured with turbine flow meters.

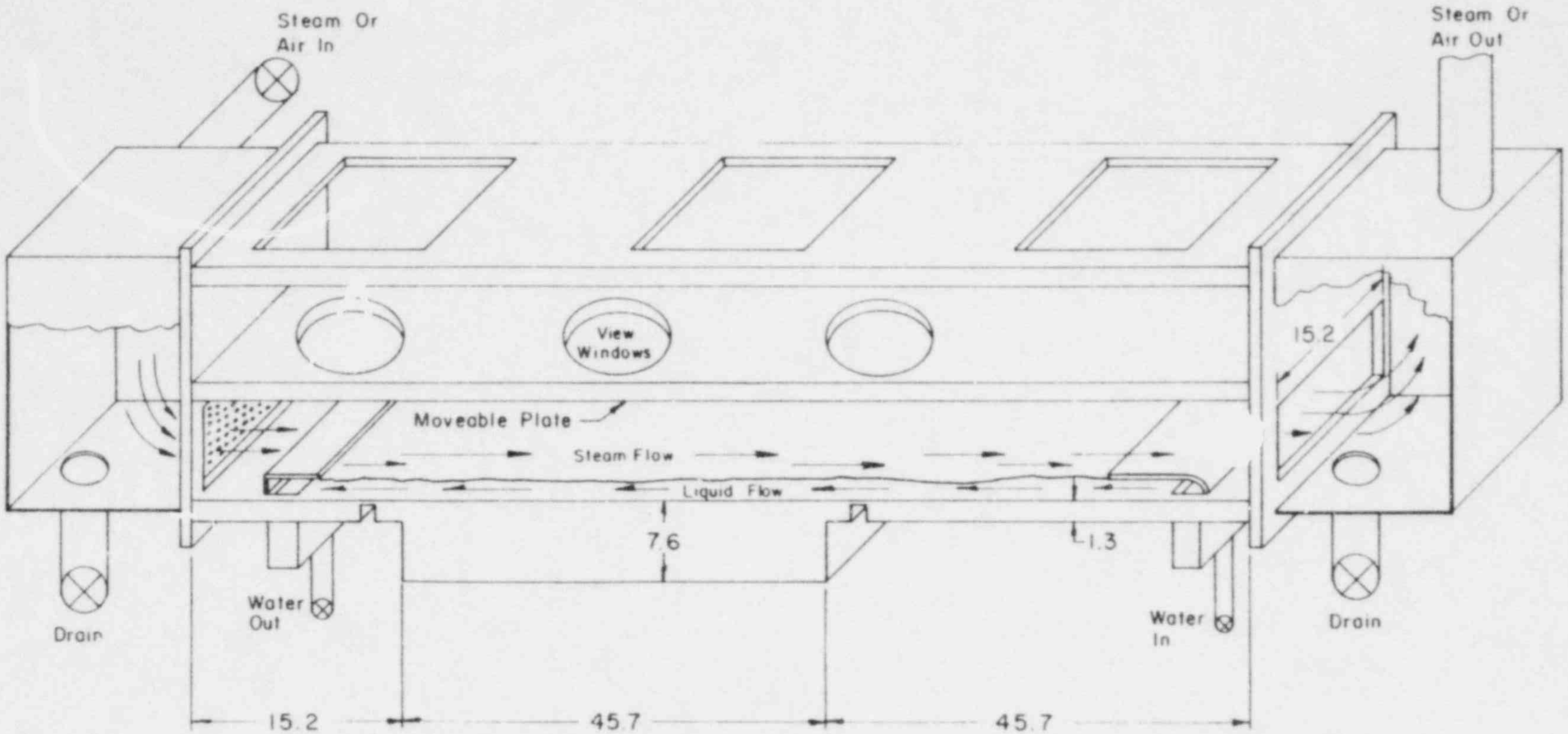

Figure 21. Schematic Di.gram of Experimental Test Section
(all measurements are in cm)

Liquid flow is introduced to the test section through an adjustable inlet port which spans the test section width. The height of the port above the plate is adjustable to provide a smooth liquid film at the entrance region. The inlet liquid volumetric flow rate is measured with a turbine flow meter. Liquid exits the test section through a similar adjustable outlet port into a tank. The weight of the tank is monitored by a load cell, from which the outlet liquid mass flow rate is determined. The height of the outlet port is adjusted to minimize interference with the inlet steam flow.

The test section is mounted such that it can be positioned at any inclination from horizontal to vertical. In the present study, the various inclinations were: 0.5° (nearly horizontal), 17°, and 45°.

Twelve thermocouples are used to monitor the liquid and solid temperatures inside the test section. A schematic sketch of their location along the centerline is shown in Figure 22. Six thermocouples are imbedded in the solid surface at various axial locations, 1.6 mm (1/16 inch) from the solid-liquid interface. Liquid temperatures are measured along the test section by six thermocouples, four of which are mounted in the top plate and two in the bottom plate. In most cases the temperatures measured by thermocouples situated in the liquid film are quite similar to the surface temperatures. However, when large waves are generated at the interface or when significant reduction in film thickness occurs, the liquid thermocouples are occasionally situated in the steam, resulting in higher temperature readings. Measurements also have shown that the local temperature gradient in the direction normal to the flow is almost zero, except very near the steam-water interface, where temperatures drop from saturated to the average film temperature over a thin layer.

Liquid film thickness is measured by micrometer-mounted conductivity contact probes located immediately upstream and downstream of the thick section. These measurements were conducted when only liquid was flowing in the test section. The average thickness along the film was correlated as a function of liquid flow rate.

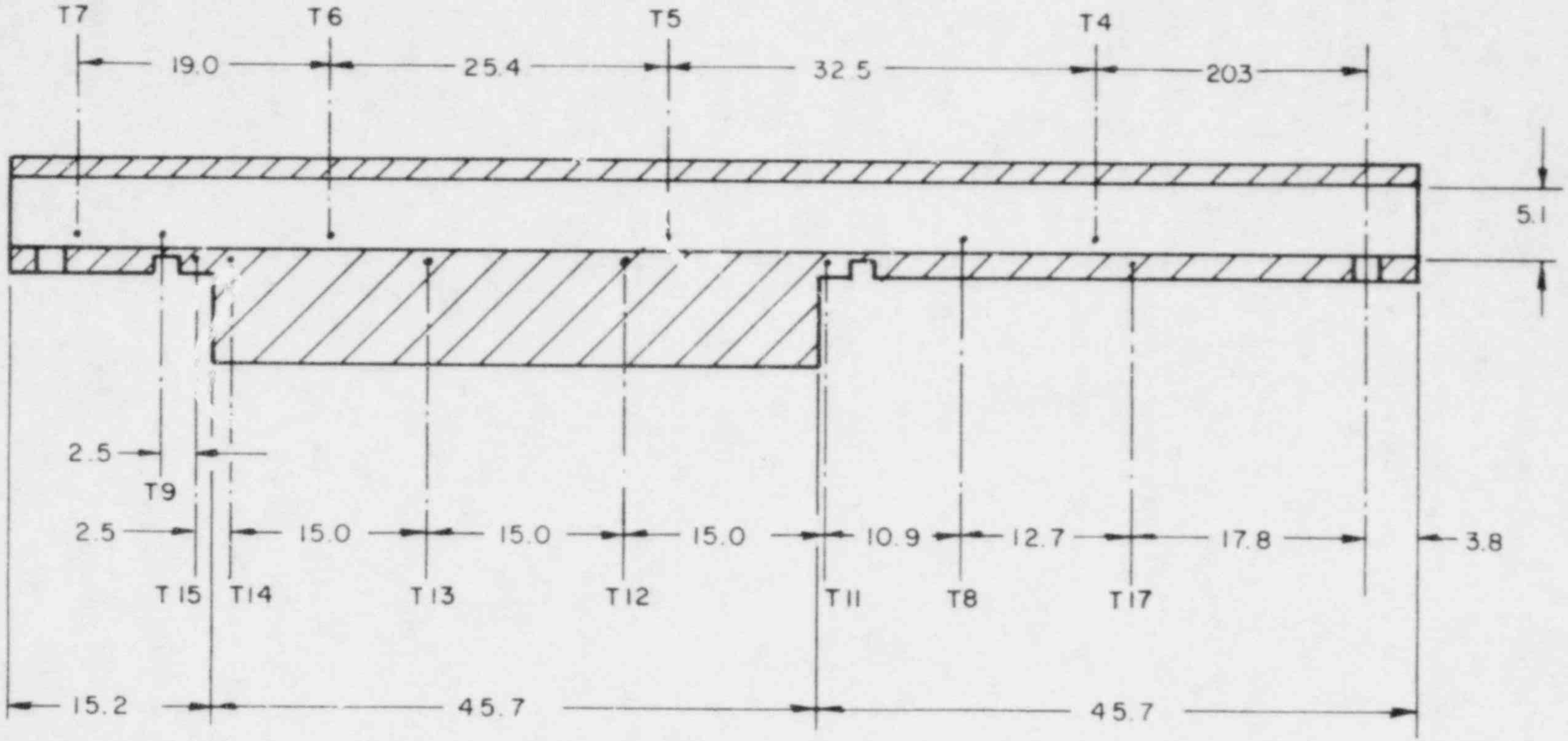

Figure 22. Schematic Sketch of Thermocouple Locations
(all measurements are in cm)

All measurements, other than film thickness, are recorded on magnetic tape every 20 msec by a minicomputer-based data acquisition system. The data are further processed on the in-house CDC computer.

Each test was conducted as follows: a predetermined liquid flow was introduced into the test section. Adjustments of the inlet and outlet ports were conducted to produce a smooth liquid film. Film thicknesses were measured and recorded. Steam flow was then introduced into the test section and was increased in small steps. For each steam flow rate the liquid drain valve, which is situated between the outlet port and the weigh tank, was adjusted to minimize the escape of steam through the liquid drain line. When liquid and adjacent wall thermocouples indicated a steady-state situation, measurements were recorded for 30 seconds. It should be noted that measurements were not taken for conditions in which the entire steam flow was completely condensed on the film. This was done to avoid uncertainties related to temperature profile evaluation.

Results

Visual observations of the flow pattern in the test section revealed that the interface between the steam and the countercurrent liquid film is characterized by the presence of wavelike disturbances. Depending mainly on the tube inclination and steam flow rate the following interfacial conditions could be observed:

1) Smooth Interface - at very low steam flow rates and with an inclined test section (17° and 45°) the interface remained practically smooth. This condition corresponds to complete condensation of steam on the lower portion of the liquid film. No measurements were taken at these low flow rates.

2) Two-Dimensional Waves - in the horizontal and inclined positions an increase of steam flow resulted in the appearance of waves which extended over the entire channel width.

3) Three-Dimensional Waves - as the steam flow was increased, three-dimensional waves were generated, giving the surface a pebbled appearance.

4) Roll Waves - at relatively high steam flow rates larger amplitude waves were generated, travelling upstream on the liquid film surface. The distance of travel depends on the steam flow rate. When the waves reach the liquid inlet injector, partial bypass occurs. At even higher steam flow rates the amplitude of a wave is increased as it travels upstream, causing complete bypass, which results in drying of the lower part of the channel and liquid circulation from the liquid injector toward the steam outlet region.

Based on the observed wave modes and the consequent heat transfer characteristics, we can define three regions which depend on the inlet steam flow rate. The range of steam flow rates which resulted in two-dimensional waves is defined as Region A. Region B includes those steam flow rates which resulted in three-dimensional waves or roll waves with complete liquid penetration. Region C covers steam flow rates which caused partial or complete bypass. Temperature measurements, and as shown below, the heat transfer coefficients are well correlated with the different regions. Figures 23-25 show typical surface temperatures as functions of inlet steam flow rate for different test section positions. The inlet liquid flow rate in those figures is 0.32 kg/s and the inlet liquid temperature is 23°C. Figure 26 describes the penetration curves for the different test section inclinations, in which the dimensionless fractional penetration rate, W_p^*, is defined as the ratio between the penetrating liquid flow rate, $W_\ell(L)$, and the injected liquid flow rate, $W_{\ell in}$.

In general, the local temperatures depend on the steam and liquid flow rates, the degree of subcooling and the test section inclination. As shown in Figure 23, the temperature profile in the horizontal position is rather uniform along the plate at low inlet steam flow rates (up to $W_g(L) \approx 0.029$ kg/s) and the temperature level is relatively low (Region A). In Region B, there is a temperature increase along the plate. This region corresponds to a uniform pebbled interface with complete penetration. At $W_g(L) \approx 0.045$ kg/s large amplitude roll waves are generated with a consequent partial bypass (Region C). This results in a reduction of liquid penetration flow rate and subsequent increase of liquid temperatures. At this point, only

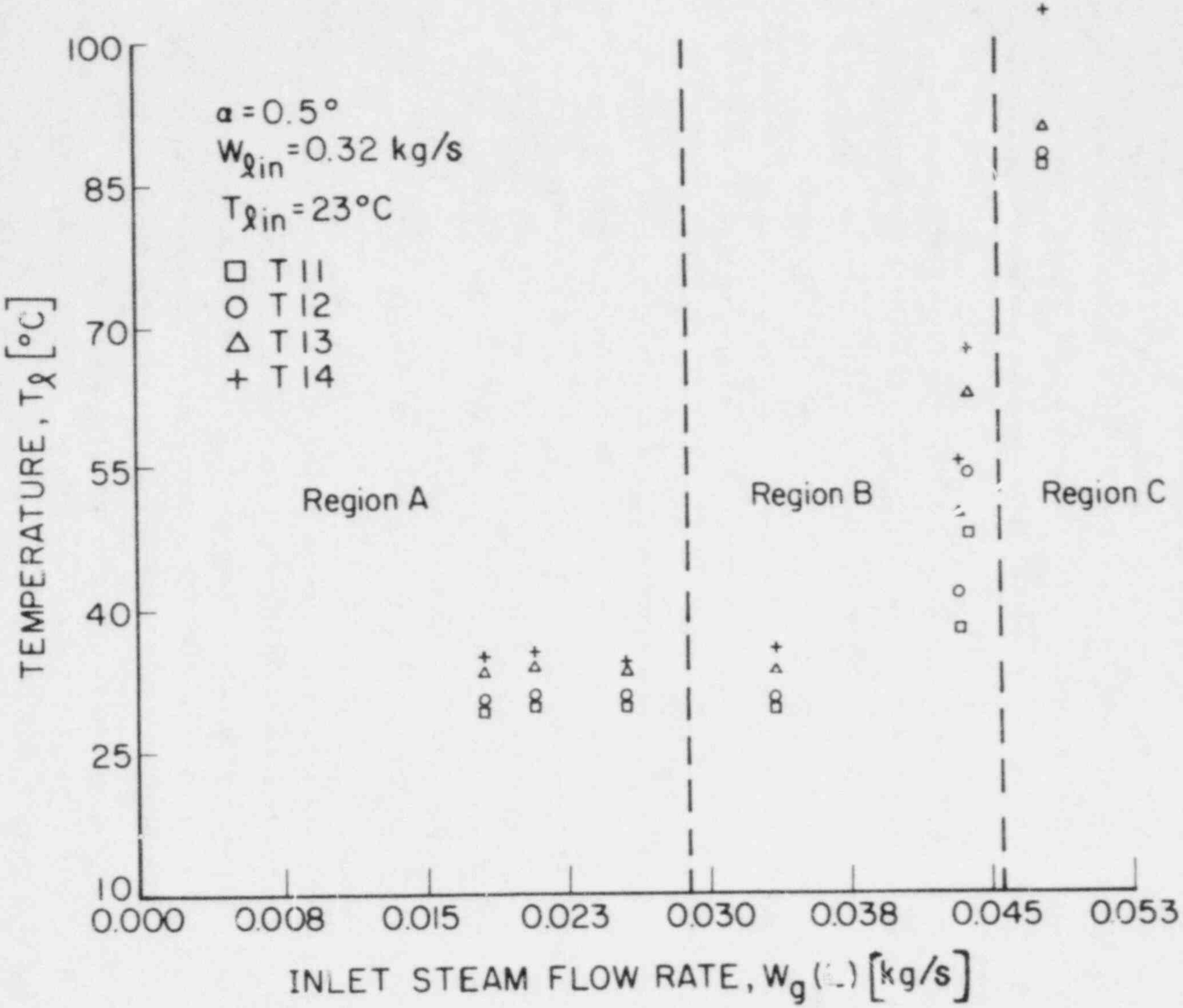

Figure 23. Liquid Temperatures for α = 0.5° and $W_{\ell in}$ = 0.32 kg/s

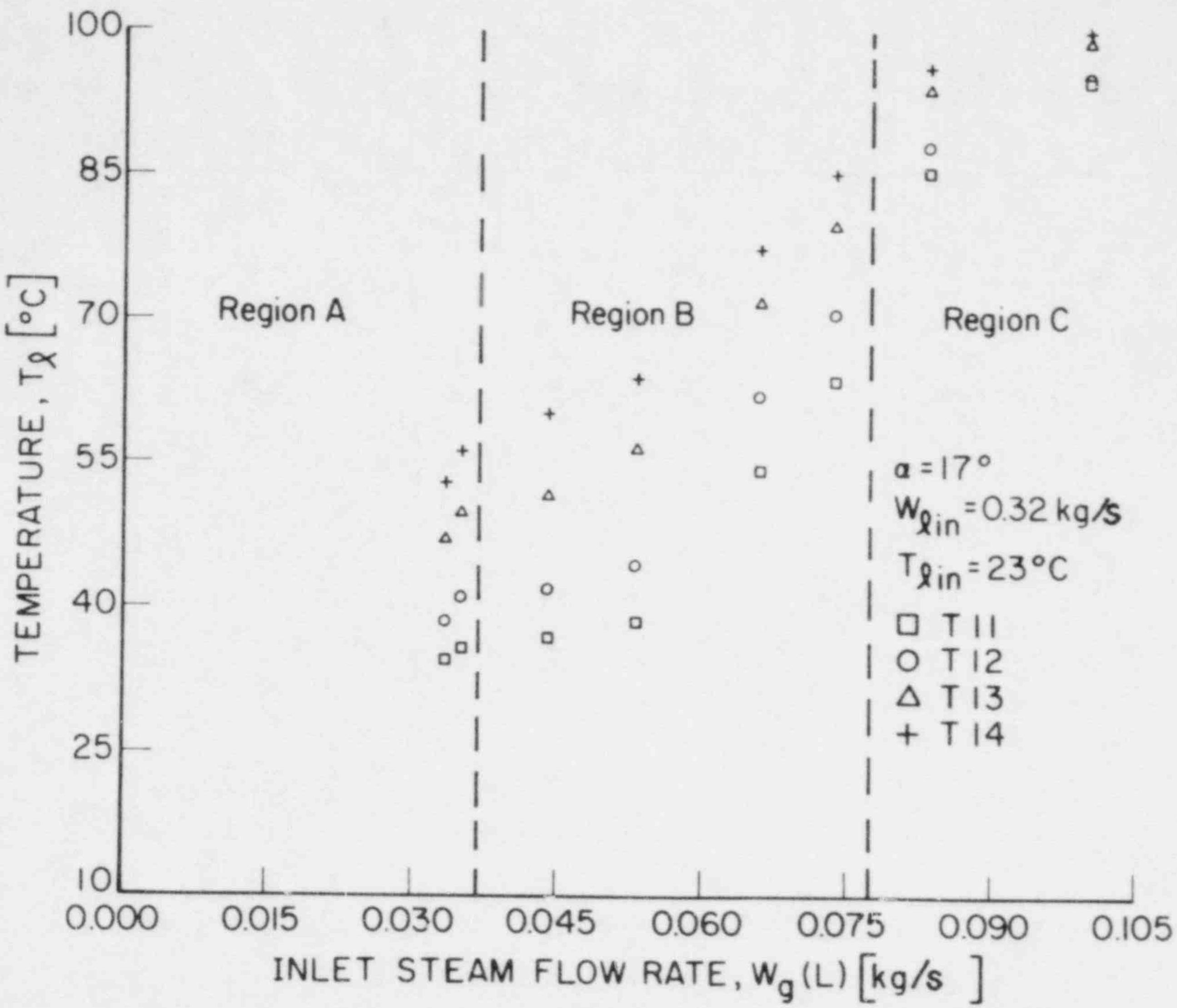

Figure 24. Liquid Temperatures for α = 17° and $W_{\ell in}$ = 0.32 kg/s

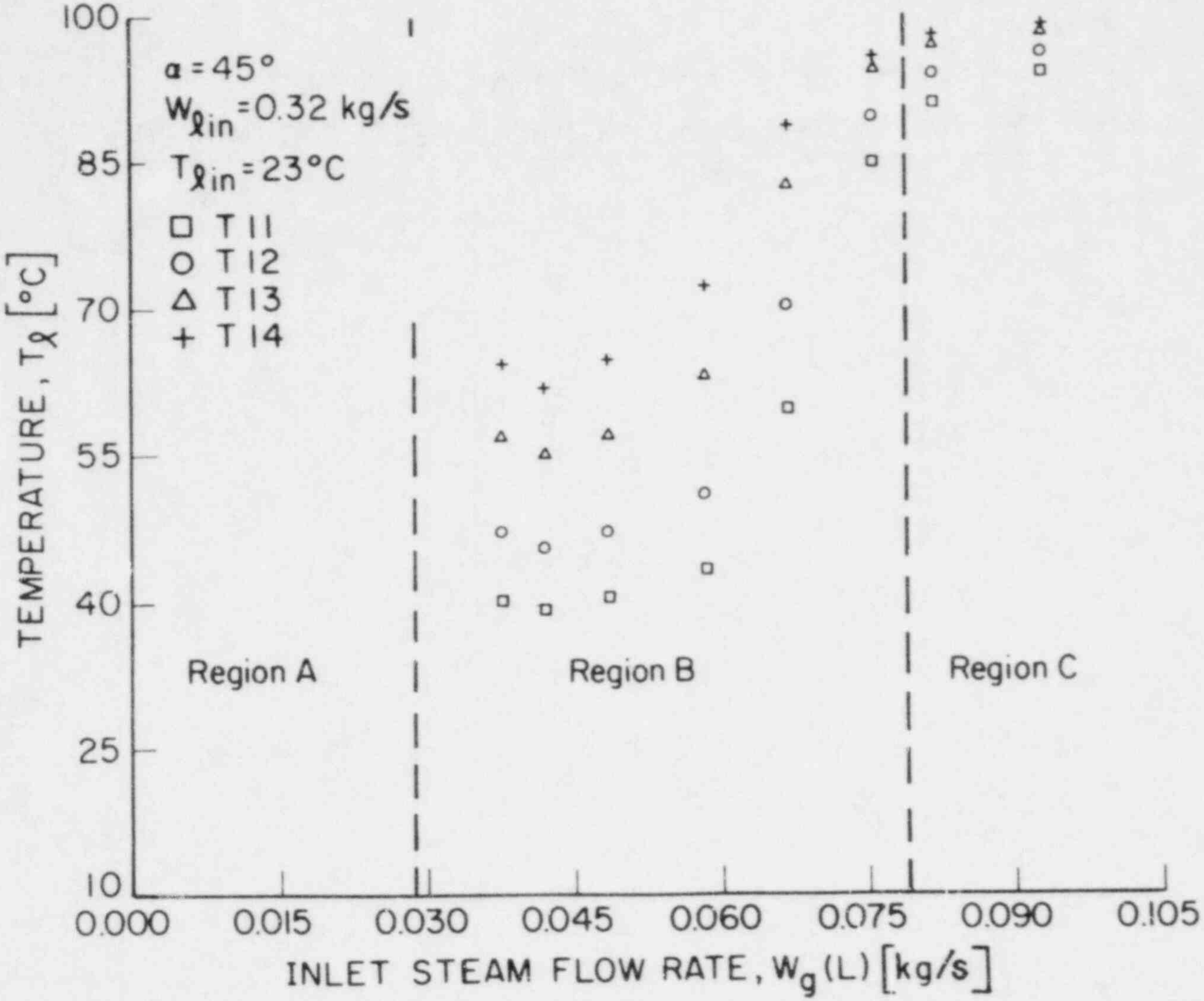

Figure 25. Liquid Temperatures for α = 45° and $W_{\ell in}$ = 0.32 kg/s

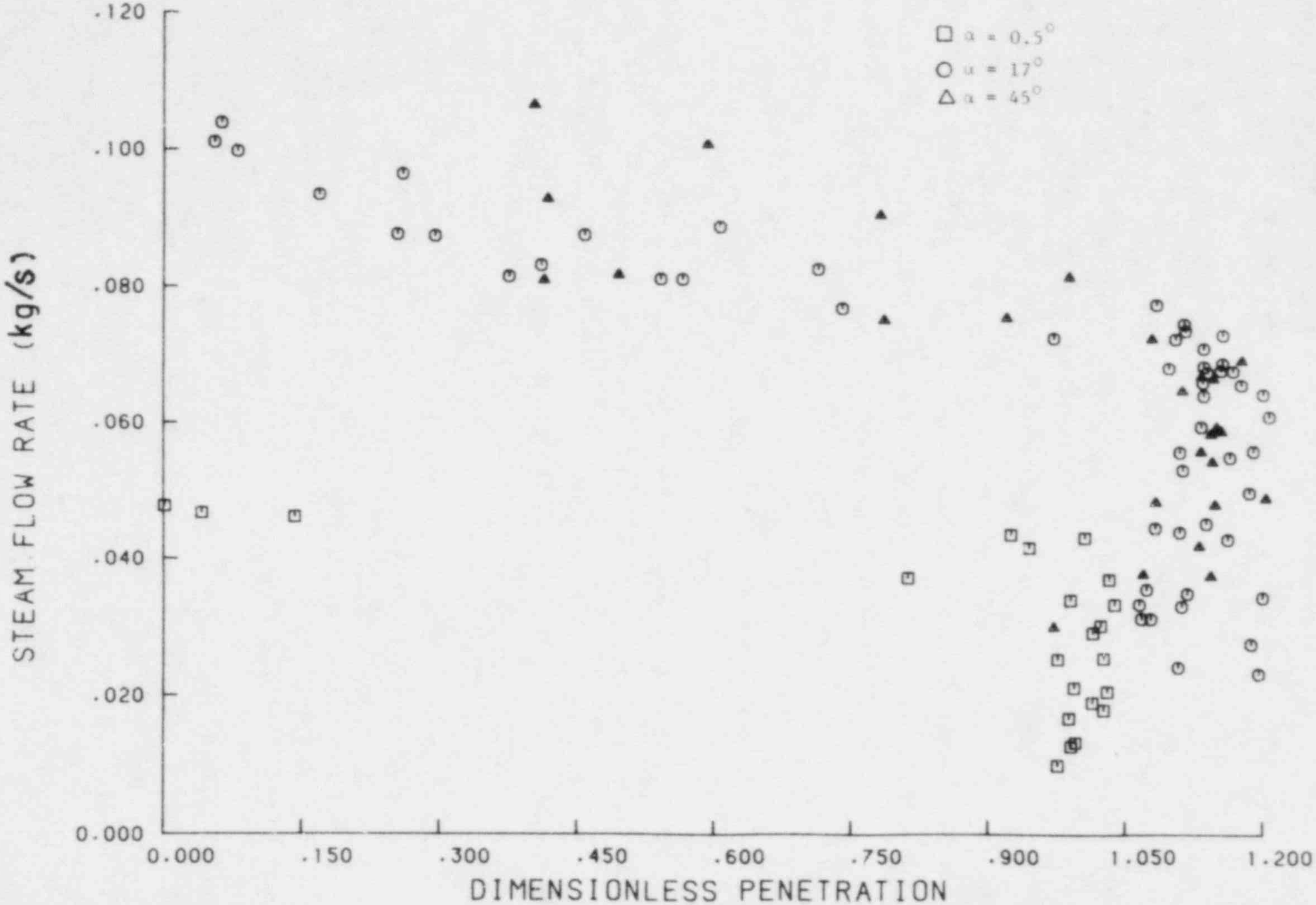

Figure 26. Liquid Penetration for Different Test Section Inclination

a slight additional increase in steam flow results in complete bypass and a sharp increase in film temperature. This last region is very sensitive to test parameters and requires a relatively longer time to reach a steady state.

When the tube inclination is increased to 17° or 45°, and the injected liquid mass flow rate remains constant, the liquid velocity increases, with an equivalent decrease in film thickness. Thus, substantially higher steam flows are required to generate flow patterns similar to those of the horizontal position. Two-dimensional waves were observed for steam flow rates up to $W_g(L) \approx 0.037$ kg/s, resulting in relatively low liquid temperatures, which are almost independent of steam flow. As $W_g(L)$ exceeds about 0.037 kg/s a pebbled interface appears with small consequent increase in film temperatures. However, a sharp increase in temperature is noticed when $W_g(L) \approx 0.077$ kg/s, which is the result of liquid bypass.

Evaluation of Heat Transfer Coefficient

For a turbulent liquid film we assume that the major heat transfer occurs through a thin layer at the liquid-vapor interface so the temperature profile across the body of the film is uniform and the bulk liquid temperature changes only in the flow direction. The resultant mass and energy equations for a time independent flow are:

$$dW_\ell = dW_c \tag{9}$$

$$\frac{d}{dz}(W_\ell h_\ell) = \frac{d}{dz}(W_c h_g) \tag{10}$$

where W_ℓ and W_c are the liquid and condensation mass flow, and h_ℓ and h_g are the liquid and vapor enthalpies, respectively, given by:

$$h_\ell = c_p(T - T_{\ell in}) \tag{11}$$

$$h_g = h_{fg} + c_p(T_s - T_{\ell in}) \tag{12}$$

where $T_{\ell in}$ and T_s are the inlet liquid and saturation temperatures, respectively, and c_p is the liquid specific heat. Assuming that $h_{fg} >> c_p(T_s - T)$ we get:

$$\frac{1}{W_\ell}\frac{dW_\ell}{dz} = \frac{c_p}{h_{fg}}\frac{dT}{dz} \tag{13}$$

which relates the local liquid flow rate to the local temperature. Assuming the steam-water interface to be smooth, the condensation heat transfer rate per unit area across the interface is

$$q' = \frac{h_{fg}}{b}\frac{dW_\ell}{dz} \tag{14}$$

where b is the channel width. Since the major resistance to heat flow is on the water side of the interface we define a condensing heat transfer coefficient which is driven by the difference between the saturated liquid temperature, and the temperature of the bulk liquid:

$$h \equiv \frac{q'}{T_s - T} \tag{15}$$

thus;

$$h = \frac{c_p W_\ell}{b(T_s - T)}\frac{dT}{dz} \tag{16}$$

The local heat transfer coefficient can be evaluated by measuring the local surface temperature and its gradient. Local temperature gradients were determined for each test by fitting a curve through the surface temperatures along the plate and differentiating the resultant profile. Runs in which the temperature difference between the lower and the upper thermocouples was less than 5°C were deleted.

17° Inclination

The dependence of the local heat transfer coefficient, h, on local steam flow rate, $W_g(z)$, is shown in Figure 27 for a given inlet liquid flow rate ($W_{\ell in}$ = 0.32 kg/s). As shown, the local heat transfer coefficient

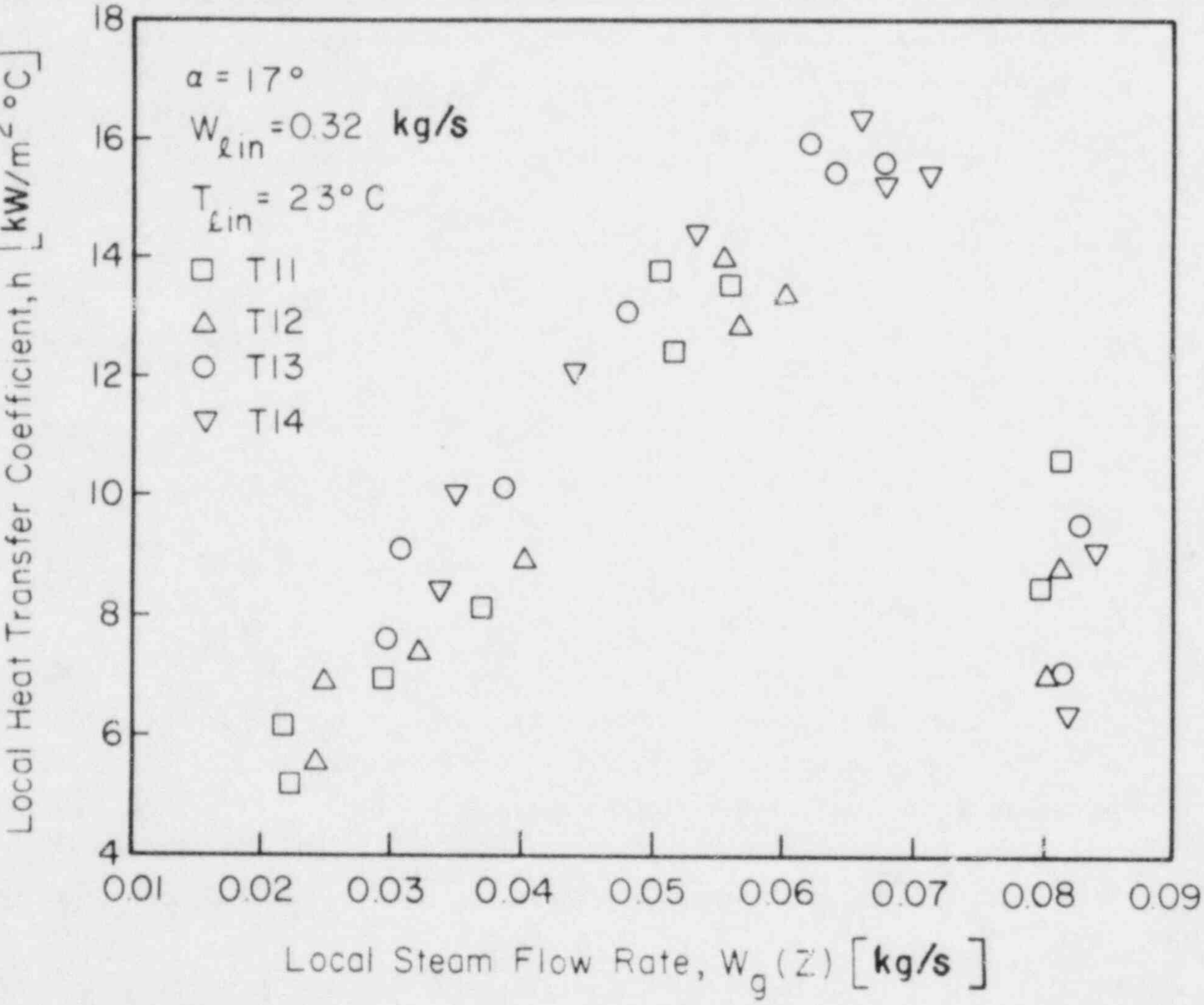

Figure 27. Local Heat Transfer Coefficient For $\alpha = 17°$ and $W_{\ell in} = 0.32$ kg/s

increases in Region B (compare with Figure 24 for region definition) with an increase in local steam flow rate. However, in Region C, where the steam flow rate is high enough to cause partial bypass, h decreases sharply, mainly due to local liquid flow rate reduction and a decrease in the temperature gradient. The dependence of h on the local value of steam flow rate rather than the inlet value suggests that a better description of the time averaged turbulent intensity, and in turn of h, is given by the local conditions rather than the averaged values. Thus, the correlations which will be developed later are based on the local Reynolds and Prandtl Numbers.

As the inlet liquid flow rate, $W_{\ell in}$, and consequently the local liquid flow rate, $W_{\ell}(z)$, increase, the surface temperatures for a given steam flow rate decrease, with a relatively smaller decrease in temperature gradient (see Figure 28). The local heat trasnfer coefficient remains almost constant except at the very high steam flow rates where the increase in inlet liquid flow rate results in higher values for h (see Figure 29). The same trends are shown when comparing temperatures and local heat transfer coefficients for $W_{\ell in}$ = 0.32 kg/s (see Figures 24 & 27) and for lower inlet liquid flow rates, $W_{\ell in}$ = 0.21 kg/s and $W_{\ell in}$ = 0.10 kg/s (see Figures 30 - 33). As shown in Figures 30 and 31, a decrease in $W_{\ell in}$ results in an overall increase of the temperature level and temperature gradient. The values for h do not change with the change of $W_{\ell in}$ at the low range of steam flow rates. However, for the higher values of $W_g(z)$ in the Region B, h is larger for higher $W_{\ell in}$ (see Figures 32 and 33).

45° Inclination

Temperature and heat transfer coefficient behavior for the 45° inclination is similar to that exhibited at 17° inclination (see Figures 25 and 34 - 38). However, it may be noticed that an increase in inclination results in an increase of h for the same local steam and liquid flow rates. This suggests that the liquid velocity or, alternatively, the liquid film thickness is an important scaling parameter, and, as will be shown later, the use of film thickness as a characteristic length dimension in the dimensionless parameters Re and Nu leads to good correlation of the data.

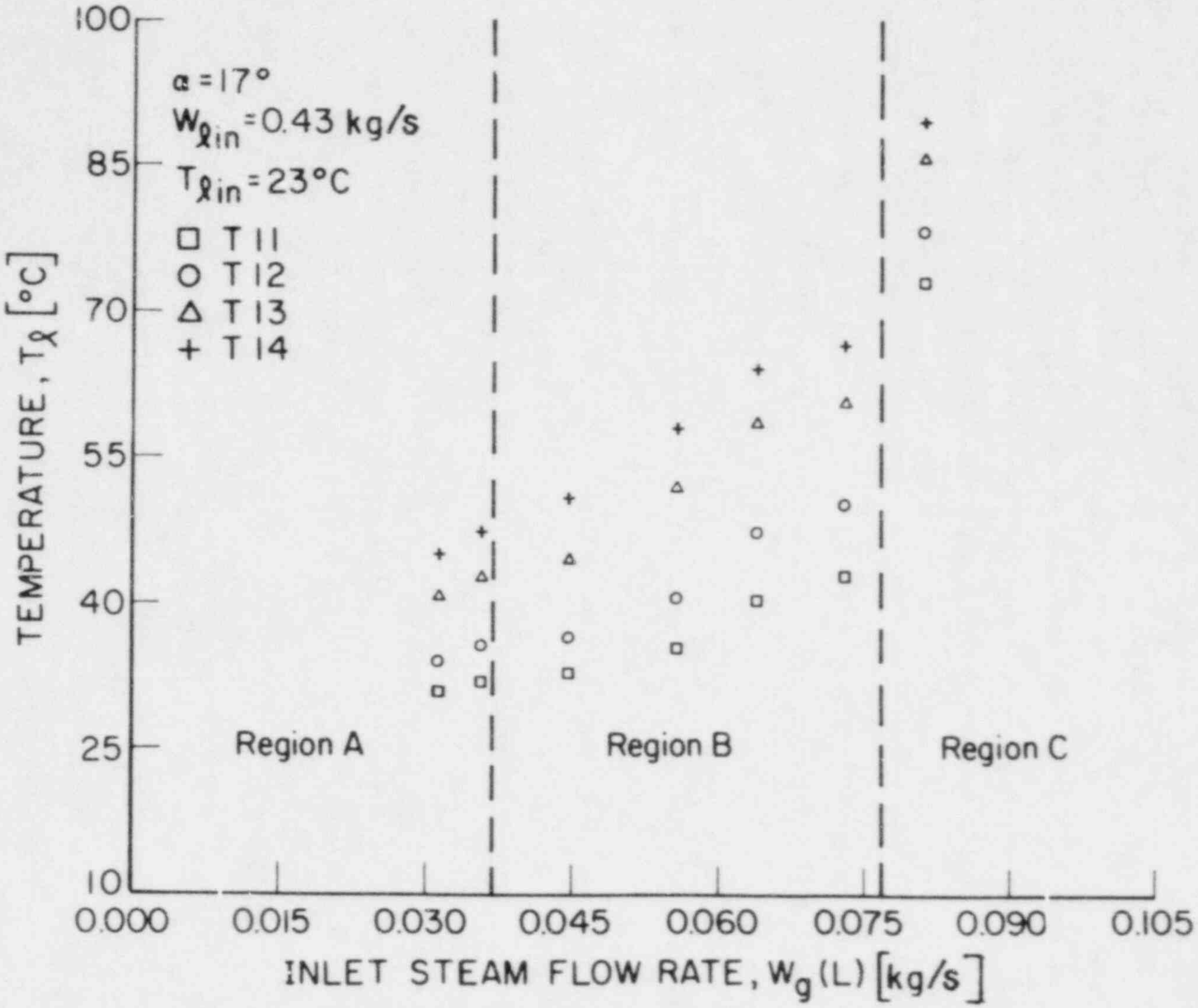

Figure 28. Liquid Temperatures for α = 17° and $W_{\ell in}$ = 0.43 kg/s

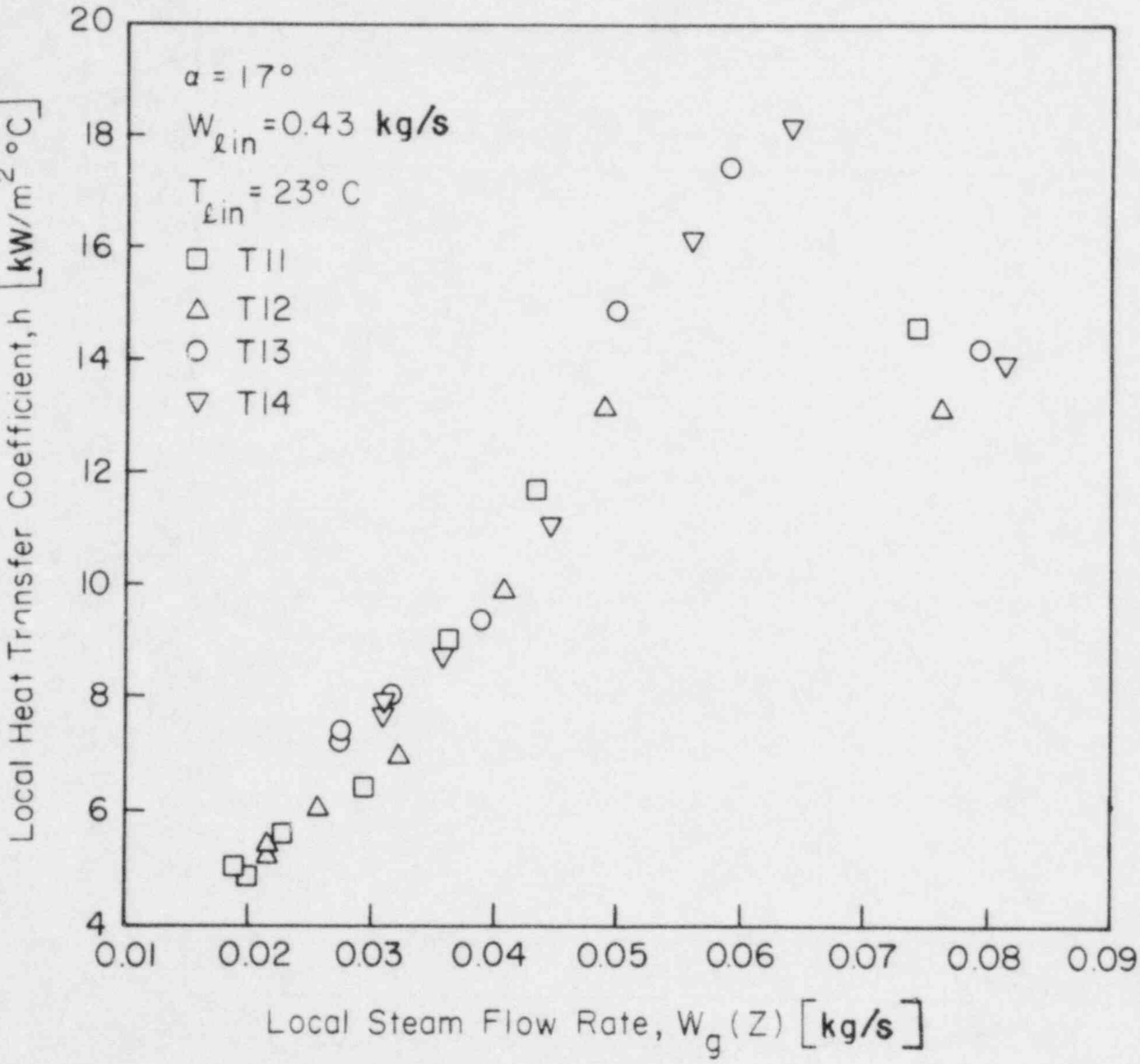

Figure 29. Local Heat Transfer Coefficient For $\alpha = 17°$ and $W_{\ell in} = 0.43$ kg/s

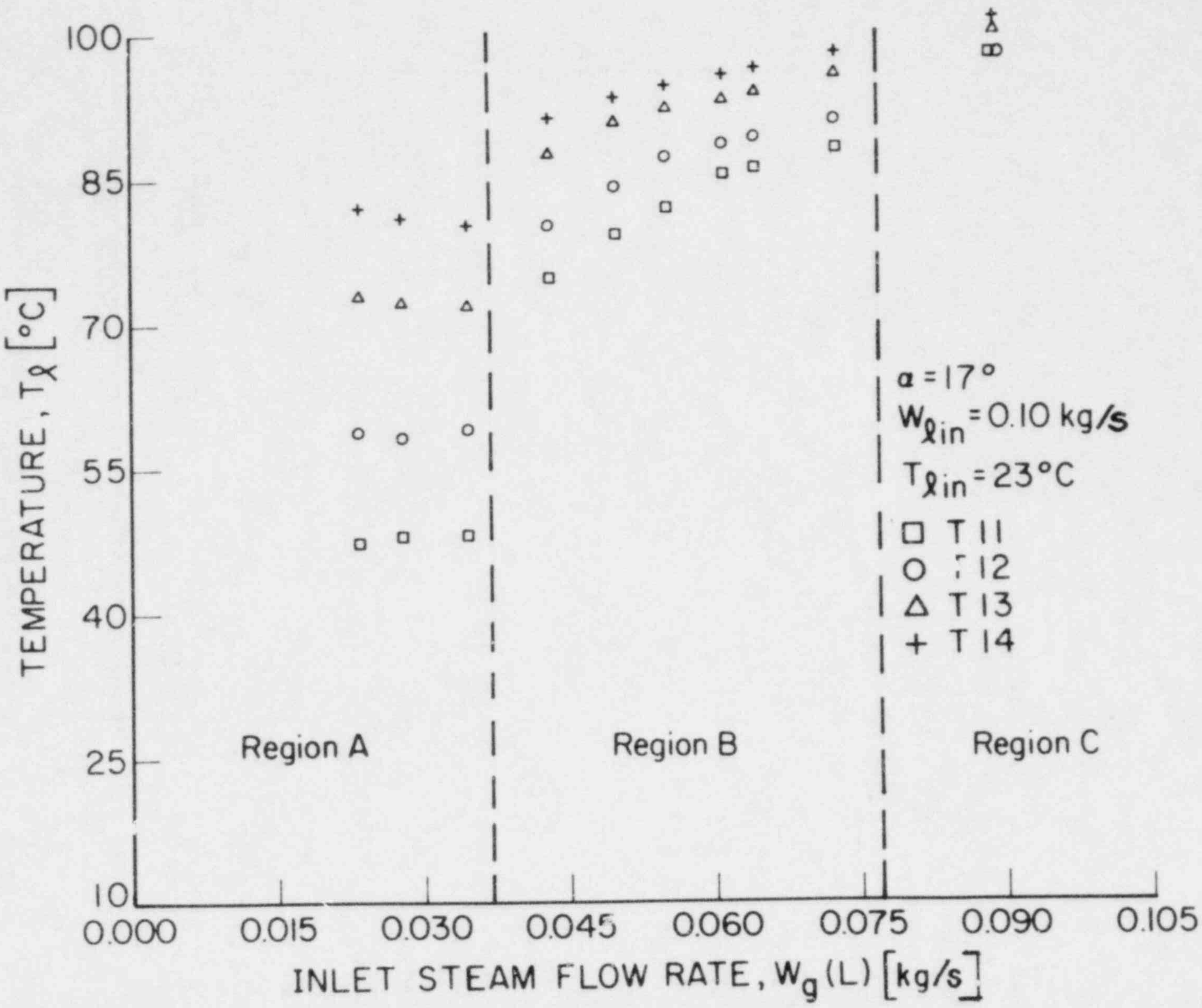

Figure 30. Liquid Temperatures for α = 17° and $W_{\ell in}$ = 0.10 kg/s

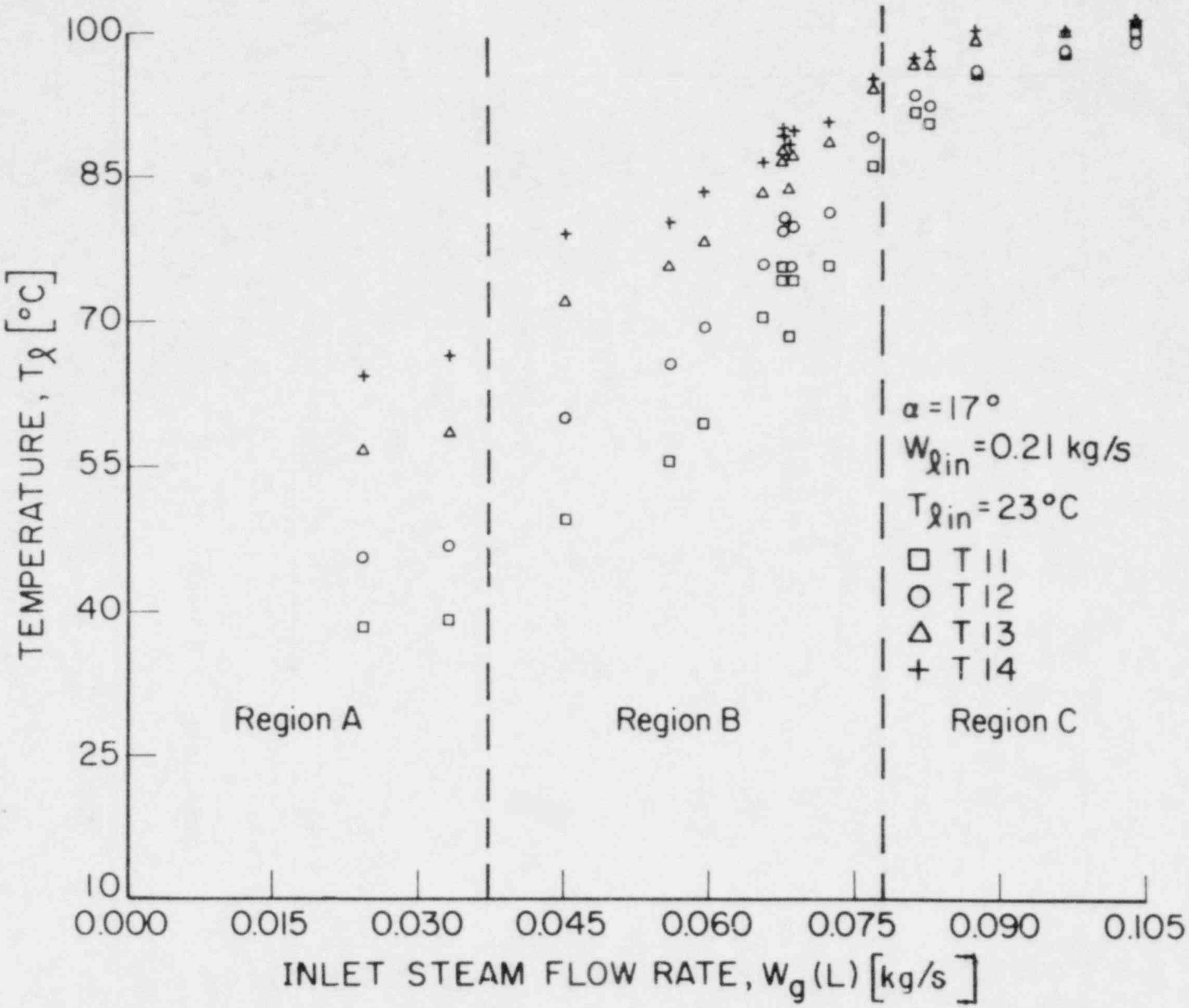

Figure 31. Liquid Temperatures for α = 17° and $W_{\ell in}$ = 0.21 kg/s

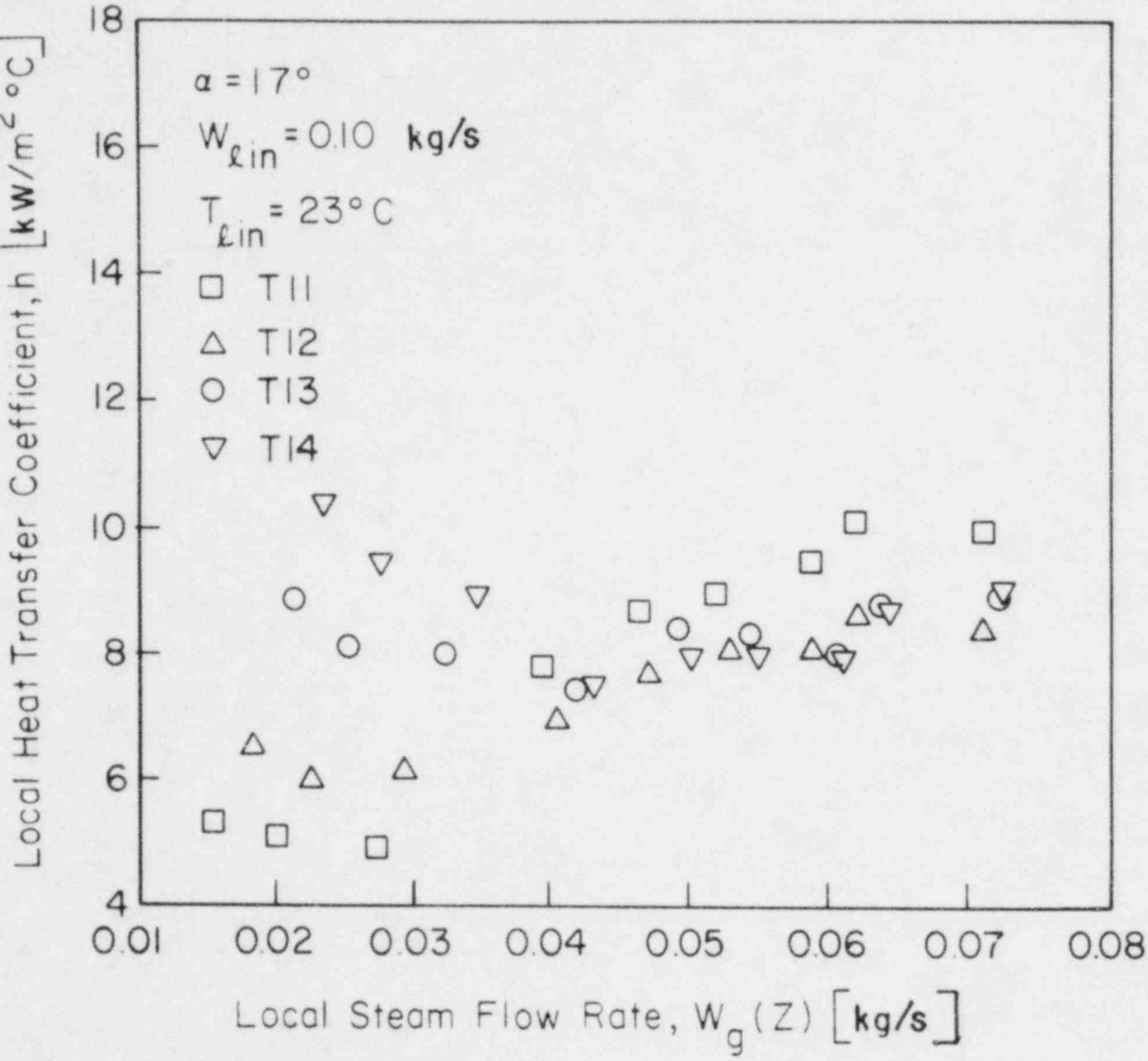

Figure 32. Local Heat Transfer Coefficient For $\alpha = 17°$ and $W_{\ell in} = 0.10$ kg/s

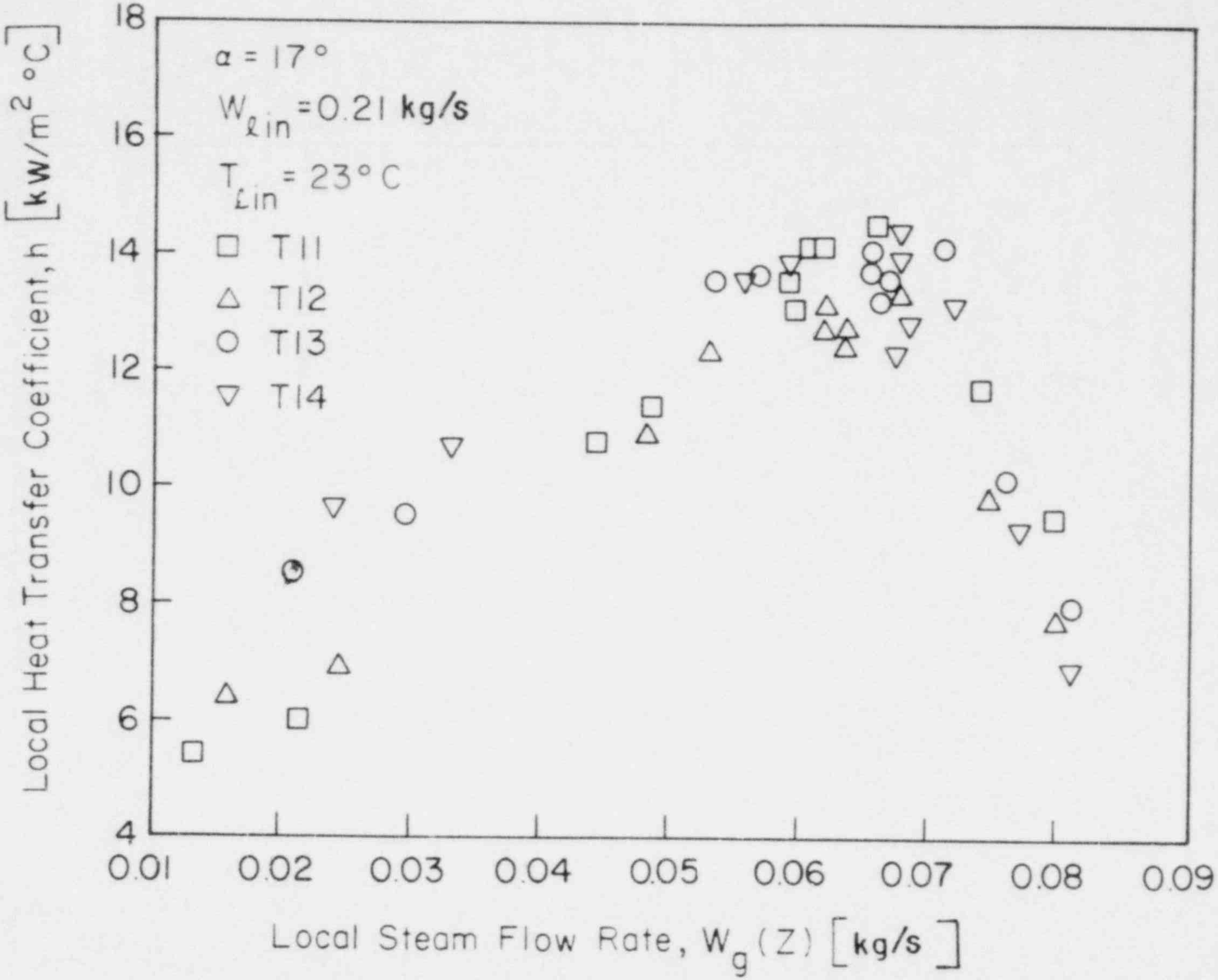

Figure 33. Local Heat Transfer Coefficient For $\alpha = 17°$ and $W_{\ell in} = 0.21$ kg/s

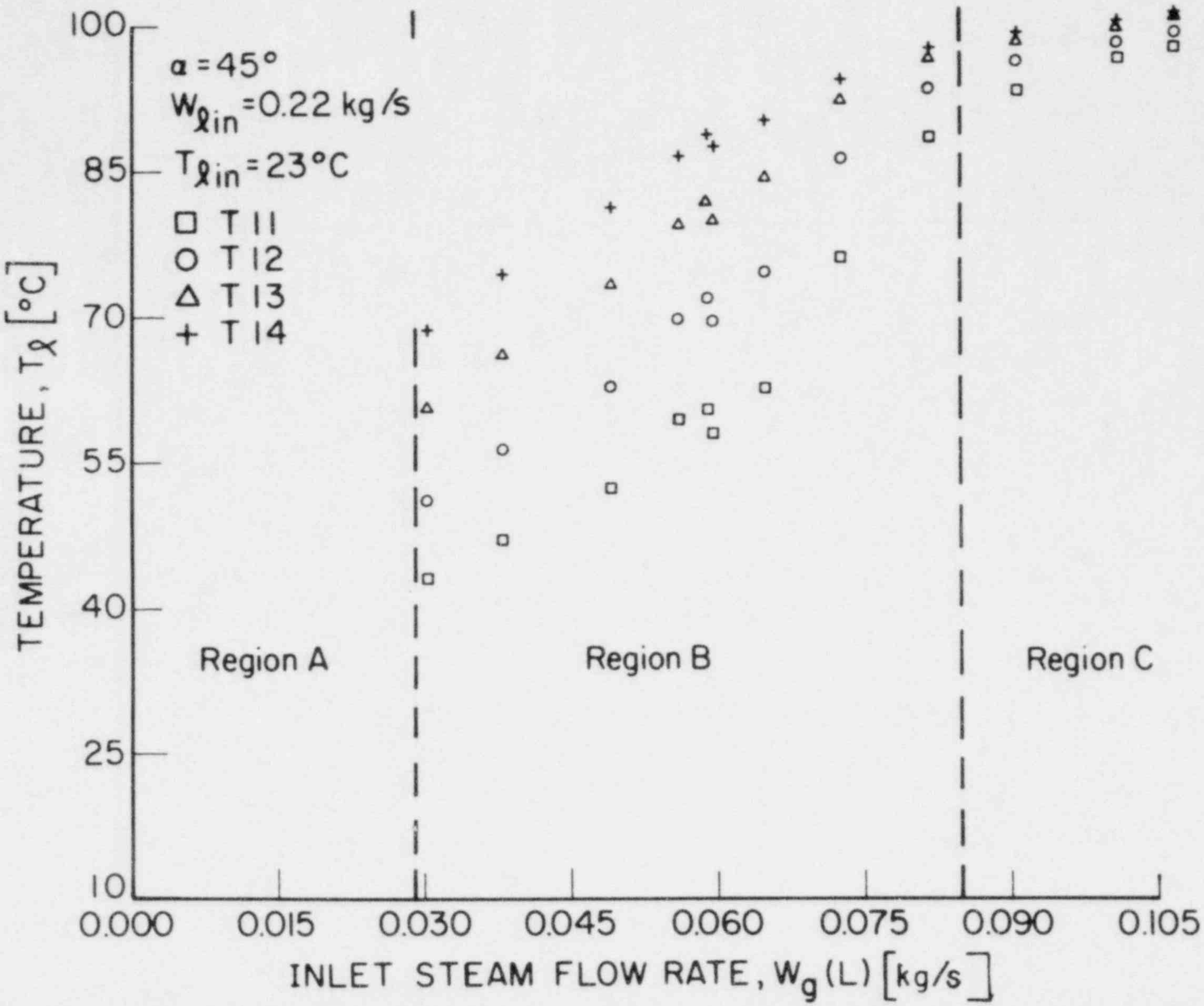

Figure 34. Liquid Temperatures for $\alpha = 45°$ and $W_{\ell in} = 0.22$ kg/s

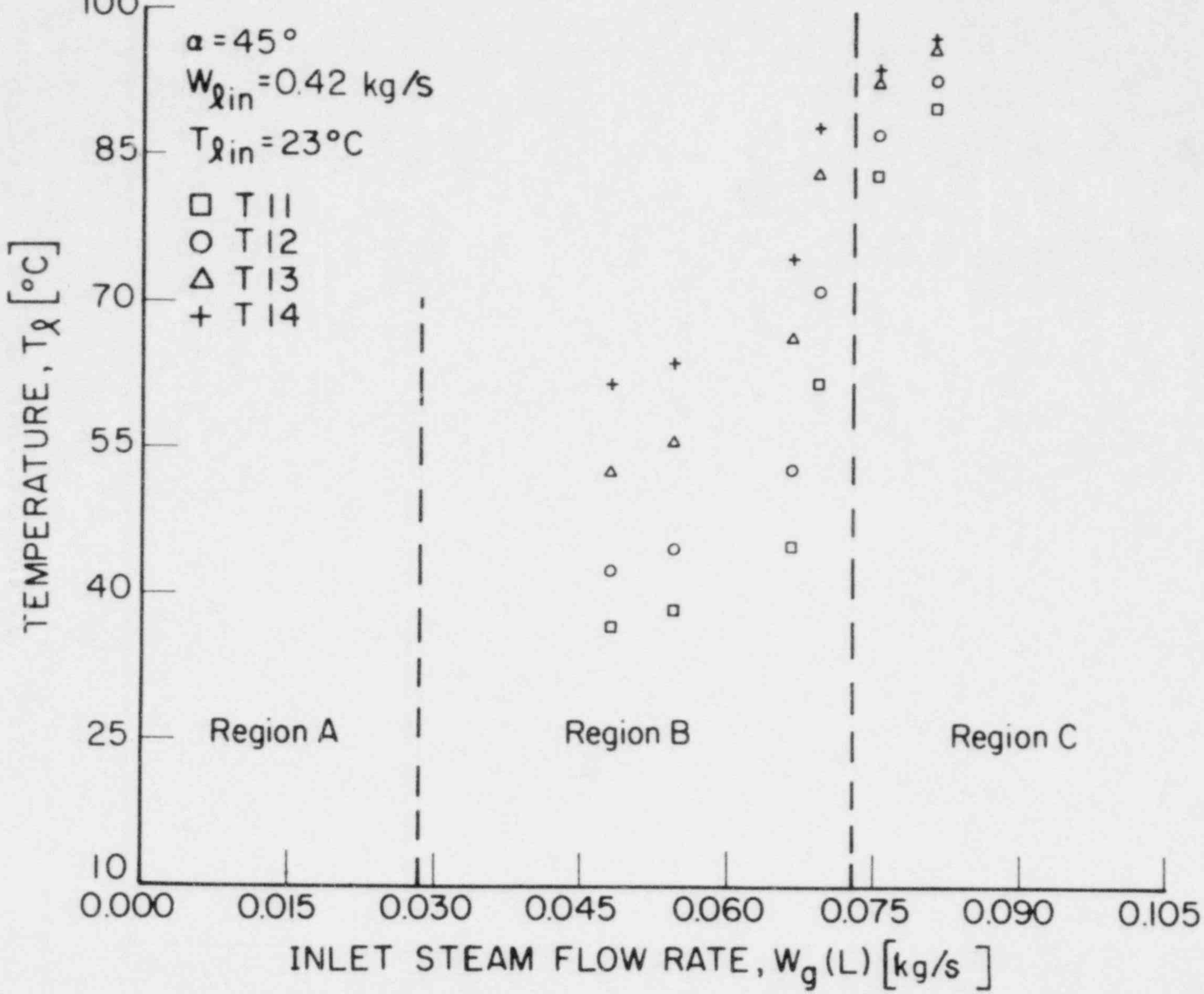

Figure 35. Liquid Temperatures for $\alpha = 45°$ and $W_{\ell in} = 0.42$ kg/s

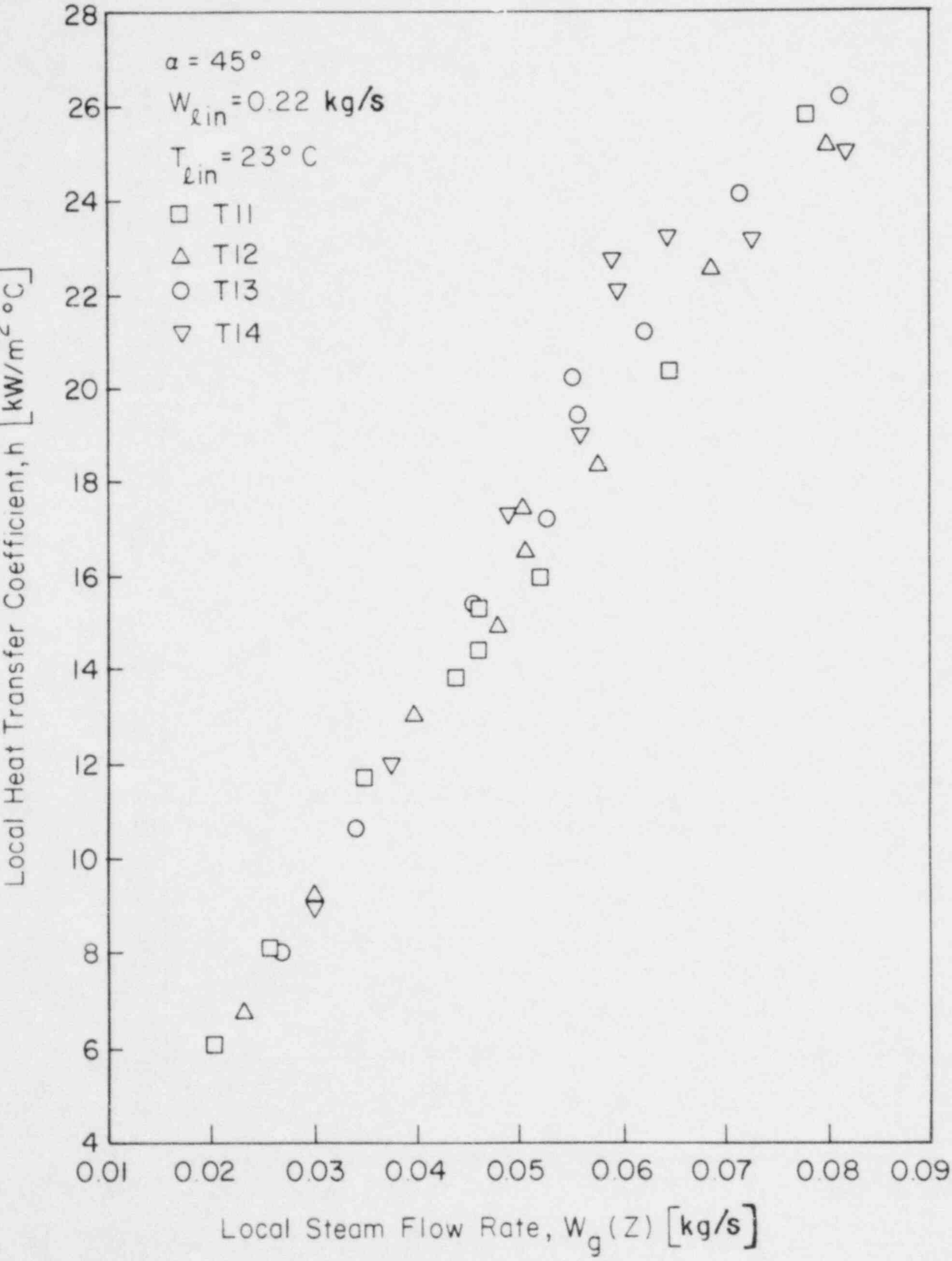

Figure 36. Local Heat Transfer Coefficient for $\alpha = 45°$ and $W_{\ell in} = 0.22$ kg/s

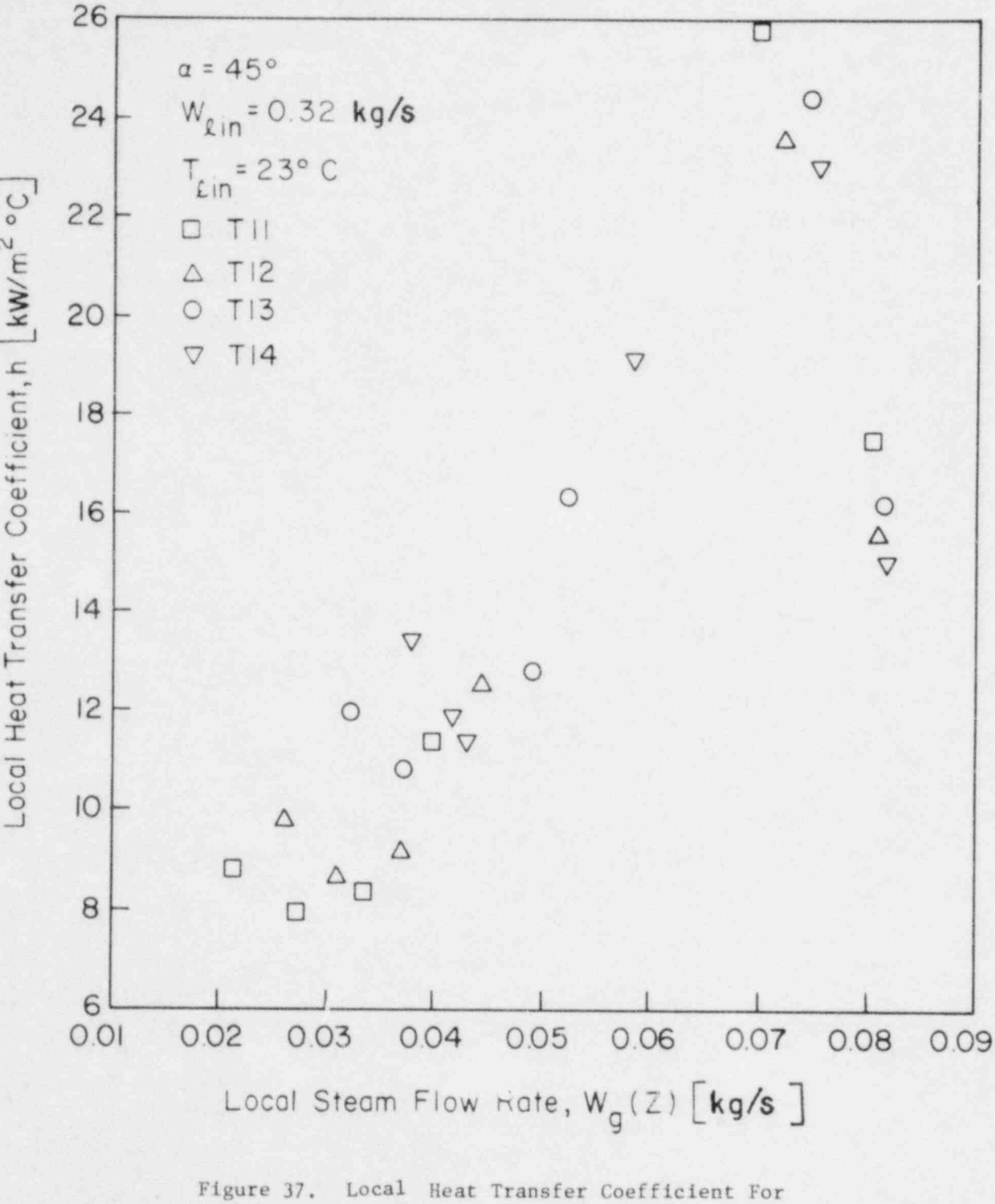

Figure 37. Local Heat Transfer Coefficient For $\alpha = 45°$ and $W_{\ell in} = 0.32$ kg/s

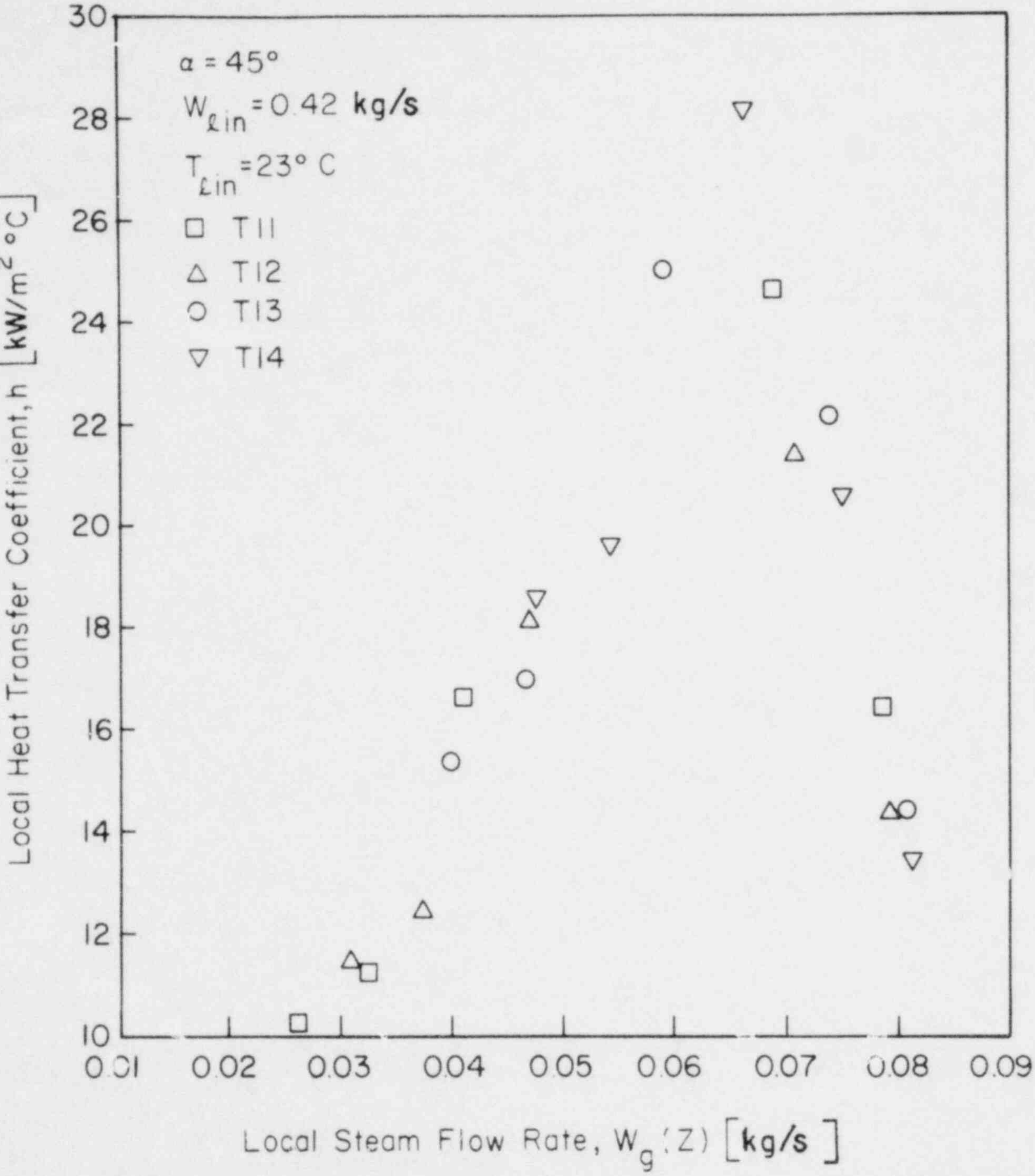

Figure 38. Local Heat Transfer Coefficient For $\alpha = 45°$ and $W_{\ell in} = 0.42$ kg/s

0.5° Inclination

Results from the horizontal position are rather unique in comparison with those of 17° and 45°. Film thicknesses are relatively large and bypass occurs immediately after roll waves are generated. However, the general dependence of h on $W_g(z)$ and $W_{\ell in}$ is similar to that seen for the inclined positions (Figures 23 and 39-41): h increases with $W_g(z)$, but decreases sharply as bypass occurs. An increase in $W_{\ell in}$ results in an increase in h, especially at the higher values of $W_g(z)$. The values of h are lower in the horizontal position than the respective values in the inclined position since the liquid velocity is lower. The main difference in the h dependence on $W_g(z)$ is seen in Region A where an almost constant value of h is calculated, a value which depends on the inlet liquid flow rate.

The Effect of Inlet Liquid Temperature

The effect of inlet liquid temperature was studied for one test section inclination and two inlet liquid flow rates. Temperature measurements for these runs are shown in Figures 42 - 44. For these low subcooling tests the wave characteristics were much less distinct than they were with cold liquid. The most pronounced difference was in the bypass mechanism. For highly subcooled inlet water the bypass is controlled by waves which are initiated near the liquid outlet. For low inlet water subcooling bypass is controlled by liquid sweepout which takes place near the liquid injector.

As shown in Figures 27, 45, and 46, the heat transfer coefficient decreases with increased liquid inlet temperature. Similarly, the dependence of h on $W_g(z)$ is reduced as inlet liquid temperature increases. Figure 45 shows that for $T_{\ell in}$ = 57°C the dependence of h on $W_g(z)$ is still noticeable, with a slight reduction of h at the higher steam flow rate. However, this dependence is diminished when the inlet liquid temperature is increased to 77°C, as shown in Figures 46 and 47 for two different liquid flow rates.

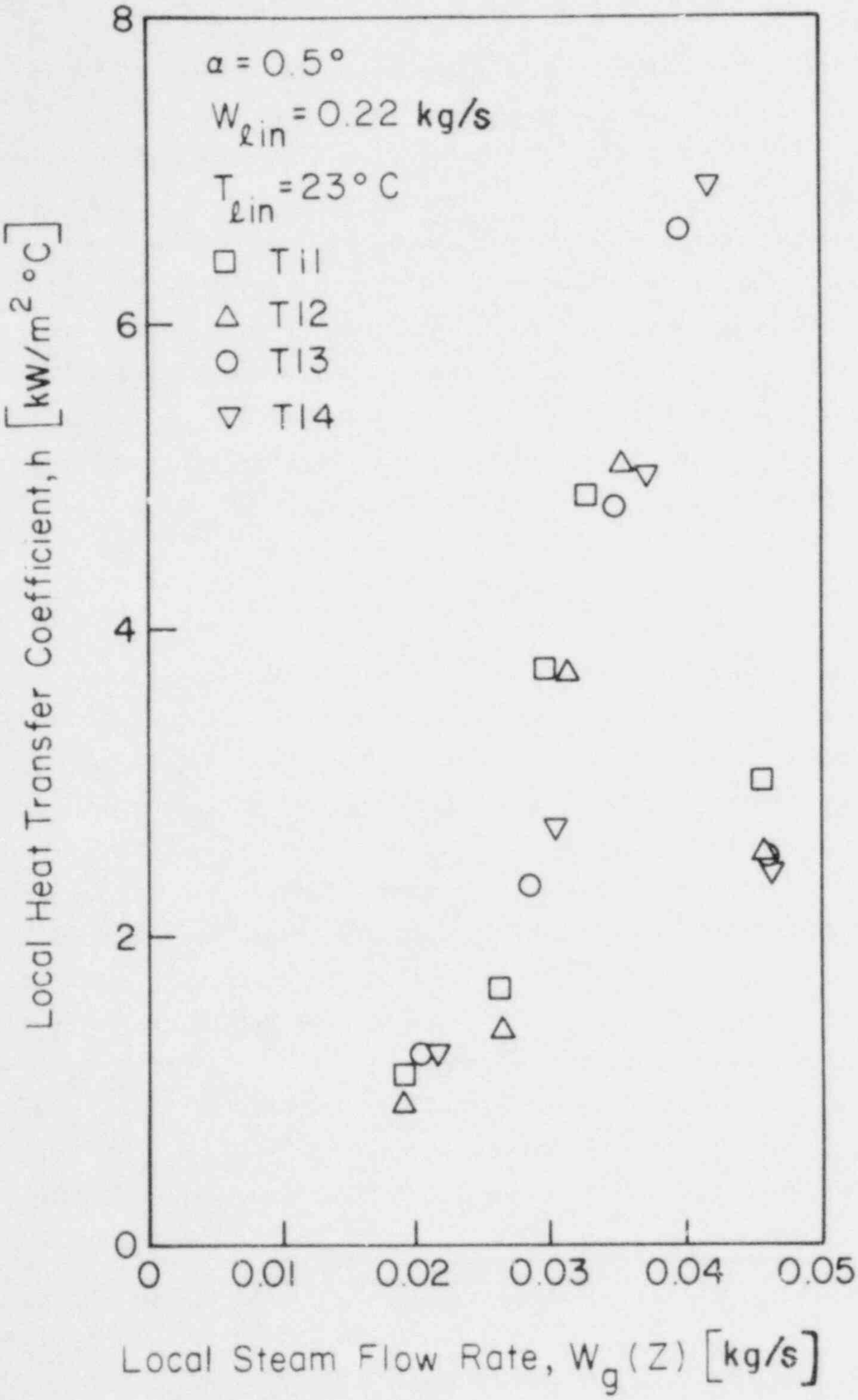

Figure 39. Local Heat Transfer Coefficient For $\alpha = 0.5°$ and $W_{\ell in} = 0.22$ kg/s

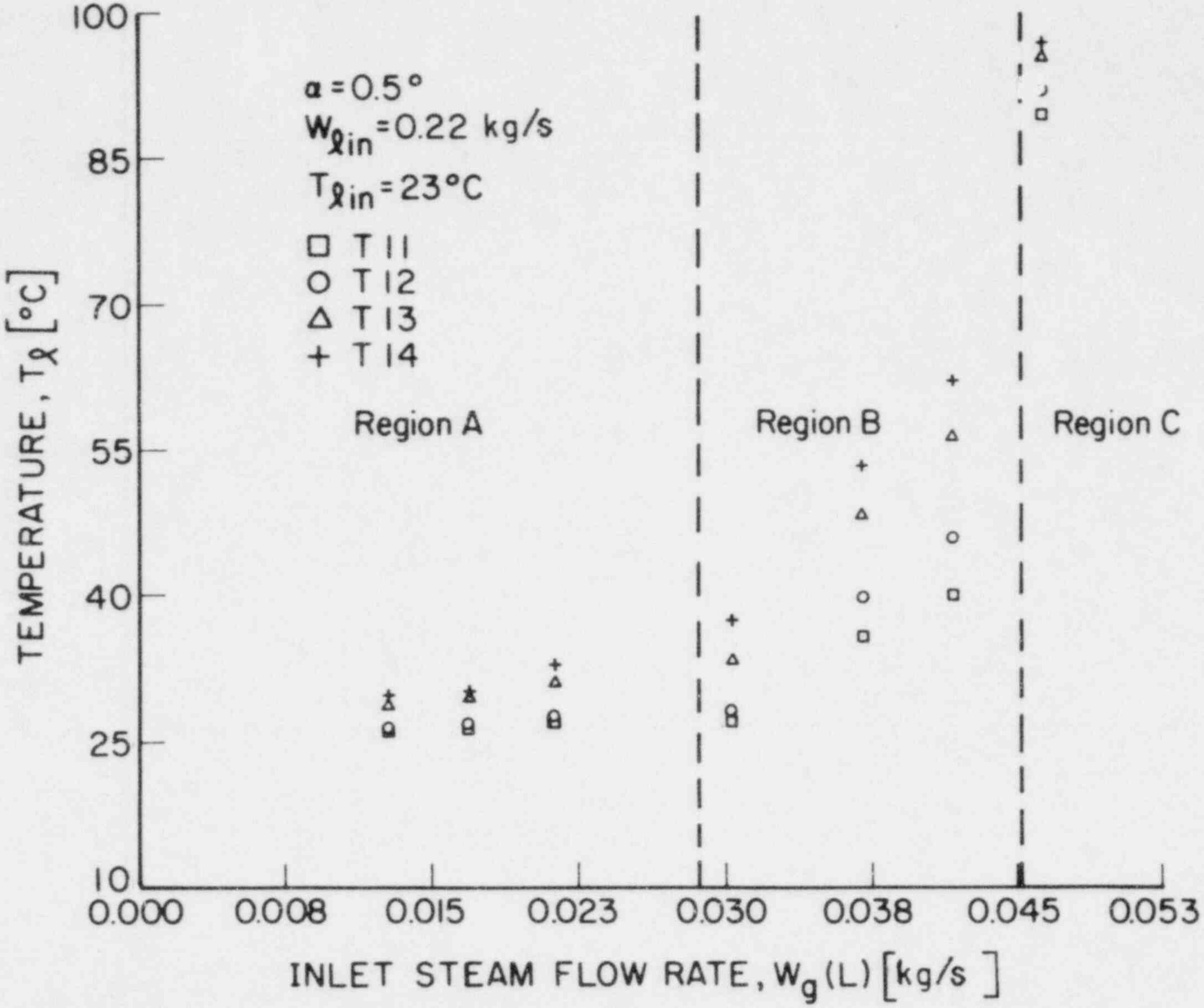

Figure 40. Liquid Temperatures for $\alpha = 0.5°$ and $W_{\ell in} = 0.22$ kg/s

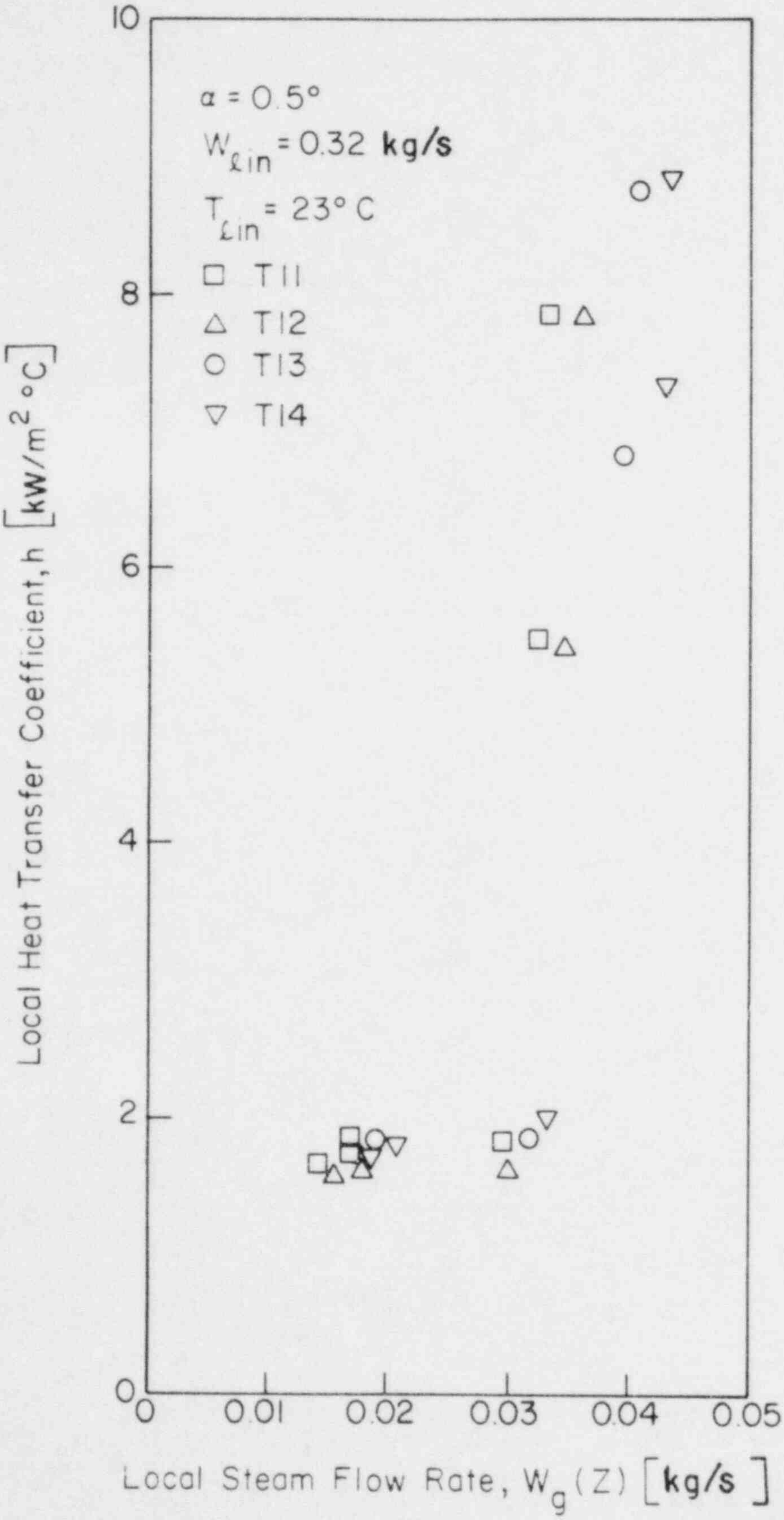

Figure 41. Local Heat Transfer Coefficient For $\alpha = 0.5°$ and $W_{\ell in} = 0.32$ kg/s

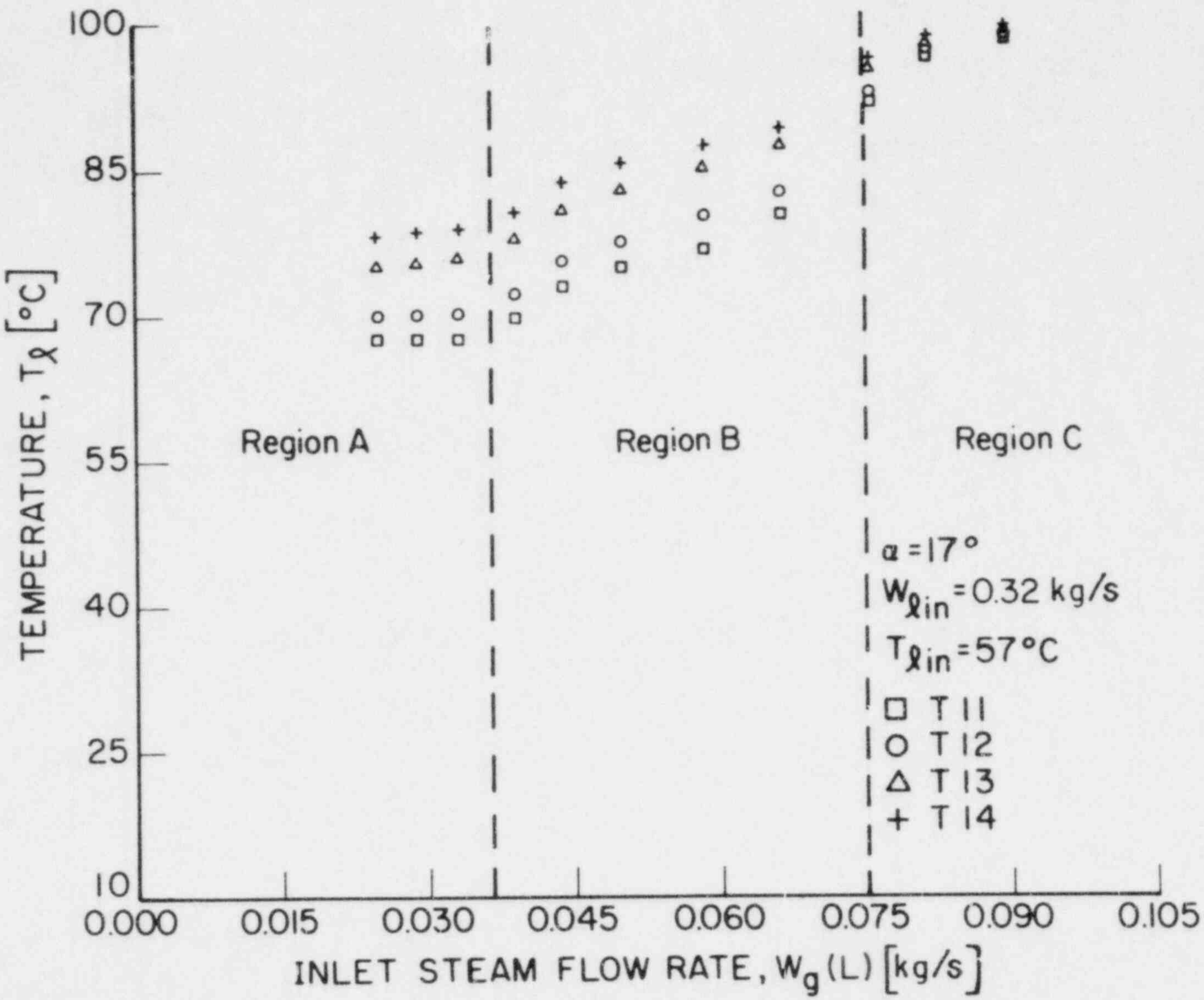

Figure 42. Liquid Temperatures for α = 17°, $W_{\ell in}$ = 0.32 kg/s and $T_{\ell in}$ = 57°C

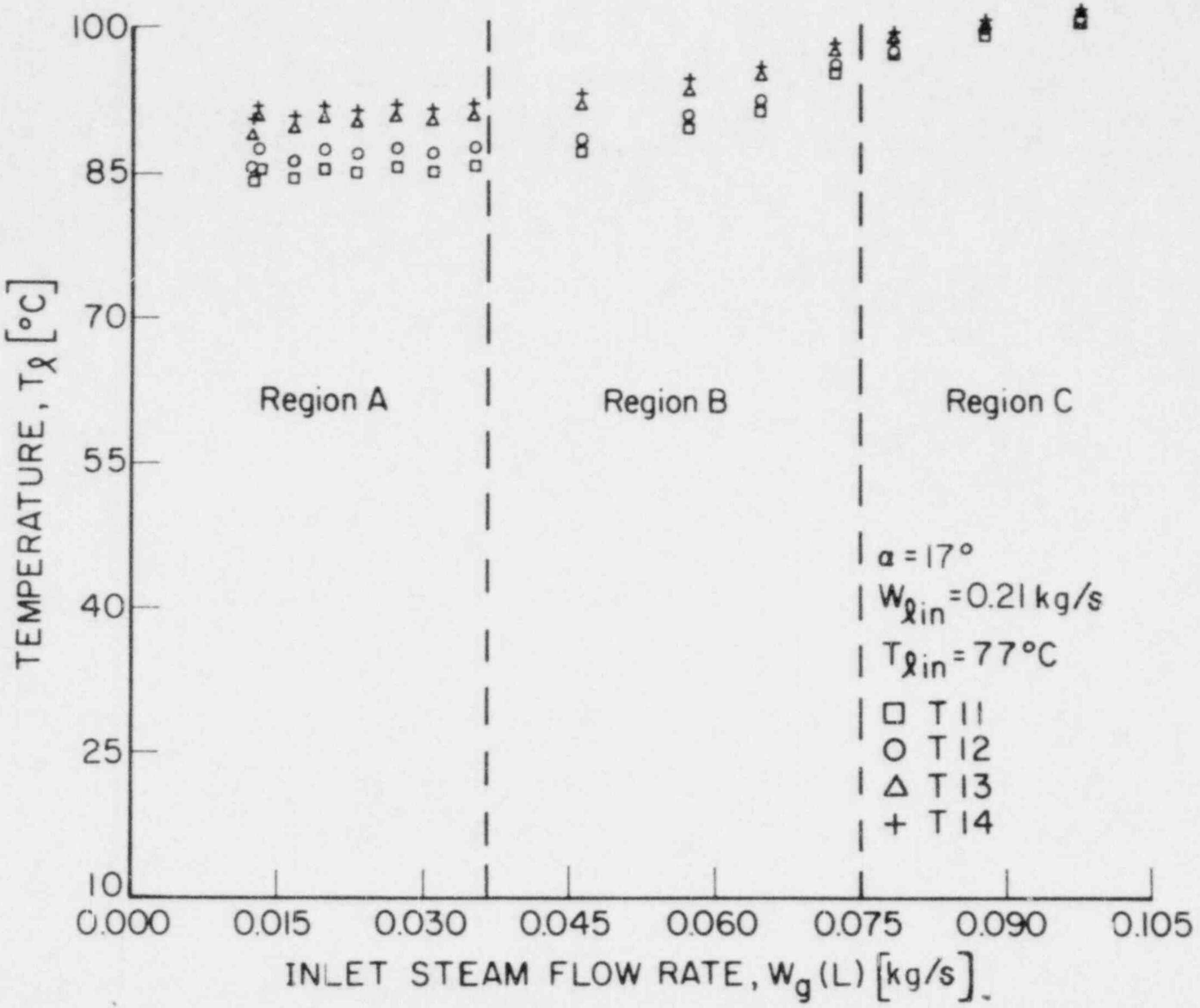

Figure 43. Liquid Temperatures for α = 17°, $W_{\ell in}$ = 0.21 kg/s and $T_{\ell in}$ = 77°C

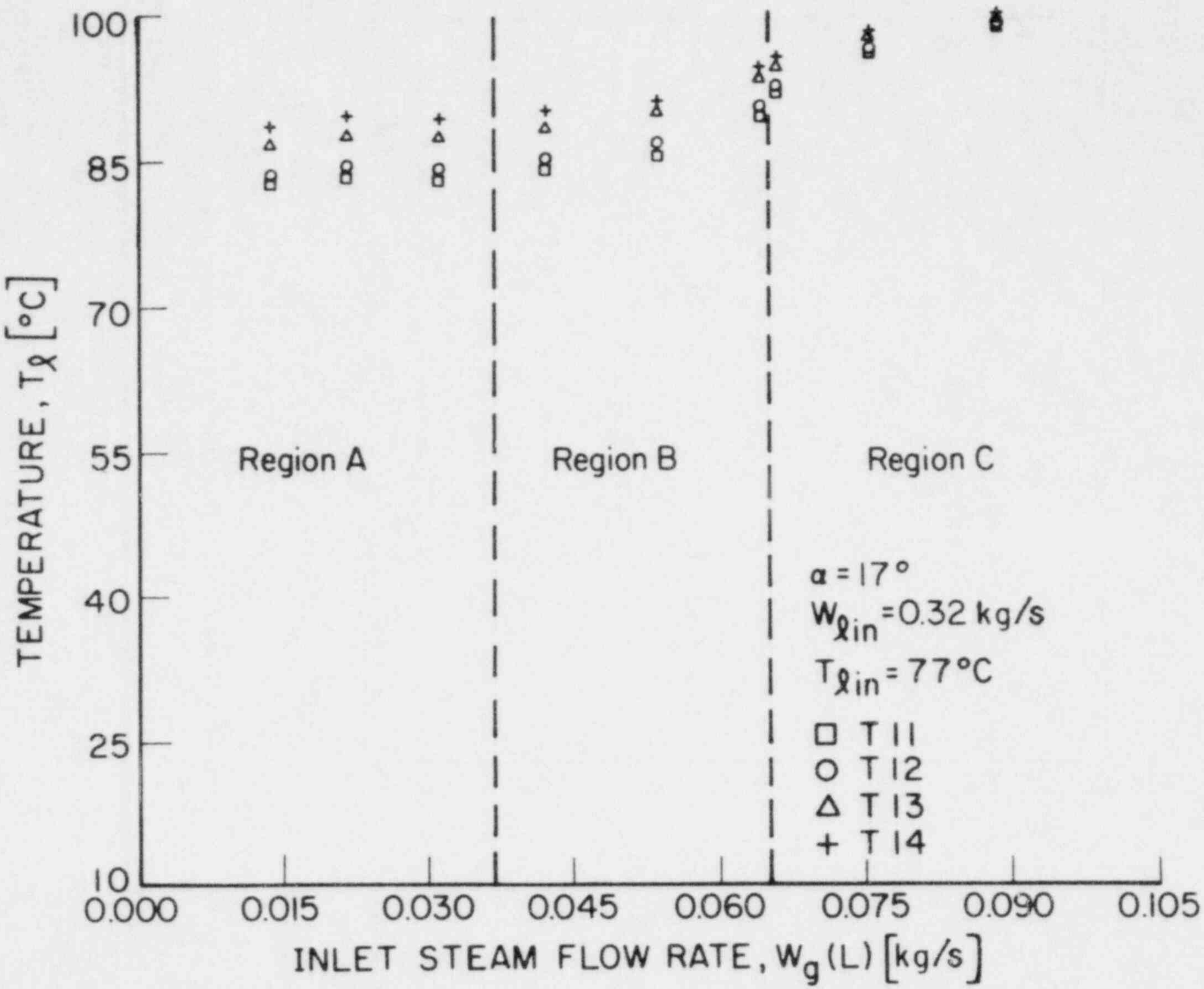

Figure 44. Liquid Temperatures for $\alpha = 17°$, $W_{\ell in} = 0.32$ kg/s and $T_{\ell in} = 77°C$

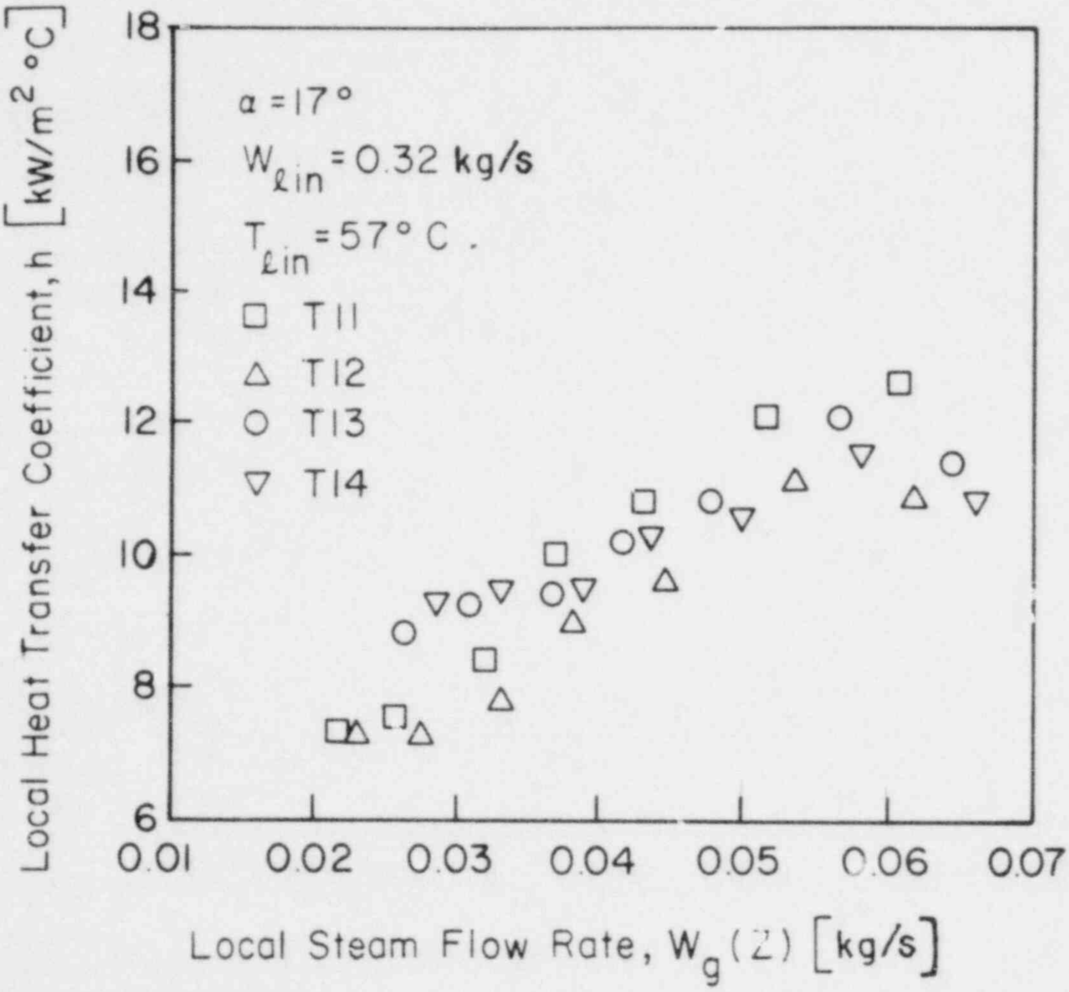

Figure 45. Local Heat Transfer Coefficient For $\alpha = 17°$, $W_{\ell in} = 0.32$ kg/s and $T_{\ell in} = 57°C$

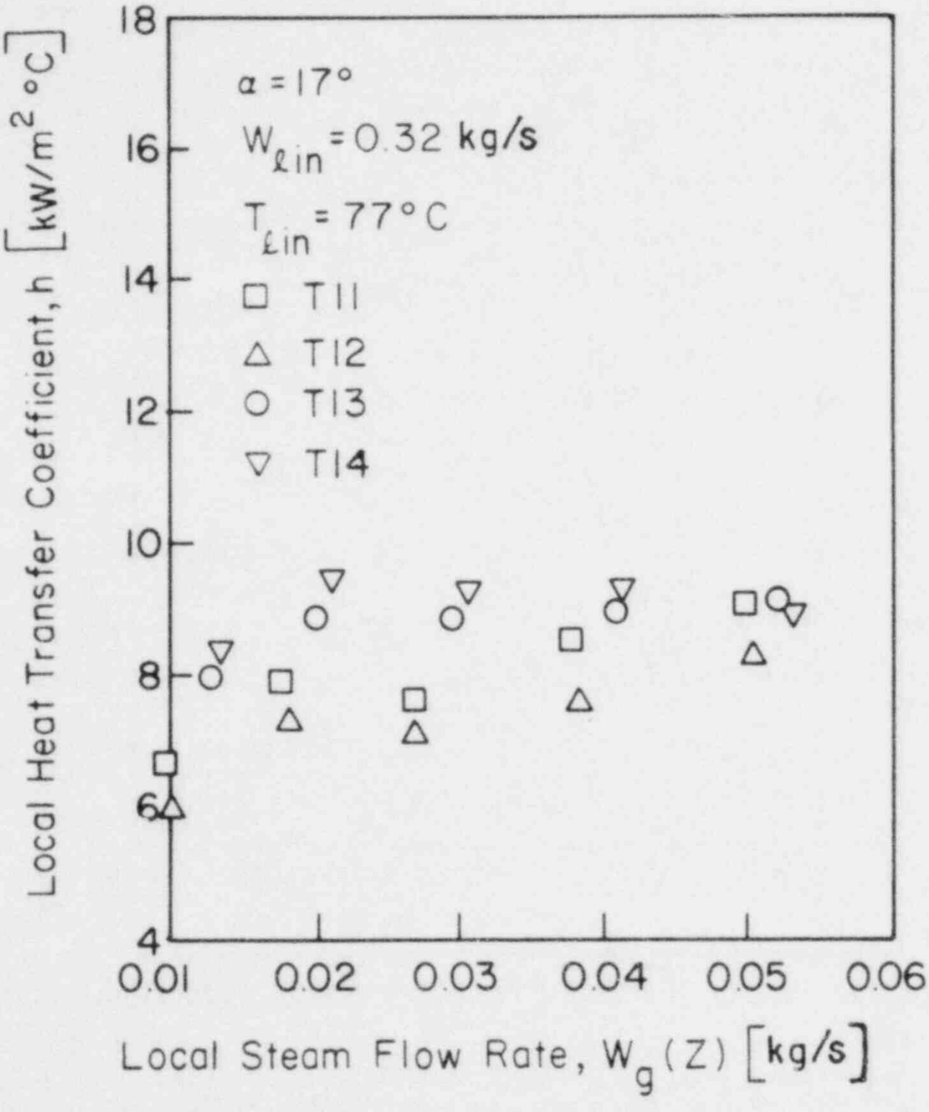

Figure 46. Local Heat Transfer Coefficient For $\alpha = 17°$, $W_{\ell in} = 0.32$ kg/s and $T_{\ell in} = 77°C$

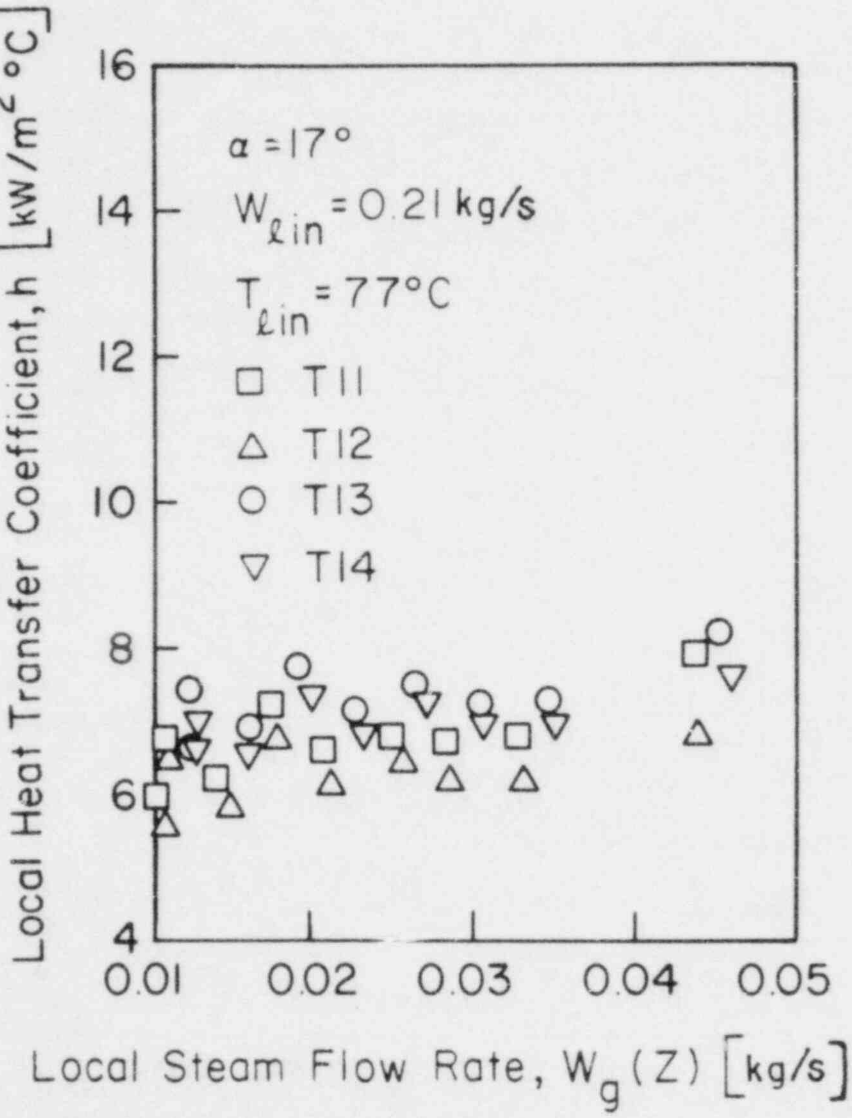

Figure 47. Local Heat Transfer Coefficient For $\alpha = 17°$, $W_{\ell in} = 0.21$ kg/s and $T_{\ell in} = 77°C$

Correlation of the Nu Number Data

A complete description of the interaction between a vapor flow and a countercurrent subcooled liquid film flow must account for a combination of very complex phenomena. One way to circumvent considering the interfacial disturbances in detail is to identify the significant parameters which directly govern the interfacial heat transfer phenomena and use these as a basis to correlate the experimental data. For turbulent forced convection on the liquid side of the interface, it is not unreasonable to expect the usual correlation form in which the Nusselt Number is related to the liquid Reynolds and Prandtl Numbers. In addition, the steam Reynolds Number should also be included since it relates to the available heat transfer area. Thus, the following interfacial heat transfer correlation will be sought:

$$Nu(z) = C \, Re_g(z)^{n_1} \, Re_\ell(z)^{n_2} \, Pr(z)^{n_3} \qquad (17)$$

where the local steam and liquid Reynolds Numbers are defined respectively as

$$Re_g(z) \equiv \frac{W_g(z)}{b\mu_g} \qquad (18)$$

$$Re_\ell(z) \equiv \frac{W_\ell(z)}{b\mu_\ell(z)} \qquad (19)$$

and the local Nusselt Number is defined by

$$Nu(z) \equiv \frac{ht}{k_\ell} \qquad (20)$$

Liquid and steam flow rates across any section normal to the wall are continuously changing along the wall because of continuous condensation at the interface. To determine the local liquid and steam flow we make use of the respective measured flow rates at the bottom of the test section:

$$W_\ell(z) = W_\ell(L)\exp\left\{[T - T(L)]\,\frac{C_p}{h_{fg}}\right\} \quad (21)$$

$$W_g(z) = W_g(L) - [W_\ell(L) - W_\ell(z)] \quad (22)$$

The correlation form, given by Equation 17 was applied separately to the data in the inclined positions (17° and 45°) and to the horizontal position. Each set of data was separated according to the respective wave structure regions observed experimentally. In the inclined positions, due to the very small number of data points in Region A, we have correlated only the data of Regions B and C which were divided according to the criterion:

$W_p^* \geq 1.0$ corresponds to Region B (no bypass), and

$W_p^* < 1.0$ corresponds to Region C (bypass).

For a given inlet liquid temperature ($T_{\ell in}$ = 23°C) a least-square fit of the data in these regions yields (see Figure 48):

(Region B:)

$$Nu = 1.16 \times 10^{-3}\ Re_g^{0.28}\ Re_\ell^{0.87}\ Pr^{0.05} \quad (23)$$

(Region C:)

$$Nu = 5.79 \times 10^{-4}\ Re_g^{0.016}\ Re_\ell^{1.08}\ Pr^{2.0} \quad (24)$$

Examination of the data points in Figure 48 reveals no systematic variation between the 17° and 45° runs but rather an apparent random scattering of the data near the correlation line. Comparing the correlations for the two regions reveals the relative effects of the different parameters. In Region B the steam and liquid Reynolds Numbers have a significant effect on Nu, whereas the local Pr is insignificant, evidently because of the relatively low liquid temperatures. In Region C where bypass occurs, the effect of Re_g diminishes and Nu drops sharply due to the strong effects of the reduced liquid

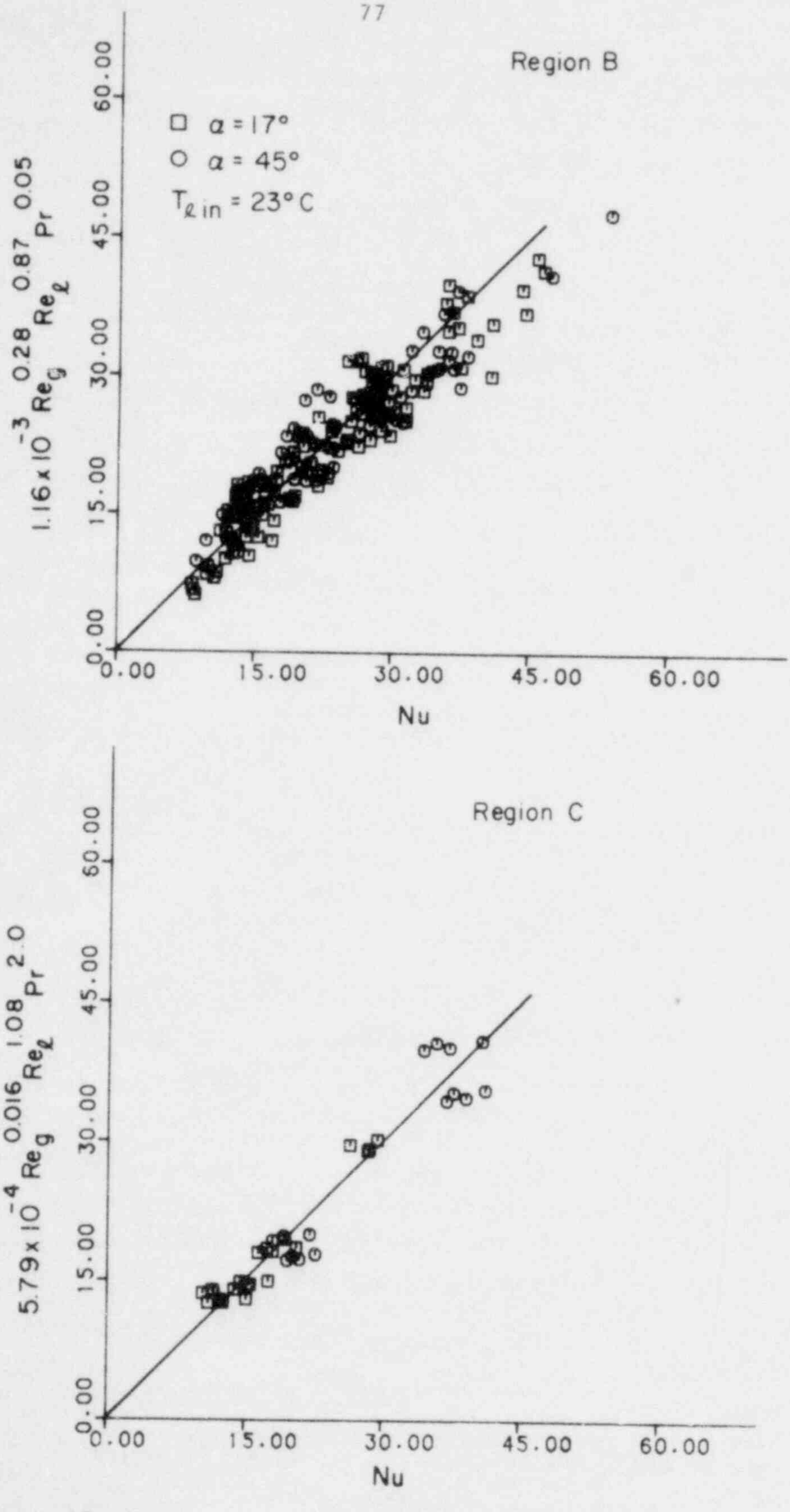

Figure 48. Comparison of Experimental and Predicted Nu For $\alpha = 17°$ and $45°$ and $T_{\ell in} = 23°C$

flow rate and, subsequently, the high liquid temperatures which are described by Re_{ℓ} and Pr, respectively. This is in full accordance with the experimental observations.

The effects of varying inlet liquid subcooling on Nu are shown when the Region B data for both 17° and 45° are correlated together (see Figure 49)

$$Nu = 8.5 \times 10^{-5} \ Re_g^{0.25} \ Re_{\ell}^{0.85} \ Pr^{0.5} \qquad (25)$$

As expected, the only significant change is in the dependence on Pr.

Data in the horizontal position have been correlated in Regions A and B and the two data points in Region C were deleted. The criterion used to divide the data between the regions was:

$W_g(L) \leq 0.029$ kg/s corresponds to Region A, and

$W_g(L) > 0.029$ kg/s corresponds to Region B.

The resultant correlations are (see Figures 50):

(Region A:)

$$Nu = 5.06 \times 10^{-5} \ Re_g^{0.012} \ Re_{\ell}^{1.45} \ Pr^{0.55} \qquad (26)$$

(Region B:)

$$Nu = 6.11 \times 10^{-6} \ Re_g^{0.58} \ Re_{\ell}^{1.21} \ Pr^{0.1} \qquad (27)$$

As shown experimentally, the Nu dependence on Re_g in Region A is very small, whereas Nu in Region B is quite sensitive to the local steam flow rate.

Correlation of Condensation Efficiency

As shown by Segev and Collier[8], the condensation efficiency is represented by the non-dimensional temperature (Θ) at the end of the core barrel:

$$f = \Theta(L) \qquad (28)$$

where $\Theta(z)$ is defined as

$$\Theta(z) = \frac{T - T_{\ell in}}{T_s - T_{\ell in}} \qquad (29)$$

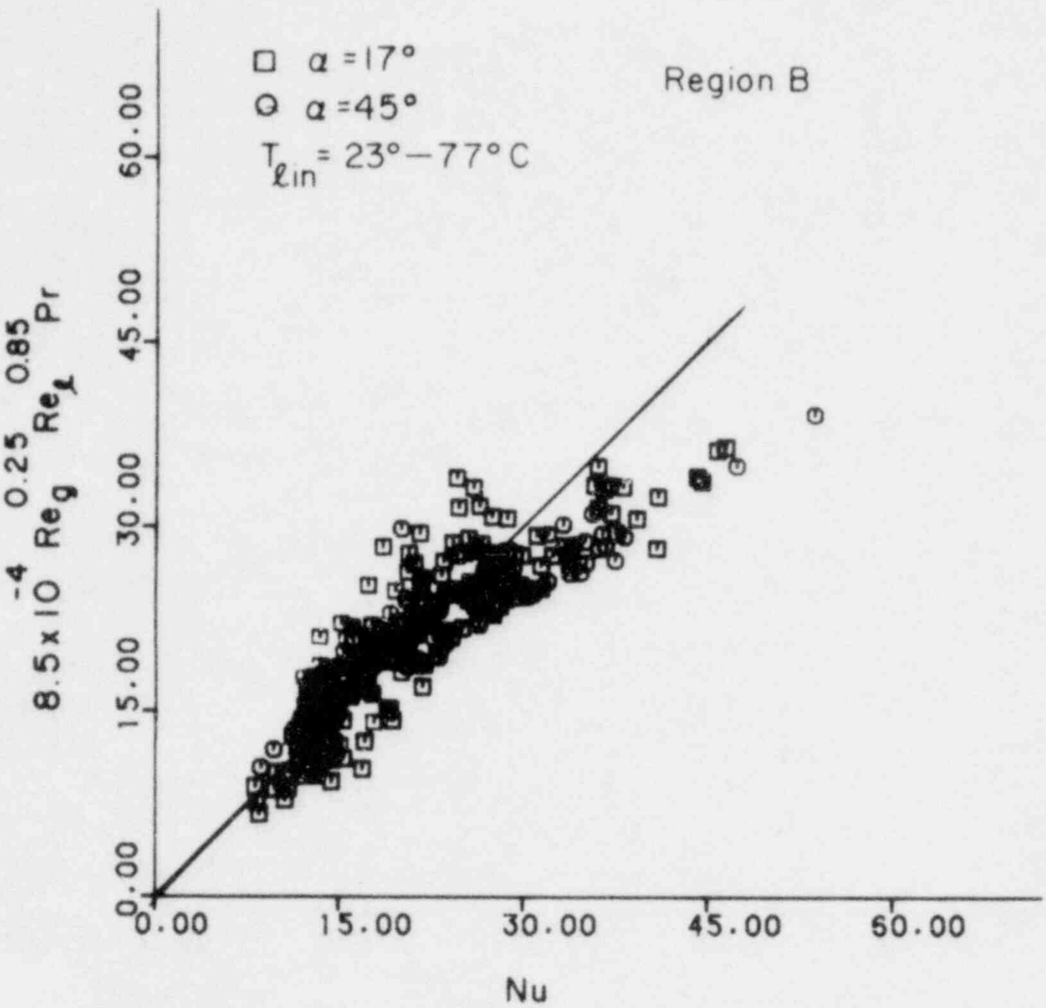

Figure 49. Comparison of Experimental and Predicted Nu For α = 17° and 45° and $T_{\ell in}$ = 23°-77°C

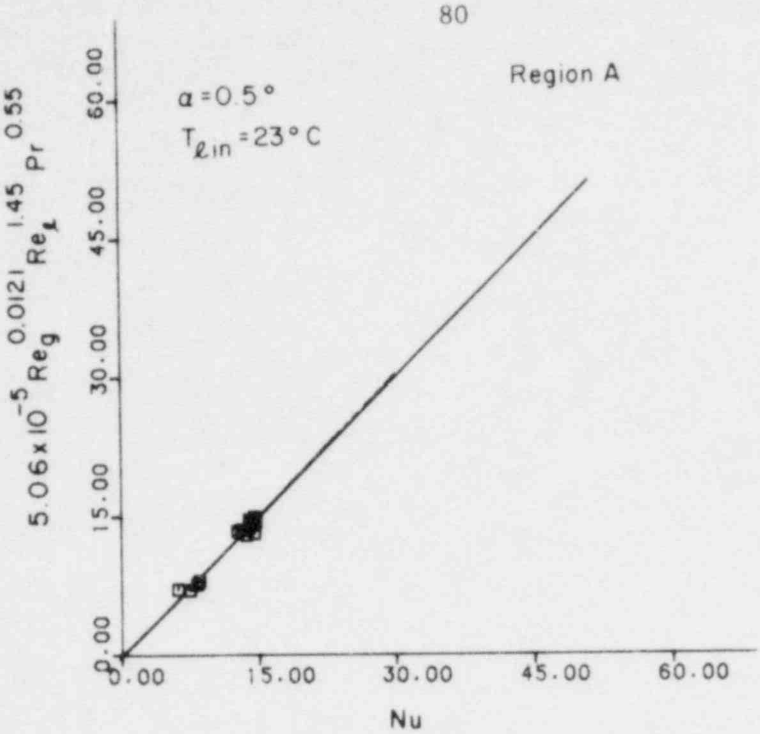

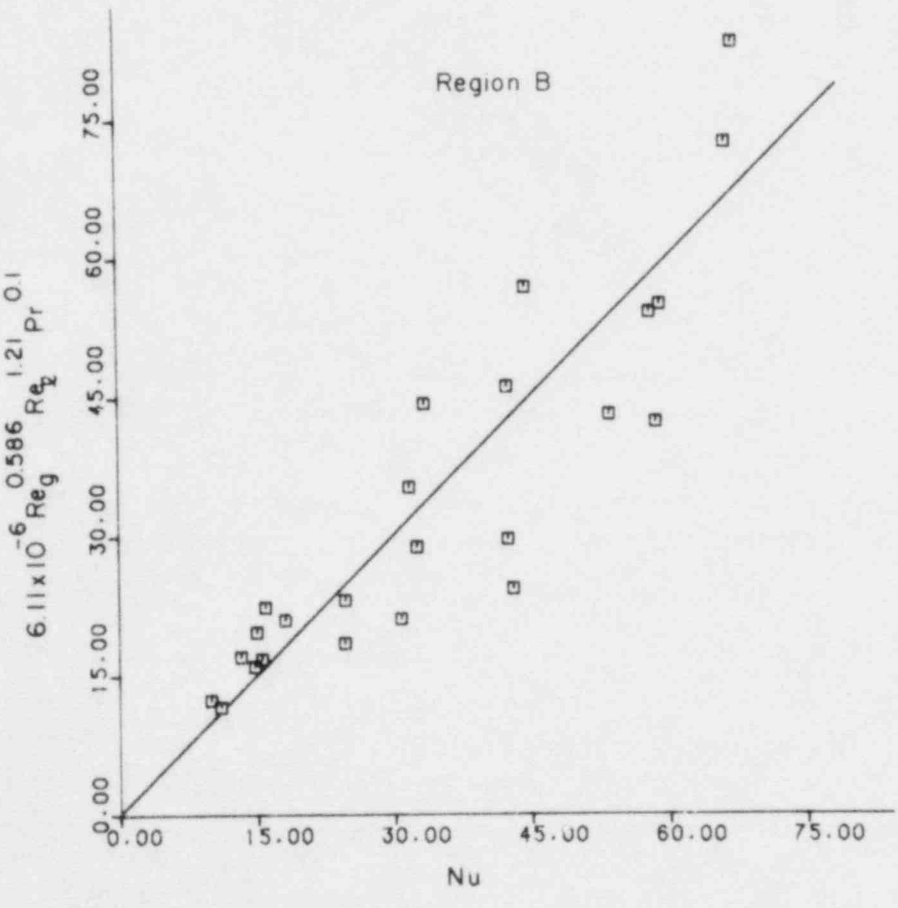

Figure 50. Comparison of Experimental and Predicted Nu For α = 0.5° and $T_{\ell in}$ = 23°C

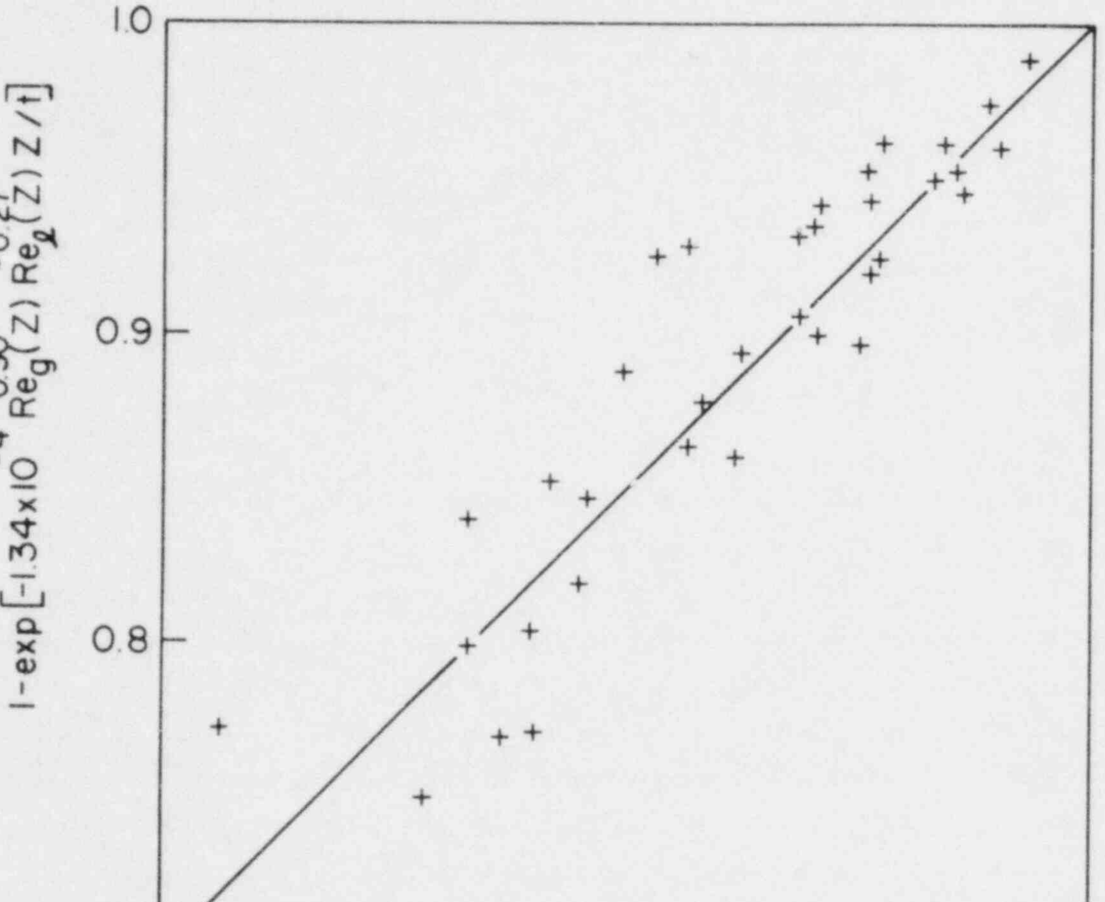

Figure 51. Comparison of Experimental and Predicted Dimensionless Liquid Temperatures

The region relevant to the ECC delivery process, which was observed experimentally in the present apparatus, is Region C where partial bypass occurs. Thus, the surface temperatures in Region C for the inclined tube positions were correlated in terms of local parameters, which resulted in (see Figure 51):

$$\Theta(z) = 1-\exp\left[-1.34.10^{-4}\ Re_g^{0.30}(z)\ Re_\ell^{-0.27}(z)\ \frac{z}{t}\right] \qquad (30)$$

from which f can be easily evaluated.

Summary

An experimental study of steam condensation on subcooled liquid films in countercurrent flow has been conducted in a small test apparatus having a rectangular cross section. Condensation heat transfer coefficients were determined and the dependence on steam and water flow rates, the degree of subcooling and test section inclination angle were all studied. The results were correlated in terms of local conditions for the different wave structure regions observed experimentally.

In the inclined tube positions, the local Nusselt number depends significantly on the local steam and liquid Reynolds numbers and on the local liquid Prandtl number when no bypass occurs. In the bypass region, the Nusselt number is almost independent of the steam flow rate, and it drops sharply due to the strong effects of the reduced liquid flow rate as bypass increases.

In the horizontal position, up to a specific steam mass flow rate, the dependence of Nu on Re_g is very small, whereas for higher steam flow rates Nu is very sensitive to Re_g.

A correlation for the dimensionless surface temperature was developed from which the condensation efficiency can be determined. This correlation is now being incorporated into a one-dimensional model[8] to better describe the downcomer behavior.

Nomenclature

b - channel width

c_p - specific heat of liquid

C - constant

f - condensation efficiency

h - local condensation heat transfer coefficient

h_{fg} - heat of vaporization

h_g - enthalpy of vapor

h_ℓ - enthalpy of liquid

k - thermal conductivity

L - length

Nu - Nusselt number

Pr - Prandtl number of liquid

q' - condensation heat transfer rate per unit area

Re - Reynolds number

T - temperature

t - film thickness

T_s - saturation temperature

W - mass flow rate

W_p^* - dimensionless fractional penetration

z - coordinate

α - degree of inclination

θ - dimensionless temperature

μ - viscosity

Subscripts

c - condensation

g - vapor

in - inlet

ℓ - liquid

REFERENCES

(1) Cudnik, R. A., et al, "Steam-Water Mixing and System Hydrodynamics Program, Task 4", Quarterly Progress Report, January-March 1978, NUREG/CR-0147, BMI-2003 (June, 1978). Available from National Technical Information Service (NTIS), Springfield, Virginia 22161.*

(2) Collier, R. P., et al, "Steam-Water Mixing and System Hydrodynamics Program, Task 4", Quarterly Progress Report, October-December 1978, NUREG/CR-0845, BMI-2028 (May, 1979). Available from National Technical Information Service (NTIS), Springfield, Virginia 22161.*

(3) Shires, G. L., and Pickering, A. R., "The Flooding Phenomenon in Countercurrent Two-Phase Flow", Proceedings, Symposium on Two-Phase Flow, Exeter, England (June 21-23, 1965).

(4) Hewitt, G. F., and Hall-Taylor, N. S., *Annular Two-Phase Flow*, Pergamon Press, p. 71 (1970).

(5) Naff, S. A., and Whitbeck, J. F., "Steady State Investigation of Entrainment and Countercurrent Flow in Small Vessels", Proceedings, ANS Topical Meeting on Water Reactor Safety, Salt Lake City, Utah (March 26-28, 1973).

(6) Collier, R. P., et al, "Status Report on ECC Penetration Scaling Research", NUREG/CR-0651, BMI-2019 (February 1979). Available from National Technical Information Service (NTIS), Springfield, Virginia 22161.*

(7) Block, J. A., et al, "Analysis of ECC Delivery", Topical Report, Creare TN-231 (April 1976). Available from National Technical Information Service (NTIS), Springfield, Virginia 22161.

(8) Segev, A., and Collier, R. P., "Condensation and Vaporization Effects on Countercurrent Steam-Water Flow in an Annulus", *Nonequilibrium Interfacial Transport Processes*, J. C. Chen and S. G. Bankoff, ed., ASME, New York (1979).

(9) Lee, L., et al, "Local Condensaion Rates in Horizontal Cocurrent Steam-Water Flow", *Nonequilibrium Interfacial Transport Processes*, J. C. Chen and S. G. Bankoff, ed., ASME, New York (1979).

---

*Also available from the NRC/GPO Sales Program, U.S. Nuclear Regulatory Commission, Washington, DC 20555.

APPENDIX A

2/15-Scale Air-Water Distorted Geometry Test Data

TABLE A-1. 2/15-SCALE AIR-WATER PLENUM FILL PENETRATION DATA LISTING FOR SHORT CORE BARREL TESTS

Explanation of Column Titles

ID - Identification number

WG - Reverse core gas flow rate, lbm/sec

WL - ECC water penetration flow rate, lbm/sec

WLIN - ECC water injection flow rate, lbm/sec

JGS - Dimensionless reverse core gas flow rate,

$$[\rho_g V_g^2 / g C_a (\rho_L - \rho_g)]^{1/2}$$

JLS - Dimensionless ECC water penetration flow rate,

$$[\rho_L V_L^2 / g C_a (\rho_L - \rho_g)]^{1/2}$$

JSLIN - Dimensionless ECC water injection flow rate,

$$[\rho_L V_{Lin}^2 / g C_a (\rho_L - \rho_g)]^{1/2}$$

PV - Lower plenum gas space pressure, psia

TLIN - ECC water temperature, F

DTLIN - ECC water subcooling, F

LAMBDA - Condensation potential,

$$[C_p (T_{sat} - T_L) / h_{fg}] (\rho_L / \rho_g)^{1/2}$$

DSTAR - Dimensionless characteristic length,

$$C_a [g(\rho_L - \rho_g)/\sigma]^{1/2}$$

Geometric data

Vessel scale	2/15
Vessel inner diameter, in	24.35
Annulus gap width, in	1.23
Annulus length, in	24.87
Annulus circumference, in	72.63
Cold leg diameter, in	4.02
Break leg diameter, in	7.63

ID	WG LBM/SEC	WL LBM/SEC	WLIN LBM/SEC	JGS	JLS	JLSIN	PV PSIA	TLIN F	DTLIN F	LAMBDA	DSTAR
23002	.037	34.556	34.47	.0020	.0640	.0639	14.39	60.22	0.00	0.000	673.71
23003	.868	15.831	34.43	.0429	.0293	.0638	16.55	60.38	0.00	0.000	673.70
23004	1.093	13.654	34.44	.0523	.0253	.0638	17.71	60.59	0.00	0.000	673.74
23005	1.228	13.089	34.44	.0576	.0243	.0638	18.55	60.75	0.00	0.000	673.78
23006	1.380	11.006	34.45	.0638	.0204	.0638	19.21	60.88	0.00	0.000	673.81
23007	1.374	10.209	34.44	.0619	.0189	.0638	20.12	61.20	0.00	0.000	673.89
23008	1.445	11.181	34.50	.0662	.0207	.0639	19.71	61.40	0.00	0.000	673.97
23009	1.738	9.434	34.43	.0763	.0175	.0638	21.49	61.63	0.00	0.000	674.01
23010	1.659	9.630	34.50	.0743	.0178	.0639	20.75	61.78	0.00	0.000	674.08
23011	1.604	10.368	34.52	.0724	.0192	.0640	20.44	61.88	0.00	0.000	674.12
23012	1.524	10.072	34.54	.0691	.0187	.0640	20.27	62.01	0.00	0.000	674.17
23013	1.844	8.603	34.46	.0797	.0159	.0639	22.27	62.33	0.00	0.000	674.23
23014	1.961	7.471	34.44	.0836	.0148	.0638	22.94	62.51	0.00	0.000	674.27
23015	1.954	8.120	34.43	.0820	.0151	.0638	23.60	62.71	0.00	0.000	674.32
23016	2.237	6.830	34.35	.0901	.0127	.0637	25.62	62.93	0.00	0.000	674.33
23017	2.307	7.589	34.37	.0922	.0141	.0637	26.03	63.18	0.00	[illegible]	674.40
23018	2.324	6.704	34.36	.0901	.0124	.0637	27.73	63.43	0.00	0.000	674.44
23019	1.908	7.335	33.75	.0777	.0136	.0626	25.01	63.98	0.00	0.000	674.71
23020	1.563	8.930	33.93	.0685	.0166	.0629	21.55	64.20	0.00	0.000	674.89
23021	1.379	10.603	33.99	.0622	.0197	.0630	20.38	64.32	0.00	0.000	674.97
23022	1.869	8.346	33.83	.0784	.0155	.0627	23.53	64.60	0.00	0.000	674.97
23023	1.735	9.035	33.90	.0754	.0168	.0629	22.00	64.83	0.00	0.000	675.10
23024	1.634	9.168	33.91	.0713	.0170	.0629	21.82	65.02	0.00	0.000	675.17
23025	1.672	8.600	33.95	.0739	.0159	.0629	21.28	65.21	0.00	0.000	675.25
23026	1.420	10.525	34.03	.0650	.0195	.0631	19.86	65.34	0.00	0.000	675.35
23027	1.339	11.551	34.06	.0622	.0214	.0631	19.20	65.42	0.00	0.000	675.39
23028	1.213	12.686	34.09	.0573	.0235	.0632	18.62	65.46	0.00	0.000	675.42
23029	1.089	13.033	34.12	.0523	.0242	.0633	18.06	65.60	0.00	0.000	675.48
23030	1.117	12.885	34.12	.0541	.0239	.0633	17.80	65.71	0.00	0.000	675.53
23031	.759	17.913	34.21	.0384	.0332	.0634	16.33	65.85	0.00	0.000	675.62
23032	1.674	9.203	33.91	.0729	.0171	.0629	21.96	66.18	0.00	0.000	675.57
23033	1.329	10.807	34.07	.0622	.0200	.0632	19.08	66.29	0.00	0.000	675.70
23034	1.479	10.699	34.00	.0671	.0198	.0631	20.28	66.37	0.00	0.000	675.70
23035	1.203	12.724	34.10	.0574	.0236	.0632	18.35	66.50	0.00	0.000	675.79
23036	1.385	11.255	34.01	.0633	.0209	.0631	20.00	66.57	0.00	0.000	675.78
23037	.986	14.940	34.16	.0484	.0277	.0633	17.34	66.71	0.00	0.000	675.90
23103	.939	18.188	52.98	.0453	.0337	.0982	17.39	66.88	0.00	0.000	675.94
23106	.523	25.080	53.24	.0265	.0465	.0987	15.76	67.63	0.00	0.000	676.25
23107	.711	22.022	53.21	.0352	.0408	.0987	16.47	67.79	0.00	0.000	676.28
23108	.782	19.785	53.17	.0381	.0367	.0986	17.09	67.95	0.00	0.000	676.33
23109	.979	19.001	53.13	.0467	.0352	.0985	17.73	68.04	0.00	0.000	676.34
23110	1.148	16.470	53.06	.0540	.0305	.0984	18.64	68.17	0.00	0.000	676.37
23111	1.356	15.200	52.57	.0614	.0282	.0975	20.18	68.30	0.00	0.000	676.37
[illegible]	[illegible]	13.684	52.43	.0723	.0254	.0973	21.66	68.46	0.00	0.000	676.38
[illegible]	[illegible]	12.830	52.30	.0736	.0238	.0970	22.75	68.54	0.00	0.000	676.37
[illegible]	[illegible]	12.769	52.27	.0801	.0237	.0970	23.45	68.68	0.00	0.000	676.39
[illegible]	[illegible]	11.912	52.22	.0787	.0221	.0969	24.10	68.76	0.00	0.000	676.40
[illegible]	1.609	14.662	52.47	.0731	.0272	.0973	21.90	68.88	0.00	0.000	676.52
[illegible]	1.428	15.836	52.60	.0640	.0294	.0976	20.75	69.02	0.00	0.000	676.61
[illegible]	1.239	17.045	52.69	.0569	.0316	.0977	19.73	69.14	0.00	0.000	676.69

ID	WG LBM/SEC	WL LBM/SEC	WLIN LBM/SEC	JGS	JLS	JLSIN	PV PSIA	TLIN F	DTLIN F	LAMBDA	DSTAR
23119	1.146	17.214	52.75	.0536	.0319	.0978	19.05	69.23	0.00	0.000	676.74
23120	.936	20.017	52.63	.0471	.0371	.0980	18.26	69.36	0.00	0.000	676.81
23121	1.016	19.998	52.67	.0490	.0371	.0981	17.91	69.49	0.00	0.000	676.86
23122	.744	19.351	52.95	.0369	.0359	.0982	17.16	69.57	0.00	0.000	676.91
23123	.729	23.147	53.02	.0365	.0423	.0983	16.58	69.67	0.00	0.000	676.96
23124	.527	27.595	53.06	.0269	.0512	.0984	15.96	69.76	0.00	0.000	677.01
23125	.337	32.589	53.15	.0176	.0604	.0986	15.31	69.84	0.00	0.000	677.06
23126	.251	37.536	53.19	.0133	.0696	.0986	14.77	69.90	0.00	0.000	677.09
23129	.446	28.463	65.35	.0226	.0528	.1212	15.86	71.15	0.00	0.000	677.49
23130	.682	24.859	65.02	.0334	.0461	.1206	16.94	71.36	0.00	0.000	677.53
23131	.819	22.819	65.02	.0396	.0423	.1206	17.72	71.61	0.00	0.000	677.61
23132	1.016	22.408	64.92	.0481	.0416	.1204	18.45	71.81	0.00	0.000	677.66
23133	1.144	19.466	64.76	.0527	.0361	.1202	19.53	71.94	0.00	0.000	677.67
23134	1.204	19.345	64.78	.0555	.0359	.1202	19.53	72.06	0.00	0.000	677.72
23135	1.230	18.875	64.65	.0553	.0350	.1200	20.43	72.28	0.00	0.000	677.76
23136	1.471	18.212	64.52	.0647	.0338	.1197	21.42	72.46	0.00	0.000	677.79
23137	1.596	16.434	64.35	.0686	.0305	.1194	22.43	72.58	0.00	0.000	677.80
23138	1.761	15.726	64.11	.0736	.0292	.1190	23.82	72.70	0.00	[illegible]	677.80
23139	1.920	14.148	64.00	.0786	.0263	.1188	24.85	72.79	0.00	0.000	677.79
23140	2.038	13.621	63.91	.0825	.0253	.1187	25.45	72.89	0.00	0.000	677.81
23141	1.910	14.186	63.96	.0775	.0263	.1187	25.37	72.95	0.00	0.000	677.83
23142	1.965	15.592	63.98	.0798	.0289	.1188	25.20	73.09	0.00	0.000	677.88
23143	1.743	16.475	64.22	.0726	.0306	.1192	23.64	73.28	0.00	0.000	678.00
23144	1.616	16.055	64.21	.0682	.0298	.1192	22.94	73.25	0.00	0.000	678.01
23145	1.547	16.051	64.11	.0667	.0298	.1190	21.96	73.27	0.00	0.000	678.05
23146	1.350	17.744	64.17	.0601	.0329	.1191	20.62	73.23	0.00	0.000	678.08
23147	1.282	19.665	64.35	.0578	.0365	.1194	20.12	73.63	0.00	0.000	678.24
23148	1.144	20.690	64.61	.0532	.0384	.1199	19.24	73.81	0.00	0.000	678.34
23149	.971	20.553	64.80	.0459	.0381	.1203	18.60	73.91	0.00	0.000	678.39
23150	.784	27.111	64.98	.0378	.0503	.1206	17.86	74.00	0.00	0.000	678.45
23151	.782	24.810	65.15	.0384	.0460	.1209	17.26	74.08	0.00	0.000	678.49
23152	.637	28.697	65.13	.0305	.0533	.1209	16.53	74.07	0.00	0.000	678.51
23153	.330	44.865	65.19	.0172	.0833	.1210	15.39	74.04	0.00	0.000	678.53
23156	.316	31.366	51.35	.0174	.0596	.0975	15.45	166.80	0.00	0.000	714.76
23157	.540	22.631	51.27	.0277	.0429	.0973	17.08	163.30	0.00	0.000	713.17
23158	.727	19.558	51.20	.0353	.0371	.0971	18.75	161.40	0.00	0.000	712.29
23159	1.077	17.794	51.09	.0485	.0337	.0968	20.50	160.50	0.00	0.300	711.82
23160	1.151	16.095	51.10	.0518	.0305	.0968	20.56	159.60	0.00	0.000	711.42
23161	1.248	15.480	51.01	.0547	.0293	.0966	21.90	158.50	0.00	0.000	710.92
23162	1.500	14.844	50.79	.0624	.0281	.0962	24.65	157.00	0.00	0.000	710.20
23163	1.745	12.818	50.67	.0710	.0243	.0959	25.83	156.30	0.00	0.000	709.87
23164	1.709	11.197	50.60	.0684	.0212	.0958	26.67	155.60	0.00	0.000	709.55
23165	1.923	10.869	50.56	.0758	.0206	.0957	27.62	154.90	0.00	0.000	709.22
23204	.732	18.107	34.73	.0362	.0334	.0644	16.44	70.64	0.00	0.000	677.29
23205	1.111	14.175	34.69	.0523	.0263	.0643	18.24	70.63	0.00	0.000	677.24
23206	1.279	12.465	34.64	.0585	.0231	.0643	19.14	70.52	0.00	0.000	677.18
23207	1.441	11.776	34.62	.0645	.0218	.0642	20.17	70.57	0.00	0.000	677.16
23208	1.634	10.740	34.73	.0701	.0199	.0645	21.14	71.94	0.00	0.000	677.61
23209	1.737	-.705	34.[illegible]0	.0723	.0180	.0646	22.65	72.34	0.00	0.000	677.69

ID	WG LBM/SEC	WL LBM/SEC	WLIN LBM/SEC	JGS	JLS	JLSIN	PV PSIA	TLIN F	DTLIN F	LAMBDA	DSTAR
23210	1.826	9.505	34.80	.0761	.0176	.0646	23.41	72.48	0.00	0.000	677.72
23211	1.825	8.477	34.78	.0741	.0157	.0646	24.70	72.64	0.00	0.000	677.73
23212	1.767	9.312	34.67	.0740	.0173	.0647	23.55	72.76	0.00	0.000	677.82
23213	1.659	9.393	34.85	.0704	.0174	.0647	22.98	72.77	0.00	0.000	677.85
23214	1.629	10.115	34.99	.0706	.0188	.0649	22.01	73.08	0.00	0.000	677.99
23215	1.526	10.750	34.94	.0670	.0200	.0649	[illegible]	73.07	0.00	0.000	678.01
23216	1.272	12.800	35.04	.0587	.0238	.0650	[illegible]	73.23	0.00	0.000	678.13
23217	1.066	14.506	35.26	.0511	.0269	.0654	[illegible]	73.46	0.00	0.000	678.25
23218	.845	16.698	35.35	.0417	.0310	.0656	16.98	73.53	0.00	0.000	678.30
23220	.242	30.175	35.48	.0127	.0560	.0658	15.08	73.73	0.00	0.000	678.42
23221	.314	30.604	35.49	.0164	.0568	[illegible]	15.08	73.83	0.00	0.000	678.46
23222	.359	30.361	35.50	.0188	.0563	.0659	15.09	73.92	0.00	0.000	678.49
23223	.325	30.990	35.51	.0170	.0575	.0659	15.08	73.99	0.00	0.000	678.51
23224	.355	30.205	35.51	.0186	.0561	.0659	15.10	74.03	0.00	0.000	678.53
23225	.328	30.416	35.50	.0172	.0564	.0659	15.10	74.09	0.00	0.000	678.55
23226	.351	30.721	35.51	.0184	.0570	.0659	15.09	74.18	0.00	0.000	678.58
23227	.233	30.378	35.51	.0122	.0564	.0659	15.11	74.25	0.00	0.000	678.61
23228	.333	30.690	35.51	.0174	.0570	.0659	15.10	74.27	0.00	0.000	678.61
23229	.696	18.371	35.46	.0346	.0341	.0658	16.43	74.51	0.00	0.000	678.65
23230	.710	18.869	35.48	.0354	.0350	.0658	16.43	74.63	0.00	0.000	678.70
23231	.739	18.495	35.48	.0368	.0343	.0659	16.47	74.68	0.00	0.000	678.71
23232	.743	18.482	35.48	.0371	.0343	.0659	16.47	74.78	0.00	0.000	678.75
23233	.764	18.376	35.48	.0381	.0341	.0659	16.48	74.88	0.00	0.000	678.79
23234	.759	18.339	35.49	.0379	.0340	.0659	16.48	74.93	0.00	0.000	678.81
23235	.696	18.232	35.49	.0347	.0338	.0659	16.48	75.03	0.00	0.000	678.84
23236	.757	18.718	35.49	.0378	.0347	.0659	16.47	75.07	0.00	0.000	678.86
23237	1.452	11.694	35.29	.0652	.0217	.0655	20.47	75.30	0.00	0.000	678.83
23238	1.411	11.806	35.29	.0632	.0219	.0655	20.61	75.36	0.00	0.000	678.84
23239	1.492	11.625	35.30	.0667	.0216	.0655	20.66	75.47	0.00	0.000	678.88
23240	1.405	11.762	[illegible]	.0629	.0218	.0656	20.62	75.54	0.00	0.000	678.91
23241	1.478	11.475	35.33	[illegible]	.0213	.0656	20.66	75.60	0.00	0.000	678.93
23242	1.475	11.600	35.33	[illegible]	.0215	.0656	20.65	75.65	0.00	0.000	678.95
23243	1.471	11.836	35.33	.0659	.0220	.0656	20.65	75.74	0.00	0 000	678.98
23244	1.381	11.705	35.33	.0618	.0217	.0656	20.68	75.80	0.00	0.000	679.00
23245	1.335	12.770	35.39	.0613	.0237	.0657	19.63	75.94	0.00	0.000	679.08
23246	1.144	14.164	35.45	.0541	.0263	.0658	18.55	76.02	0.00	0.000	679.14
23247	.998	15.708	35.51	.0484	.0292	.0659	17.63	76.13	0.00	0.000	679.20
23248	.721	18.192	35.59	.0362	.0338	.0661	16.42	76.22	0.00	0.000	679.27
23249	.495	24.056	35.65	.0255	.0447	.0662	15.54	76.36	0.00	0.000	679.34
23250	.201	34.721	35.68	.0106	.0645	.0662	14.86	76.46	0.00	0.000	679.40
23251	.192	35.725	51.32	.0101	.0679	.0975	15.15	169.00	0.00	0.000	715.70
23252	.291	33.823	51.32	.0150	.0643	.0975	15.62	168.40	0.00	0.000	715.42
23253	.458	25.948	51.30	.0234	.0493	.0974	16.43	166.10	0.00	0.000	714.38
23254	.551	21.900	50.95	.0272	.0416	.0967	17.53	163.70	0.00	0.000	713.30
23255	.724	20.600	50.81	.0345	.0391	.0964	18.69	162.40	0.00	0.000	712.70
23256	.930	18.925	51.35	[illegible]	.0359	.0974	19.67	161.20	0.00	0.000	712.15
23257	1.042	17.870	51.27	[illegible]	.0339	.0972	20.68	160.40	0.00	0.000	711.78
23258	1.161	16.879	51.21	.0515	.0320	.0971	21.59	159.80	0.00	0.000	711.50
23259	1.214	16.432	51.18	.0533	.0311	.0970	22.03	159.00	0.00	0.000	711.14
23260	1.070	16.916	51.26	.0476	.0320	.0971	21.43	158.50	0.00	0.000	[illegible]
23261	.827	18.794	51.39	.0381	.0356	.0973	20.00	157.80	0.00	0.000	710.68
23262	.906	19.536	51.47	.0425	.0370	.0975	19.34	157.20	0.00	0.000	710.44
23263	.736	20.162	51.55	.0352	.0382	.0976	18.61	156.80	0.00	0.000	710.29
23264	.654	22.120	51.65	.0321	.0419	.0978	17.60	156.20	0.00	0.000	710.06

ID	WG LBM/SEC	WL LBM/SEC	WLIN LBM/SEC	JGS	JLS	JLSIN	PV PSIA	TLIN F	DTLIN F	LAMBDA	DSTAR
23265	.441	25.641	51.75	.0224	.0485	.0979	16.55	155.80	0.00	0.000	709.92
23266	.330	32.570	51.64	.0172	.0616	.0981	15.71	155.50	0.00	0.000	709.82
23267	.781	20.870	51.60	.0377	.0395	.0976	18.34	155.00	0.00	0.000	709.53
23268	1.217	16.730	51.33	.0543	.0317	.0971	21.44	154.40	0.00	0.000	709.18
23269	1.275	15.975	51.25	.0558	.0302	.0970	22.26	154.00	0.00	0.000	708.99
23270	1.323	15.526	51.25	.0574	.0294	.0969	22.68	153.50	0.00	0.000	708.77
23271	1.448	15.351	51.15	.0620	.0290	.0967	23.28	153.00	0.00	0.000	708.54
23272	1.518	14.632	51.05	.0632	.0277	.0965	24.55	152.50	0.00	0.000	708.29
23273	1.673	13.283	50.93	.0678	.0251	.0963	25.92	151.90	0.00	0.000	708.00
23274	1.778	12.974	50.66	.0710	.0245	.0961	26.71	151.30	0.00	0.000	707.73
23275	1.319	12.445	50.79	.0714	.0235	.0960	27.61	150.60	0.00	0.000	707.41
23276	1.892	12.197	50.79	.0732	.0230	.0960	28.02	149.80	0.00	0.000	707.05
23277	1.307	12.207	50.63	.0698	.0231	.0960	27.93	148.70	0.00	0.000	706.59
23278	1.728	12.332	50.65	.0669	.0233	.0960	27.78	147.90	0.00	0.000	706.25
23279	1.633	12.323	50.67	.0652	.0233	.0960	27.74	147.10	0.00	0.000	705.92

TABLE A-2. 2/15-SCALE AIR-WATER PLENUM FILL PENETRATION DATA LISTING FOR EXTENDED CORE BARREL TESTS

Explanation of Column Titles

ID - Identification number

WG - Reverse core gas flow rate, lbm/sec

WL - ECC water penetration flow rate, lbm/sec

WLIN - ECC water injection flow rate, lbm/sec

JGS - Dimensionless reverse core gas flow rate,

$[\rho_g V_g^2/gC_a(\rho_L - \rho_g)]^{1/2}$

JLS - Dimensionless ECC water penetration flow rate,

$[\rho_L V_L^2/gC_a(\rho_L - \rho_g)]^{1/2}$

JSLIN - Dimensionless ECC water injection flow rate,

$[\rho_L V_{Lin}^2/gC_a(\rho_L - \rho_g)]^{1/2}$

PV - Lower plenum gas space pressure, psia

TLIN - ECC water temperature, F

DTLIN - ECC water subcooling, F

LAMBDA - Condensation potential,

$[C_P(T_{sat} - T_L)/h_{fg}](\rho_L/\rho_g)^{1/2}$

DSTAR - Dimensionless characteristic length,

$C_a[g(\rho_L - \rho_g)/\sigma]^{1/2}$

Geometric data

Vessel scale	2/15
Vessel inner diameter, in	24.35
Annulus gap width, in	1.23
Annulus length, in	66.00
Annulus circumference in	72.63
Cold leg diameter,	4.02
Break leg diamete in	7.63

ID	WG LBM/SEC	WL LBM/SEC	WLIN LBM/SEC	JGS	JLS	JLSIN	PV PSIA	TLIN F	DTLIN F	LAMBDA	DSTAR
23703	.834	15.972	34.35	.0418	.0296	.0637	16.25	72.19	0.00	0.000	677.84
23704	1.305	6.822	34.20	.0609	.0127	.0635	18.68	72.34	0.00	0.000	677.83
23705	1.274	4.393	34.17	.0582	.0082	.0634	19.50	72.40	0.00	0.000	677.83
23706	1.277	3.152	34.14	.0582	.0058	.0634	19.61	72.53	0.00	0.000	677.87
23707	1.363	3.523	34.15	.0616	.0065	.0634	20.04	72.60	0.00	0.000	677.88
23708	1.375	2.776	34.12	.0615	.0052	.0633	20.47	72.69	0.00	0.000	677.90
23709	1.294	3.053	34.14	.0582	.0057	.0634	20.34	72.78	0.00	0.000	677.94
23710	1.201	3.775	34.10	.0546	.0070	.0633	19.92	72.87	0.00	0.000	677.99
23711	1.602	2.825	34.10	.0712	.0052	.0633	20.78	71.72	0.00	0.000	677.55
23712	1.781	1.579	34.02	.0760	.0029	.0631	22.61	71.48	0.00	0.000	677.40
23713	1.584	2.433	34.10	.0697	.0045	.0633	21.21	71.51	0.00	0.000	677.46
23714	1.269	3.265	34.15	.0574	.0061	.0634	20.10	71.33	0.00	0.000	677.44
23715	1.259	4.581	34.23	.0584	.0085	.0635	19.05	71.57	0.00	0.000	677.55
23716	1.158	7.853	34.27	.0555	.0146	.0636	17.88	71.71	0.00	0.000	677.63
23717	.866	13.571	34.00	.0375	.0252	.0631	21.92	71.88	0.00	0.000	677.57
23718	.730	21.407	52.84	.0321	.0397	.0981	21.26	71.41	0.00	0.000	677.43
23719	.994	13.088	52.93	.0446	.0243	.0982	20.32	71.19	0.00	0.000	677.38
23720	1.312	6.999	52.93	.0584	.0130	.0982	20.70	71.52	0.00	0.000	677.48
23721	1.592	3.257	52.85	.0691	.0060	.0981	21.79	70.84	0.00	0.000	677.21
23722	1.739	2.036	52.66	.0729	.0038	.0977	23.42	71.39	0.00	0.000	677.34
23723	1.774	2.070	52.52	.0732	.0038	.0975	24.67	70.93	0.00	0.000	677.15
23724	1.343	7.826	52.81	.0581	.0145	.0980	22.52	71.40	0.00	0.000	677.39
23725	1.281	9.161	52.82	.0559	.0170	.0980	22.13	70.95	0.00	0.000	677.25
23726	1.050	9.673	52.88	.0462	.0179	.0981	21.70	71.26	0.00	0.000	677.37
23727	1.072	10.180	52.97	.0477	.0189	.0983	21.01	71.03	0.00	0.000	677.31
23728	.921	15.344	52.79	.0398	.0285	.0980	22.26	71.26	0.00	0.000	677.34
23729	.499	24.430	53.02	.0226	.0453	.0984	20.17	71.43	0.00	0.000	677.48
23730	.437	29.387	65.53	.0186	.0545	.1216	22.72	70.53	0.00	0.000	677.06
23731	.560	23.246	65.77	.0245	.0431	.1220	21.71	70.77	0.00	0.000	677.19
23732	.698	21.379	65.81	.0307	.0397	.1221	21.26	70.96	0.00	0.000	677.27
23733	.769	17.450	65.60	.0329	.0324	.1217	22.41	71.08	0.00	0.000	677.27
23734	.891	17.020	65.60	.0382	.0316	.1217	22.31	71.26	0.00	0.000	677.33
23735	1.055	13.813	65.36	.0438	.0256	.1213	23.88	70.80	0.00	0.000	677.11
23736	1.182	10.434	65.29	.0483	.0194	.1212	24.61	71.13	0.00	0.000	677.20
23737	1.206	9.688	65.23	.0491	.0180	.1211	24.88	71.20	0.00	0.000	677.22
23738	1.342	6.298	65.07	.0539	.0117	.1208	25.99	71.10	0.00	0.000	677.15
23739	1.506	5.393	64.90	.0597	.0100	.1205	26.74	70.98	0.00	0.000	677.09
23740	1.523	3.649	64.78	.0597	.0068	.1203	27.39	71.21	0.00	0.000	677.14
23741	1.599	4.181	64.72	.0623	.0078	.1201	27.83	70.40	0.00	0.000	676.84
23742	1.610	3.798	64.73	.0626	.0071	.1202	27.92	70.95	0.00	0.000	677.03
23743	1.631	3.466	64.71	.0637	.0064	.1201	27.75	71.16	0.00	0.000	677.11
23744	1.543	3.580	64.74	.0602	.0066	.1202	27.82	71.33	0.00	0.000	677.17
23745	1.475	4.580	64.60	.0579	.0085	.1203	27.45	71.45	0.00	0.000	677.23
23746	1.534	4.266	64.79	.0599	.0079	.1203	27.78	70.83	0.00	0.000	677.00
23747	1.544	4.229	64.85	.0608	.0078	.1204	27.33	71.27	0.00	0.000	677.17
23748	1.524	4.759	64.90	.0603	.0088	.1205	27.03	70.70	0.00	0.000	676.98
23749	1.275	7.381	65.07	.0516	.0137	.1208	25.81	70.94	0.00	0.000	677.11
23750	1.010	11.842	65.28	.0419	.0220	.1211	24.61	71.22	0.00	0.000	677.26

ID	WG LBM/SEC	WL LBM/SEC	WLIN LBM/SEC	JGS	JLS	JLSIN	PV PSIA	TLIN F	DTLIN F	LAMBDA	DSTAR
23751	.886	15.770	65.62	.0379	.0293	.1218	22.88	71.40	0.00	0.000	677.38
23752	.592	23.780	65.77	.0257	.0441	.1220	22.12	70.31	0.00	0.000	677.02
23753	.403	28.444	65.03	.0160	.0528	.1207	26.30	70.82	0.00	0.000	677.04
23754	.393	29.239	34.15	.0144	.0543	.0634	30.92	71.49	0.00	0.000	677.11
23755	.492	27.474	34.19	.0185	.0510	.0635	29.59	71.13	0.00	0.000	677.02
23756	.520	25.113	34.21	.0197	.0466	.0635	28.87	71.47	0.00	0.000	677.17
23757	.904	18.591	34.21	.0340	.0345	.0635	29.18	71.72	0.00	0.000	677.24
23758	1.047	13.540	34.32	.0407	.0251	.0637	27.24	71.31	0.00	0.000	677.17
23759	1.122	12.381	34.15	.0415	.0230	.0634	30.13	71.52	0.00	0.000	677.13
23760	1.260	7.513	34.36	.0497	.0139	.0638	26.40	71.76	0.00	0.000	677.36
23761	1.451	6.107	34.27	.0553	.0113	.0636	28.74	70.73	0.00	0.000	676.92
23762	1.613	2.714	34.44	.0665	.0050	.0639	24.82	71.03	0.00	0.000	677.18
23763	1.698	2.534	34.38	.0687	.0047	.0638	25.84	71.43	0.00	0.000	677.28
23764	1.700	1.684	34.56	.0735	.0031	.0641	22.63	71.61	0.00	0.000	677.46
23765	1.865	1.264	34.52	.0790	.0023	.0641	23.59	71.40	0.00	0.000	677.36
23766	1.903	1.476	34.48	.0798	.0027	.0640	24.12	71.74	0.00	0.000	677.46
23767	1.644	1.790	34.56	.0713	.0033	.0641	22.56	71.61	0.00	0.000	677.47
23768	1.471	3.701	34.49	.0632	.0069	.0640	23.02	71.68	0.00	0.000	677.48
23769	1.186	5.597	34.62	.0543	.0104	.0642	20.20	71.46	0.00	0.000	677.50
23770	.593	23.070	34.42	.0252	.0428	.0639	23.52	71.74	0.00	0.000	677.48
23802	.235	23.226	51.29	.0102	.0441	.0974	26.11	166.80	0.00	0.000	714.51
23803	.374	20.288	51.74	.0176	.0385	.0983	21.29	166.20	0.00	0.000	714.35
23804	.513	20.225	51.61	.0230	.0384	.0980	22.38	165.50	0.00	0.000	713.98
23805	.728	16.914	51.30	.0301	.0321	.0974	25.60	165.00	0.00	0.000	713.65
23806	.891	12.132	51.55	.0380	.0230	.0979	23.61	164.40	0.00	0.000	713.43
23807	1.025	10.290	51.43	.0424	.0195	.0976	25.06	163.80	0.00	0.000	713.13
23808	1.170	5.539	51.74	.0518	.0105	.0982	22.25	163.10	0.00	0.000	712.92
23809	1.290	5.164	51.68	.0562	.0098	.0980	22.98	162.60	0.00	0.000	712.68
23810	1.363	3.867	51.55	.0582	.0073	.0978	24.10	162.10	0.00	0.000	712.43
23811	1.453	2.734	51.50	.0610	.0052	.0977	24.95	161.70	0.00	0.000	712.2[illegible]
23812	1.564	2.061	51.45	.0646	.0039	.0976	25.71	161.10	0.00	0.000	711.[illegible]6
23813	1.680	1.804	51.42	.0686	.0034	.0975	26.29	160.40	0.00	0.000	71[illegible].64
23814	1.780	1.393	51.38	.0714	.0026	.0974	27.23	159.60	0.00	0.000	711.27
23815	1.833	1.134	51.36	.0732	.0021	.0973	27.54	158.10	0.00	0.000	710.61
23816	1.879	1.014	51.35	.0745	.0019	.0973	27.94	157.20	0.00	0.000	710.21
23817	1.940	1.116	51.34	.0761	.0021	.0972	28.46	156.40	0.00	0.000	709.86
23818	1.795	1.404	51.51	.0723	.0027	.0975	27.05	155.60	0.00	0.000	709.56
23819	1.565	2.114	51.69	.0650	.0040	.0978	25.42	154.80	0.00	0.000	709.26
23820	1.502	2.816	51.79	.0638	.0053	.0980	24.33	154.30	0.00	0.000	709.08
23821	1.256	4.694	52.01	.0555	.0089	.0984	22.45	153.60	0.00	0.000	708.84
23822	1.097	5.211	52.15	.0497	.0099	.0986	21.38	153.10	0.00	0.000	708.65
23823	.831	9.925	52.27	.0387	.0188	.0988	20.18	152.60	0.00	0.000	708.48
23824	.726	14.319	51.98	.0317	.0271	.0983	23.00	152.30	0.00	0.000	708.27
23825	.628	18.990	52.18	.0288	.0359	.0986	20.81	152.00	0.00	0.000	708.21
23826	.437	21.456	52.35	.0211	.0406	.0989	18.48	152.00	0.00	0.000	708.26

ID	WG LBM/SEC	WL LBM/SEC	WLIN LBM/SEC	JGS	JLS	JLSIN	PV PSIA	TLIN F	DTLIN F	LAMBDA	DSTAR
24703	.003	14.935	16.82	.0002	.0277	.0312	16.38	73.23	0.00	0.000	678.22
24705	.003	14.189	16.83	.0002	.0263	.0312	16.18	72.13	0.00	0.000	677.84
24708	.382	13.258	16.94	.0180	.0246	.0314	18.48	69.30	0.00	0.000	676.78
24709	.537	12.219	16.92	.0247	.0227	.0314	19.57	69.13	0.00	0.000	676.69
24710	.742	10.018	16.94	.0334	.0186	.0314	20.26	69.91	0.00	0.000	676.94
24711	.892	8.966	16.93	.0408	.0166	.0314	19.82	69.86	0.00	0.000	676.94
24712	.962	6.923	16.93	[illegible]	.0128	.0314	19.87	70.15	0.00	0.000	677.04
24713	1.103	3.776	16.88	.0485	.0070	.0313	21.44	70.36	0.00	0.000	677.06
24714	1.035	5.074	16.89	.0461	.0094	.0313	20.82	70.61	0.00	0.000	[illegible]
24715	1.194	3.337	16.84	.0510	.0062	.0313	22.67	70.91	0.00	0.000	677.20
24716	1.162	2.832	16.86	.0496	.0053	.0313	22.73	71.18	0.00	0.000	677.30
24717	1.246	2.622	16.66	.0522	.0049	.0309	23.74	71.59	0.00	0.000	677.41
24718	1.222	1.800	16.70	.0596	.0033	.0310	17.80	71.77	0.00	0.000	677.67
24719	1.327	1.200	16.69	.0638	.0022	.0310	18.29	72.14	0.00	0.000	677.79
24720	1.358	1.263	16.70	.0651	.0023	.0310	18.48	72.58	0.00	0.000	677.94
24727	.358	29.323	35.00	.0177	.0544	.0649	16.86	69.68	0.00	0.000	676.96
24728	.434	22.334	35.03	.0222	.0414	.0650	15.62	69.49	0.00	0.000	676.92
24729	.481	21.487	35.06	.0244	.0399	.0650	15.93	69.41	0.00	0.000	676.88
24730	.518	21.488	34.97	.0260	.0399	.0648	16.47	68.84	0.00	0.000	676.67
24731	.556	21.942	34.99	.0275	.0407	.0649	16.89	68.96	0.00	0.000	676.70
24736	.112	35.006	53.09	.0054	.0649	.0985	17.81	69.65	0.00	0.000	676.92
24737	.175	32.571	52.71	.0077	.0604	.0978	21.75	69.78	0.00	0.000	676.85
24739	.375	29.322	53.16	.0180	.0544	.0986	17.89	69.89	0.00	0.000	677.00
24740	.452	26.742	52.96	.0211	.0496	.0983	19.03	70.08	0.00	0.000	677.04
24741	.527	21.338	52.85	.0238	.0396	.0981	20.35	70.13	0.00	0.000	677.02
24742	.587	21.634	52.67	.0257	.0401	.0977	21.55	70.17	0.00	0.000	676.99
24746	.088	46.419	66.62	.0047	.0861	.1236	14.79	71.62	0.00	0.000	677.70
24747	.154	39.104	66.41	.0078	.0725	.1232	15.89	71.87	0.00	0.000	677.75
24748	.233	44.815	66.28	.0117	.0831	.1230	16.56	71.87	0.00	0.000	677.73
24750	[illegible]	25.477	65.86	.0168	.0473	.1222	19.59	72.12	0.00	0.000	677.74
24752	.498	22.820	[illegible]	.0233	.0423	.1224	18.81	71.34	0.00	0.000	677.48
24753	.576	21.343	66.10	.0272	.0396	.1226	18.40	71.03	0.00	0.000	677.38
24754	.626	20.977	66.30	.0302	.0389	.1230	17.73	70.81	0.00	0.000	677.33
24755	.047	12.542	16.10	.0024	.0239	.0306	17.19	173.60	0.00	0.000	717.73
24756	.171	12.917	16.10	.0087	.0246	.0306	17.06	173.50	0.00	0.000	717.68
24757	.239	12.464	16.10	.0113	.0237	.0306	17.77	173.40	0.00	0.000	717.61
24758	.326	13.084	16.09	.0170	.0249	.0306	16.48	173.40	0.00	0.000	717.66
24759	.411	12.070	16.09	.0211	.0230	.0306	17.10	173.40	0.00	0.000	717.64
24760	.380	11.904	16.05	.0187	.0227	.0306	17.97	173.30	0.00	0.000	717.55
24761	.531	10.804	16.03	.0255	.0206	.0305	19.01	173.00	0.00	0.000	717.39
24762	.549	10.708	16.07	.0283	.0204	.0306	16.34	173.10	0.00	0.000	717.51
24763	.612	10.086	16.06	.0314	.0192	.0306	16.97	173.00	0.00	0.000	717.46
24764	.695	8.517	16.03	.0343	.0162	.0305	18.37	172.80	0.00	0.000	717.33
24765	.819	6.442	16.10	.0395	.0122	.0306	19.21	168.70	0.00	0.000	715.48

ID	WG LBM/SEC	WL LBM/SEC	WLIN LBM/SEC	JGS	JLS	JLSIN	PV PSIA	TLIN F	DTLIN F	LAMBDA	DSTAR
24766	.860	4.364	16.20	.0405	.0083	.0308	20.26	165.50	0.00	0.000	714.04
24767	.846	6.605	16.20	.0408	.0125	.0307	19.25	164.40	0.00	0.000	713.58
24768	.949	3.840	16.19	.0443	.0073	.0307	20.55	164.00	0.00	0.000	713.37
24769	.889	2.446	16.20	.0447	.0046	.0307	17.72	163.90	0.00	0.000	713.41
24770	.902	3.541	16.19	.0457	.0067	.0307	17.39	164.00	0.00	0.000	713.46
24771	.902	3.347	16.19	.0457	.0064	.0307	17.39	164.00	0.00	0.000	713.46
24772	.978	2.058	16.18	.0486	.0039	.0307	18.04	163.90	0.00	0.000	713.40
24773	1.040	2.115	16.16	.0511	.0040	.0307	18.43	163.80	0.00	0.000	713.34
24774	1.126	1.400	16.15	.0546	.0027	.0306	18.90	163.80	0.00	0.000	713.33
24775	1.176	1.486	16.13	.0569	.0028	.0306	19.03	163.70	0.00	0.000	713.28
24802	.163	31.050	34.22	.0082	.0590	.0650	18.40	166.40	0.00	0.000	714.50
24803	.211	31.054	34.22	.0107	.0590	.0650	18.65	166.10	0.00	0.000	714.38
24804	.330	27.297	34.09	.0159	.0518	.0647	20.27	165.80	0.00	0.000	714.20
24805	.377	23.191	34.10	.0178	.0440	.0647	20.52	165.60	0.00	0.000	714.09
24806	.461	19.513	34.07	.0218	.0370	.0647	20.58	165.40	0.00	0.000	714.00
24807	.518	18.395	34.05	.0236	.0349	.0647	21.22	165.10	0.00	0.000	713.83
24808	.589	15.816	33.99	.0261	.0300	.0645	22.27	164.90	0.00	0.000	713.70
24809	.666	13.594	33.97	.0286	.0258	.0645	23.47	164.50	0.00	0.000	713.48
24810	.740	12.133	34.02	.0326	.0230	.0646	22.19	164.00	0.00	0.000	713.30
24811	.830	10.169	34.00	.0367	.0193	.0645	22.08	163.90	0.00	0.000	713.26
24812	.877	8.016	34.19	.0403	.0152	.0649	20.23	163.50	0.00	0.000	713.14
24813	.829	7.851	34.19	.0383	.0149	.0649	20.37	163.10	0.00	0.000	712.97
24814	.960	6.174	34.45	.0438	.0117	.0653	20.85	162.60	0.00	0.000	712.74
24815	1.034	4.780	34.32	.0465	.0091	.0651	21.33	162.30	0.00	0.000	712.60
24816	1.077	4.427	34.38	.0484	.0084	.0652	21.83	161.70	0.00	0.000	712.33
24817	1.190	3.210	34.42	.0526	.0061	.0653	22.57	161.30	0.00	0.000	712.14
24818	1.255	2.857	34.38	.0548	.0054	.0652	23.07	160.70	0.00	0.000	711.86
24819	1.204	3.111	34.40	.0531	.0059	.0652	22.67	160.50	0.00	0.000	711.79
24820	1.266	3.021	34.22	.0549	.0057	.0649	23.44	159.90	0.00	0.000	711.51
24821	1.271	2.871	34.37	.0546	.0054	.0651	23.84	159.50	0.00	0.000	711.32
24822	1.382	2.801	34.06	.0593	.0053	.0645	23.92	159.10	0.00	0.000	711.15
24823	1.376	2.553	34.24	.0586	.0048	.0649	24.24	158.70	0.00	0.000	710.97
24824	1.434	2.665	34.27	.0610	.0050	.0649	24.32	158.40	0.00	0.000	710.83
24825	1.400	2.432	34.39	.0594	.0046	.0651	24.39	157.70	0.00	0.000	710.53
24826	1.406	2.473	34.42	.0595	.0047	.0652	24.24	157.30	0.00	0.000	710.36
24827	1.312	2.144	34.42	.0556	.0041	.0652	24.40	156.90	0.00	0.000	710.18
24828	1.402	2.228	34.41	.0592	.0042	.0652	24.57	156.70	0.00	0.000	710.09
24830	1.485	1.776	34.40	.0620	.0034	.0651	25.18	155.70	0.00	0.000	709.69
24831	1.603	1.608	34.38	.0658	.0030	.0651	26.03	155.10	0.00	0.000	709.37
24832	1.641	1.571	34.36	.0667	.0030	.0650	26.51	154.60	0.00	0.000	709.14
24834	.204	26.204	52.57	.0096	.0499	.1000	21.79	172.00	0.00	0.000	716.92
24835	.324	27.784	52.36	.0147	.0529	.0997	23.07	172.30	0.00	0.000	717.02
24836	.390	25.869	52.34	.0170	.0492	.0996	23.79	172.10	0.00	0.000	716.87
24838	.454	25.188	52.54	.0203	.0479	.1000	23.01	171.40	0.00	0.000	716.60
24839	.361	22.774	52.49	.0160	.0433	.0999	23.54	171.10	0.00	0.000	716.45
24841	.577	18.537	52.23	.0253	.0353	.0994	23.91	171.00	0.00	0.000	716.39
24842	.214	35.764	64.71	.0100	.0680	.1230	22.40	169.30	0.00	0.000	715.71
24845	.376	28.217	64.51	.0166	.0536	.1226	23.91	168.90	0.00	0.000	715.47
24847	.416	25.026	64.66	.0182	.0476	.1229	23.26	168.60	0.00	0.000	715.32
24848	.538	23.850	64.37	.0234	.0453	.1224	24.09	168.50	0.00	0.000	715.27

ID	WG LBM/SEC	WL LBM/SEC	WLIN LBM/SEC	JGS	JLS	JLSIN	PV PSIA	TLIN F	DTLIN F	LAMBDA	DSTAR
24849	.572	21.491	64.59	.0250	.0408	.1228	23.78	168.40	0.00	0.000	715.23
24850	.185	30.844	63.78	.0088	.0596	.1232	22.04	210.90	0.00	0.000	735.56
24851	.152	25.822	63.67	.0072	.0499	.1230	22.50	210.20	0.00	0.000	735.21
24852	.354	21.689	63.30	.0160	.0419	.1222	23.25	210.00	0.00	0.000	735.04
24853	.427	21.214	63.34	.0194	.0408	.1220	23.29	202.80	0.00	0.000	731.42
24854	.535	17.985	63.51	.0233	.0346	.1222	24.14	201.40	0.00	0.000	730.67
24855	.630	15.650	63.51	.0265	.0301	.1222	25.48	200.40	0.00	0.000	730.13
24856	.738	13.298	63.43	.0304	.0256	.1220	26.32	199.90	0.00	0.000	729.85
24857	.810	13.693	63.26	.0330	.0263	.1217	27.26	199.70	0.00	0.000	729.73
24858	.877	9.857	63.15	.0377	.0190	.1214	24.89	199.20	0.00	0.000	729.57
24859	.943	8.728	62.13	.0398	.0168	.1195	25.63	198.70	0.00	0.000	729.30
24860	1.041	7.547	62.08	.0435	.0145	.1193	26.24	198.10	0.00	0.000	728.99
24862	1.124	6.018	62.02	.0458	.0116	.1192	27.68	196.80	0.00	0.000	728.31
24863	1.266	4.918	61.94	.0509	.0094	.1190	28.36	196.30	0.00	0.000	728.05
24864	1.289	4.069	61.85	.0510	.0078	.1188	29.15	195.40	0.00	0.000	727.58
24865	1.394	3.543	61.73	.0546	.0068	.1185	29.70	194.80	0.00	0.000	727.27
24866	1.408	3.125	61.78	.0545	.0060	.1186	30.33	194.00	0.00	0.000	726.87
24867	1.425	2.748	61.77	.0543	.0053	.1185	30.96	193.10	0.00	0.000	726.41
24868	1.509	2.236	60.68	.0570	.0043	.1162	31.32	188.90	0.00	0.000	724.39
24869	1.624	1.965	61.67	.0606	.0038	.1182	32.16	190.80	0.00	0.000	725.27
24870	1.729	1.878	61.50	.0642	.0036	.1178	32.34	189.00	0.00	0.000	724.41
24871	1.734	1.808	61.67	.0644	.0035	.1181	32.39	187.80	0.00	0.000	723.84
24872	1.647	1.549	61.58	.0609	.0030	.1179	32.77	186.70	0.00	0.000	723.31
24873	.146	27.197	50.99	.0068	.0525	.0985	21.55	211.10	0.00	0.000	735.64
24874	.234	23.502	51.05	.0114	.0453	.0985	21.95	207.20	0.00	0.000	733.70
24876	.391	21.738	50.48	.0173	.0419	.0973	25.39	204.40	0.00	0.000	732.18
24877	.420	19.114	50.46	.0182	.0368	.0972	26.96	203.60	0.00	0.000	731.75
24878	.500	17.426	50.60	.0216	.0336	.0974	26.09	203.00	0.00	0.000	731.45
24879	.562	16.495	50.60	.0236	.0318	.0974	25.62	202.60	0.00	0.000	731.21
24880	.662	14.865	50.59	.0274	.0286	.0974	25.99	202.10	0.00	0.000	730.94
24881	.726	13.840	50.59	.0302	.0266	.0974	25.62	201.70	0.00	0.000	730.75
24882	.779	8.835	50.79	.0330	.0170	.0977	24.59	201.10	0.00	0.000	730.48
24883	1.020	6.560	50.84	.0423	.0126	.0978	25.63	200.70	0.00	0.000	730.25
24885	1.061	5.324	50.60	.0427	.0102	.0973	27.08	199.70	0.00	0.000	729.71
24886	1.233	4.146	50.62	.0497	.0080	.0974	27.94	199.40	0.00	0.000	729.57
24887	1.395	3.333	50.66	.0551	.0064	.0974	28.97	198.90	0.00	0.000	729.29
24888	1.392	2.949	50.46	.0543	.0057	.0970	29.67	198.10	0.00	0.000	728.88
24889	1.437	2.288	50.38	.0551	.0044	.0968	30.60	197.40	0.00	0.000	728.50
24890	1.599	2.054	50.30	.0606	.0039	.0967	31.31	196.60	0.00	0.000	728.09
24891	1.697	1.781	50.27	.0639	.0034	.0965	31.69	195.70	0.00	0.000	727.64
24892	1.708	1.549	50.21	.0635	.0030	.0964	32.34	194.40	0.00	0.000	726.99
24893	1.730	1.427	50.25	.0643	.0027	.0964	32.45	191.90	0.00	0.000	725.79
24902	.296	31.497	33.18	.0131	.0608	.0641	25.23	210.70	0.00	0.000	735.37
24903	.388	25.691	33.19	.0169	.0496	.0641	27.47	210.10	0.00	0.000	735.05
24904	.454	22.086	33.09	.0197	.0427	.0639	26.97	210.30	0.00	0.000	735.14
24905	.519	19.003	33.23	.0239	.0367	.0642	23.32	210.10	0.00	0.000	735.12
24906	.603	16.155	33.30	.0270	.0312	.0642	23.50	207.00	0.00	0.000	733.50
24907	.720	14.767	33.32	.0314	.0285	.0643	24.82	206.20	0.00	0.000	733.06
24908	.683	14.279	33.32	.0288	.0275	.0642	25.97	205.40	0.00	0.000	732.61
24909	.636	11.624	33.43	.0274	.0224	.0644	24.44	205.10	0.00	0.000	732.49

ID	WG LBM/SEC	WL LBM/SEC	WLIN LBM/SEC	JGS	JLS	JLSIN	PV PSIA	TLIN F	DTLIN F	LAMBDA	DSTAR
24911	1.008	7.646	33.67	.0447	.0147	.0649	23.38	204.60	0.00	0.000	732.28
24912	1.074	6.329	33.74	.0474	.0122	.0650	23.42	204.30	0.00	0.000	732.12
24913	1.074	5.688	33.49	.0462	.0110	.0645	24.00	203.90	0.00	0.000	731.89
24914	1.200	4.726	33.42	.0508	.0091	.0644	24.55	203.40	0.00	0.000	731.62
24915	1.211	4.457	33.43	.0506	.0086	.0644	25.23	202.90	0.00	0.000	731.35
24916	1.329	4.144	33.76	.0558	.0080	.0650	25.78	202.20	0.00	0.000	731.01
24917	1.397	3.386	33.57	.0583	.0065	.0646	26.24	201.80	0.00	0.000	730.80
24918	1.458	2.875	33.42	.0598	.0055	.0643	27.04	200.40	0.00	0.000	730.09
24919	1.596	2.122	33.33	.0640	.0041	.0641	28.10	199.70	0.00	0.000	729.71
24920	1.666	1.745	33.31	.0657	.0034	.0640	28.85	198.20	0.00	0.000	728.94
24921	1.738	1.584	33.33	.0681	.0030	.0641	29.14	197.10	0.00	0.000	728.39
24922	1.739	1.394	33.34	.0676	.0027	.0640	29.58	195.80	0.00	0.000	727.75
24924	1.779	1.225	33.49	.0688	.0024	.0643	29.92	193.40	0.00	0.000	726.58
24925	.204	14.958	15.75	.0094	.0289	.0304	21.72	211.20	0.00	0.000	735.68
24926	.436	14.440	15.70	.0204	.0279	.0303	22.25	211.40	0.00	0.000	735.80
24927	.322	15.225	15.80	.0147	.0294	.0305	23.63	211.10	0.00	0.000	735.62
24928	.566	13.227	15.77	.0266	.0256	.0305	21.74	210.90	0.00	0.000	735.55
24929	.517	12.415	15.66	.0239	.0240	.0302	22.07	210.80	0.00	0.000	735.48
24930	.708	10.803	15.76	.0320	.0209	.0304	22.89	210.50	0.00	0.000	735.30
24931	.823	10.266	15.71	.0364	.0198	.0303	23.22	210.40	0.00	0.000	735.21
24932	.782	9.014	15.66	.0362	.0174	.0302	20.73	210.20	0.00	0.000	735.17
24933	1.007	5.986	15.69	.0455	.0116	.0303	21.54	210.20	0.00	0.000	735.14
24934	1.013	5.298	15.70	.0458	.0102	.0303	21.99	209.80	0.00	0.000	734.94
24935	1.084	4.875	15.75	.0487	.0094	.0304	22.46	209.70	0.00	0.000	734.88
24936	1.183	4.308	15.73	.0528	.0083	.0304	22.88	209.40	0.00	0.000	734.72
24937	1.195	3.814	15.77	.0528	.0074	.0304	23.45	209.10	0.00	0.000	734.55
24938	1.316	3.416	15.78	.0576	.0066	.0305	23.87	208.90	0.00	0.000	734.44
24939	1.331	2.945	15.74	.0577	.0057	.0304	24.33	208.50	0.00	0.000	734.22
24940	1.359	2.495	15.73	.0581	.0048	.0304	24.88	208.10	0.00	0.000	734.00
24941	1.474	2.323	15.72	.0619	.0045	.0303	25.66	206.60	0.00	0.000	733.21
24942	1.583	2.115	15.88	.0667	.0041	.0305	25.50	198.60	0.00	0.000	729.24
24943	1.631	1.881	15.97	.0683	.0036	.0307	25.69	196.40	0.00	0.000	728.16
24944	1.602	1.661	15.99	.0666	.0032	.0307	26.04	195.10	0.00	0.000	727.51
24945	1.675	1.548	15.98	.0692	.0030	.0307	26.35	194.50	0.00	0.000	727.21
24946	1.738	1.328	16.02	.0711	.0025	.0307	26.73	193.70	0.00	0.000	726.31
24947	1.763	1.482	16.03	.0718	.0028	.0307	26.90	193.20	0.00	0.000	726.57
24948	1.722	1.425	16.00	.0700	.0027	.0307	27.06	193.30	0.00	0.000	726.61
24949	1.739	1.264	15.98	.0704	.0024	.0307	27.26	193.10	0.00	0.000	726.91

NRC FORM 335 (7-77) U.S. NUCLEAR REGULATORY COMMISSION **BIBLIOGRAPHIC DATA SHEET**		1. REPORT NUMBER (Assigned by DDC) NUREG/CR-1557 BMI-2038	
4. TITLE AND SUBTITLE (Add Volume No., if appropriate) Steam-Water Mixing and System Hydrodynamics Program - Task 4 - Quarterly Progress Report April 1, 1979 - June 30, 1979		2. (Leave blank)	
		3. RECIPIENT'S ACCESSION NO.	
7. AUTHOR(S) Robert P. Collier and others		5. DATE REPORT COMPLETED MONTH June	YEAR 1980
9. PERFORMING ORGANIZATION NAME AND MAILING ADDRESS (Include Zip Code) Battelle Columbus Laboratories 505 King Avenue Columbus, Ohio 43201		DATE REPORT ISSUED MONTH July	YEAR 1980
		6. (Leave blank)	
		8. (Leave blank)	
12. SPONSORING ORGANIZATION NAME AND MAILING ADDRESS (Include Zip Code) Division of Reactor Safety Research U. S. Nuclear Regulatory Commission Washington, D.C. 20555		10. PROJECT/TASK/WORK UNIT NO.	
		11. CONTRACT NO. FIN No. A4048	
13. TYPE OF REPORT Quarterly Progress Report	PERIOD COVERED (Inclusive dates) April 1, 1979 - June 30, 1979		
15. SUPPLEMENTARY NOTES		14. (Leave blank)	

16. ABSTRACT (200 words or less)

During this quarter analysis included additional development of the I^* scaling parameter for tubes, review of results from air-water tests in distorted geometries, and correlation of results from countercurrent flow condensation tests in a rectangular test section.

Experimental work this quarter included completion of condensation tests and heat partitioning studies in the rectangular test section, and air-water and steam-water tests in the 2/15-scale model with shortened and extended annulus lengths. The instrumented break leg spool piece was received from INEL and installed in the 2/15-scale facility.

17. KEY WORDS AND DOCUMENT ANALYSIS

ECC Bypass
Scaling
Condensation
Analysis
Experiments

17a. DESCRIPTORS

17b. IDENTIFIERS/OPEN-ENDED TERMS

18. AVAILABILITY STATEMENT	19. SECURITY CLASS (This report)	21. NO. OF PAGES
Unlimited	Unclassified	
	20. SECURITY CLASS (This page)	22. PRICE $

NRC FORM 335 (7-77)